LBL--26904

DE89 012486

# Molecular Beam Photodissociation Studies of Polyatomic Molecules and Radicals

Eric J. Hintsa
(Ph.D. Thesis)

Department of Chemistry
University of California
and
Materials and Chemical Sciences Division
Lawrence Berkeley Laboratory
1 Cyclotron Road
Berkeley, California 94720
USA

March 1989



---

## Abstract

This thesis contains the results of a series of molecular beam photodissociation experiments in which the identity, relative amounts, and velocity distributions of the products were measured, to determine the photochemical pathways and the energy released into translation. Chapter I provides an introduction to the molecular beam photofragmentation technique and a description of the apparatus used in chapters II and III.

A study of the infrared multiphoton dissociation of ethyl and methyl acetate is presented in chapter II. For both molecules, there was competition between simple bond rupture to produce $CH_3CO_2^{\cdot}$ and ethyl or methyl radical and a concerted reaction. Ethyl acetate dissociated almost entirely through concerted reaction to produce acetic acid and ethylene. Methyl acetate underwent simple bond rupture and reaction producing ketene and water in about equal amounts. The dynamics of translational energy release between simple bond rupture and concerted reactions are compared. Using the branching ratio between the two channels, the translational energy release for simple bond rupture, and RRKM calculations, the barrier for concerted reaction in methyl acetate was determined to be 69 ± 3 kcal/mol.

Chapter III describes the photodissociation of 2-bromoethanol and 2-chloroethanol at 193 nm. Both molecules have only one primary dissociation channel, elimination of the halogen atom, with an average of about 34 kcal/mol released into translation. In the photodissociation of 2-bromoethanol, some of the $C_2H_4OH$ product underwent secondary dissociation with a forward-backward peaked secondary angular distribution similar to that found in the decay of long-lived complexes in crossed molecular beams experiments.

The production and photodissociation of cold polyatomic radicals is the subject of chapter IV. $CCl_3$ radicals were produced by photolysis of $CCl_4$ at 193 nm inside a teflon nozzle, thermalyzed in the high-pressure region of the source, then cooled in a supersonic expansion. $CCl_3$ was found to absorb at 308 nm and dissociate to produce $CCl_2$ and Cl, with less than a third of the available energy released into translation.

## Acknowledgements

Earning a Ph.D. in chemical physics requires either lots of hard work or a great deal of help from others. Having relied heavily on the second approach at Berkeley, I have many debts to acknowledge.

First and foremost I would like to thank Yuan Lee for all the help he has given me. His enthusiasm for good science and his expertise in the design and interpretation of experiments may be unmatched anywhere. His eternal optimism, whether on the softball field ("Only down by seven?") or in lab ("Should be all right."), was always inspirational. He really merits most of the praise he receives, and none of its attendant headaches. Bernice Lee also deserves thanks, both for tolerating all this dedication to science and for kind treatment of the group, not to mention for dealing with the press at all hours of the day.

Laurie Butler and Alec Wodtke raised and weaned me up in Building 70A, showing me a healthy blend of hard work and fun, careful thought and irreverence, safety and total recklessness. I will be forever grateful for their calm competence and their gentle and supportive teaching, especially since at one time I must have held the record for asking the most questions in the group. Zhao Xinsheng arrived at the beginning of my second year, and after an initial moment of dismay at his intellect and dedication

(both higher than mine) he became a valued and trusted coworker and friend. Though the "senior" students are supposed to teach the "junior" students, I ended up relying on Xinsheng for all the computer programming I was too lazy to do myself, as well as for any theoretical work requiring more than one sheet of paper.

The Rotating Source Machine (RSM) has been a temporary home for several visitors with whom it has been my pleasure to work. Walter Miller will always be remembered for his wisdom, competence, good stories, and willingness to further the cause in any way (synthesizing S-tetrazine for Xinsheng, building electronics for me). Zhu Qihe was an altogether different kind of person, his perseverance and enthusiasm in the face of staggering (at least for spoiled Americans) obstacles are truly amazing. I wish I had spent more time with Atsushi Yokoyama while he was here, but I enjoyed working on the Benzene Monomer Campaign and playing softball with him. While Bill Jackson is the latest arrival, he has already generated enough good ideas to keep half a dozen graduate students busy for a decade, and proven to be an enthusiastic metalworker. I have also worked with Anne-Marie Schmoltner, Marion Helfand, and John Allman, and learned something from each of them. As I leave, the RSM now rests in the capable hands of Deon Anex.

Throughout the years, the Lee group has held an interesting assortment of people. Barbara Balko and Kerry

(Busarow) Cogen helped me out many times as we suffered through the fun of being first year graduate students together. I certainly learned a great deal from Tim Minton, ranging from the assessment of current technologies (most were pronounced deficient in one key feature or another) to the art of carrying on several different conversations simultaneously. Howard Nathel, though not officially a Lee group student, was often around to answer questions; he also reinvented the Gentec $CO_2$ laser. Mitchio Okumura stood out like an island of thoughtful calm among the turbulent waters of the rest of the group. My first office-mate was Gary Robinson, who introduced me to the Trinity Alps, cheap tickets at the S.F. Opera, sick humor, and calm political debate. Gil Nathanson, with whom I shared an office on campus, showed me a boundless interest in science as well as a willingness to drop anything just to work on someone else's problem. Though no one can replace Gil, Evan Cromwell and Deon have helped to keep the office a safe haven. I have enjoyed friendship and many discussion with Lisa Yeh, on science and other subjects, and from her I have learned something about honesty and integrity. Mike Covinsky provided welcome distractions with a deck of cards, and Dijia Liu was good company on road trips and during poster-making sessions. Looking at the younger students and postdocs I have no doubt that the Lee group will remain an interesting place for some time to come.

Two people in the group deserve special praise (with an honorable mention for Pam Chu, who made the computer center into a productive working area). Not only has Bob Continetti been a key source of information on many aspects of science, he also sacrificed a year out of his graduate career to help the group find a workable "common ground" in Giauque Hall. Finally, of course, is E. Ann Weightman, who has kept the group running on an even keel since pre-collimation, through the move, the Nobel fiasco, and beyond. Though I didn't always agree with her (perhaps because of that) I learned quite a lot from her, and will be perpetually grateful for help received.

Outside the group I would especially like to thank I-Chia Chen, who helped keep me going in the early days and has been a true friend ever since. Bill Ham has been a loyal roommate for my entire stay in Berkeley, and also rekindled my interest in mountaineering and environmentalism. Special thanks go to him and two former roommates (Jeff Cogen and Bill Lubell) and significant others for a great deal of good food, entertainment, and kindness. Thanks also to Spencer and Yvonne Anthony-Cahill and other friends both far and near, for camping trips to Point Reyes, some truly fabulous meals, and general maintenance of sanity.

The support staff both at LBL and on campus do a tremendous job of providing a good environment in which to

do science. Fred Vogelsberg, Henry Chan, Tom Giannotti, and Yau-man Chan have always kept my electronics smoothly humming. Andy Anderson, George Weber, Ron Dal Porto (and of course Fred Wolff before them) managed to ensure that all my machine shop orders were ready as I needed them. Tony Moscarelli introduced me to metalworking (and car-buying too), but it was Steve Willett who really showed me the joys of working in the student shop. Hans Graetsch actually built most of my machine shop orders and also taught me how to machine teflon. Harry Chiladakis kept many things running in Giauque Hall and elsewhere, and was always a good person to have around.

David Wells, a high school teacher, is probably responsible for my majoring in chemistry. In college, Steve Cooper taught me a great deal of what I know about the subject and first turned me on to Berkeley; Gary McClelland first pointed me towards Yuan Lee. From these two scientists, as well as from Hassan Minor and his crew at Brandeis, I learned a great deal that would come in handy surviving in the Lee group.

My parents are really responsible for me being here, in more ways than one. I am grateful for their everlasting confidence and support. Finally, I need to thank someone far away in China, who has patiently accepted my time in graduate school and who provided much of the inspiration to accomplish what follows.

This work was supported by the Office of Naval Research under Contract No. N00014-83-K-0069, and by the Director, Office of Basic Energy Sciences, Chemical Sciences Division of the U.S. Department of Energy under Contract No. DE-AC03-76SF00098.

**Table of Contents**

To My Parents

# Chapter I

## Introduction

Photodissociation is an ideal method for studying the mechanism and dynamics of unimolecular chemical reactions. In a typical experiment, molecules absorb energy from a source of electromagnetic radiation and then decompose into two or more fragments. This can range from IR single[1] or multiphoton dissociation (MPD)[2] to the preparation of excited electronic states with visible or UV photons followed by dissociation.[3] The observable quantities are the identity and amount of each product formed; the product vibrational, rotational, translational, and/or electronic energies; the angular distribution of the products; and the dissociation lifetimes.[4] From this information, one can gain an understanding of the primary (and secondary) photochemistry, the relative yields of each product, and the detailed dynamics of the photodissociation process and the potential energy surface (PES) on which it occurs.

The earliest photodissociation experiments involved irradiating a bulk sample and spectroscopically analyzing the products.[5] One potential problem with such experiments is that if unstable fragments are produced they can undergo further bimolecular reactions in the high pressure environment where they are formed, and may never be detected.[6] This is especially true of reactions producing radicals,

which can recombine, disproportionate, react on the walls, or initiate chain reactions. Many ingenious experiments have been designed to trap these unstable fragments and chemically transform them into something which can be measured,[7] but the results may still be difficult to interpret.

Two technological advances have helped to overcome these problems and vastly extend the amount of information extractable from photodissociation experiments. The first to appear was the molecular beam technique, which allowed experiments to be performed under single-collision conditions.[8] In a photodissociation experiment, all the fragments now survive long enough to be detected, unless they have enough energy to undergo secondary dissociation. Since the molecules in a molecular beam are all traveling in the same direction with roughly the same velocity, the laboratory angular and velocity distributions, as well as the identity of the products, can now be measured. Among the first molecular beam photodissociation experiments were those performed by Wilson and coworkers.[9] Their apparatus consisted of a molecular beam source chamber, an interaction chamber where the beam was crossed by radiation from a light source, and a mass spectrometer detector. The molecular beam, incident radiation, and the direction of detection were mutually perpendicular. By varying the polarization of the light and measuring the velocity distributions of the

products, they were able to determine the initially excited states and the dissociation dynamics of small molecules.[9]

The second major advance in the field of photochemistry was the advent of high-power pulsed lasers. This development, which revolutionized other areas of physical chemistry as well, opened up a great many possibilities for photodissociation experiments. Many experiments previously restricted by signal-to-noise (S/N) considerations became relatively simple with these new high-intensity light sources. Since laser energy is already in a reasonably narrow bandwidth, wavelength-specific experiments were now as feasible as previous broadband excitation experiments. Lasers proved to be very compatible with molecular beam techniques since laser beams are generally narrow, intense, and to some extent wavelength-tunable. The short pulses are ideal for time-of-flight (TOF) measurements such as we do: the laser sets t = 0 and the products are measured as a function of their arrival time after traveling over a known distance. Since the laser pulses are on a nanosecond or shorter timescale, two-laser pump-probe experiments can be carried out in a gas cell or molecular beam where the nascent fragments are probed before they collide with other molecules or a wall. Very elegant and detailed experiments have been performed to measure the internal state distributions of the photodissociation fragments of small molecules,[10] and some experiments have even measured the

evolution of a laser-initiated unimolecular reaction in real time.[11]

Photodissociation can be thought of as a half-collision. Instead of the archetypal reaction A + BC → AB + C, we study the reaction ABC + $h\nu$ → AB + C, or A + BC, or AC + B, or even A + B + C. Since the experiment starts with the "collision complex" already prepared, information is gained only about the exit channel of the PES. Therefore it is complementary to crossed-beams reactive scattering, where both the initial approach of the reactants and the exit channel affect the energy partitioning and the angular distribution. For example, it has been shown that in the ground electronic state, for a simple bond rupture reaction where two polyatomic radicals are produced with no exit channel barrier, dissociation occurs along the attractive part of the PES and there is very little energy released into translation.[2] In contrast, for a concerted reaction, where there is a sizable reaction barrier in the exit channel in addition to the endothermicity, a large fraction (up to 70%) of the exit barrier is released into translation as the closed-shell products repel each other down the exit channel of the PES.[2] In an excited electronic state of a polyatomic molecule, if excitation occurs to a directly repulsive state, about half the excess energy often ends up in translation.[3] If the molecule undergoes internal conversion (IC) to the ground state it behaves as if the

energy had been initially deposited into the ground state, and the total amount of energy has little effect on the translational energy release.[12]

The most basic question to be answered is, however, what are the products? Though we have performed some completely original experiments in this area, such as demonstrating the possibility of bond-selective (bs) photochemistry by varying the excitation wavelength for bromoiodo compounds,[13] many of our experiments involve previous work by other researchers. Since we can find the primary dissociation pathways of most molecules "in a day", there have been a great many short and not-so-short experiments performed to determine the primary photochemistry of a particular system.[14] Unfortunately, our experience has shown that much primary photochemistry was either unknown (benzene and substituted aromatics),[15] known incorrectly (RDX, s-tetrazine),[12,15] only partially known (methyl acetate, nitromethane),[16] or some combination thereof (dimethyl nitramine).[17] In at least some of these cases we have been able to clear up the previous confusion.

For several reasons, photodissociation research is now enjoying a period of steady growth. Sadly, one of the main reasons is that within the field of physical chemistry, it's among the easier experiments to do. Almost anyone can get a laser, blast apart some molecule, detect something, and publish the results. It is not, however, easy to do well,

or else several of the papers mentioned above would not have been necessary. To do the perfect experiment is quite difficult, and even the oft-studied $CH_3I$ is still the subject of controversy.[18]

In defense of photodissociation, it can also yield very accurate and detailed information on chemical reaction dynamics. The photodissociation dynamics of water[19] and formaldehyde,[20] just for example, are now quite well understood. Our molecular beam photodissociation experiments have not focused on any one molecule to such a high level of detail, but rather we have looked at a whole range of chemistry and dissociation dynamics. The goals have been to gain a predictive power of the primary photochemistry and the rough features of translational energy release for general classes of molecules. There have also been applications to atmospheric and combustion chemistry, including the photodissociation of $CCl_4$,[21] a source of atmospheric Cl, and the precise determination of the C-H bond energy in $C_2H_2$,[22] a quantity needed for combustion modeling. In the photodissociation of 2-bromoethanol,[23] we were originally interested in how much energy remained in the $CH_2CH_2OH$ fragment following excitation at 193 nm, and whether it could spontaneously fall apart. $CH_2CH_2OH$ is the intermediate in the reaction of OH + $C_2H_4$ at low temperatures, and may be important in the combustion of ethylene.[24] We found that not only could we produce and measure the $CH_2CH_2OH$, it

spontaneously underwent secondary dissociation to $C_2H_4$ and OH with a forward-backward symmetric angular distribution governed by angular momentum constraints,[23] thus leading back to reaction dynamics and the observation of long-lived complexes in crossed molecular beam scattering experiments.

The experiments described in chapters 2 and 3 were carried out on the Rotating Source Machine (RSM), a crossed laser-molecular beam apparatus designed specifically for photodissociation. A somewhat detailed description of the apparatus is contained in the remainder of this chapter and a schematic of the machine is shown in fig. 1. The molecular beam is formed by flowing gas out the end of a nozzle (a .125 mm platinum electron microscope aperture from Ted Pella, Inc.) into the source chamber. The resulting supersonic expansion internally cools the molecules and leaves them with a narrow velocity distribution. The expansion then passes through two skimmers, keyed into the source and differential regions, resulting in a well-collimated (nominally ±1.5° angular divergence) beam. The source chamber opens up in the back (behind the page) and is pumped by two Varian 6" diffusion pumps (replaced by Edwards Diffstaks in 1986). The differential region is pumped by a Leybold-Heraeus turbomolecular pump in front (coming out of the page) which exhausts back into the source. The main chamber is pumped by a 3500 l/sec diffusion pump (Edwards) and by liquid nitrogen cryopanels along the bottom, as well

as a liquid nitrogen cooled "beam-stop" near the detector. The differential pumping allows the main chamber pressure to remain unchanged ($10^{-7}$ Torr) even with the source running (P = 1-3 x $10^{-4}$ Torr). The entire source rotates inside the main chamber from 0° (straight into the detector) to 90° (straight down).

Molecular beams of many different molecules can be made quite easily. Gaseous species are prepared by mixing a tank of the target molecule seeded in some buffer gas, and condensed phase molecules are introduced into molecular beams by passing the buffer gas through the liquid or solid of choice and picking up its equilibrium vapor pressure. The seeded beams generated in the RSM typically have velocity spreads of less than 15% of the peak velocity, both of which can be measured by a spinning slotted wheel in the main chamber.[25] The wheel can be raised into position for beam TOF, then lowered externally without interrupting the experiment.

In the main chamber, the molecular beam is crossed by a laser beam coming out of the page. The molecules absorb energy from the laser and dissociate, with the fragments scattered in the center-of-mass (c.m.) frame with a distribution of c.m. velocities. A small fraction of the fragments have the correct c.m. velocity and angle such that they pass through the aperture (±1.5° resolution) of the detector. They travel through two regions of differential

pumping into a Brink-type electron bombardment ionizer (~$1/10^5$ efficiency). The ions are extracted and focused into a quadrupole mass spectrometer. The mass-selected ions are then detected with near unit efficiency by a Daly-type detector. The ions are accelerated at -30 kV onto a flat Aluminum "doorknob", the secondary electrons produce photons in a scintillator opposite the doorknob, and the photons are collected and amplified in a photomultiplier tube. A discriminator is used to reject spurious signal from dark current.

Data is taken by sending the detector output to a multichannel scaler. The laser pulse typically sets t = 0, then all the signal in the first time increment (usually 1-10 $\mu$sec, though the new scalers can go to 150 nsec) goes to the first bin of the scaler, the signal in the second increment goes to the second bin, and so forth, giving a TOF spectrum, examples of which are shown in the following chapters. These are taken at all mass-to-charge ratios (m/e) where signal is detected, and at different beam-to-detector angles as needed.

Since these are low signal experiments (typically 0.02-1.0 counts/laser pulse integrated over the whole TOF spectrum, though we can do .001 counts/pulse in some cases), great effort has been spent to achieve good S/N. The displayed TOF spectra are the average of many thousands of laser shots. The scalers accumulate signal in each bin for

each laser shot, then dump the data to an LSI-11 minicomputer at the end of each "sweep" (usually 1,000-20,000 triggers). A 100,000 shot scan at 100 Hz ($CO_2$ or excimer laser) takes about 15 minutes, but almost 3 hours at 10 Hz (YAG laser). Scans of over a million shots are sometimes needed, but fortunately not often.

To reduce background, great care is taken to keep the ionizer region of the detector as clean as possible, including more differential pumping. The first two differential regions of the detector are pumped by conventional grease-sealed turbomolecular pumps, and the third region, containing the ionizer, is pumped by a magnetically suspended turbo pump and enclosed in a liquid nitrogen cooled insert. The magnetically suspended turbo can run at higher speeds and has no background from lubricating grease. The quadrupole and ion detection system are pumped by a fourth turbo pump, in contrast to the "nested" design of the crossed beam machines. (Space is not so much of a consideration when the detector need not rotate inside a vacuum chamber. Even with a less-than-compact detector, the RSM is much smaller than any of the crossed beam machines, yet its neutral flight length from the interaction region to the ionizer, which determines the ultimate resolution, is the longest. It was originally designed to be 36.7 cm, but can be relatively easily extended to 80 cm.[26]) In this case, the differential pumping does not decrease the ultimate

pressure in the ionizer region, but serves to reduce the partial pressures of gas molecules effusing in from the main chamber, which contribute strongly to the background in the TOF spectra of the photofragments. Unfortunately this does not help much with ions originating in the detector, such as at m/e = 2 ($H_2^+$) or 28 ($CO^+$).

With a triply-differentially pumped detector, most of the molecules reaching the ionizer from the main chamber do not effuse though the differential regions, but rather have a velocity in the same direction as the photofragments and will not be reduced by any amount of differential pumping. Since at $10^{-7}$ Torr the mean free path is many meters, this "direct-through" background comes almost entirely from molecules bouncing off a surface in the line-of-sight of the detector. To eliminate this, a closed-cycle Helium refrigerator cools a small plate behind the interaction region to ~30 K, so the detector always sees a cryocooled surface, which pumps away any erstwhile direct-through background. Most of the residual background now comes directly from the beam (at small beam-to-detector angles) or from inside the ionizer.

Data analysis proceeds by assigning the primary (and secondary, if any) dissociation channels and determining their translational energy release. In the c.m. frame, pairs of fragments must have equal and opposite momenta as they dissociate. By constructing a Newton diagram (see fig.

2), the c.m. velocities of the neutral fragments can be determined to see if they "momentum match". Based on chemical intuition and the conservation of momentum, a fairly good idea of which reaction channels are occurring can be obtained. The TOF spectra are fit by assuming a trial translational energy distribution ($P(E_T)$) (obtained from Newton diagrams, direct inversion, or a guess) and simulating the data with forward convolution techniques. The $P(E_T)$ is then adjusted until the simulated and the real data match. There has been no complete discussion of data analysis from theory all the way to the computer strategy and algorithms, and it certainly will not be given here, but ref. 27 contains a summary of the kinematic relations and ref. 28 has a derivation of the theory from first principles as well as a listing of a program which treats primary and also secondary dissociation. Ref. 29 also contains a simpler (though slightly incorrect in its treatment of secondary dissociation) version of the program, which is also reasonably well annotated.

The RSM has proven to be a versatile and high-yield apparatus. Many chemical systems have been investigated, among which three are discussed in the following chapters. The IR multiphoton dissociation of ethyl and methyl acetate is described in the next chapter. A $CO_2$ laser was used to "heat" the molecules in the beam and study their "thermal" chemistry. For both molecules, competition between concer-

ted reaction and simple bond rupture was observed. The dynamics of translational energy release are discussed and barrier heights for the concerted reaction are determined. The photodissociation of 2-bromoethanol and 2-chloroethanol at 193 nm is described in chapter III. After excitation to a repulsive electronic state, loss of a halogen atom occurs with large amounts of energy channelled into translation and rotation. Very interesting secondary dissociation dynamics were observed, similar to long-lived collision complexes in crossed molecular beams experiments. The experiments in the last chapter were begun on the RSM but completed on a crossed-beams apparatus. As part of an effort to develop a source of cold polyatomic radicals, we produced a pulsed beam of $CCl_3$ from the photolysis of $CCl_4$ at 193 nm in the source. The $CCl_3$ was then dissociated at 308 nm and the products were measured.

**References**

1. Z. S. Huang, K. W. Jucks, and R. E. Miller, J. Chem. Phys. **85**, 3338 (1986); D. C. Dayton, K. W. Jucks, and R. E. Miller, J. Chem. Phys., in press; K. G. H. Baldwin and R. O. Watts, J. Chem. Phys. **87**, 873 (1987).

2. P. A. Schulz, Aa. S. Sudbø, D. J. Krajnovich, H. S. Kwok, Y. R. Shen, and Y. T. Lee, Annu. Rev. Phys. Chem. **30**, 379 (1979); F. Huisken, D. Krajnovich, Z. Zhang, Y. R. Shen, and Y. T. Lee, J. Chem. Phys. **78**, 3806 (1983); L. J. Butler, R. J. Buss, R. J. Brudzynski, and Y. T. Lee, J. Phys. Chem. **87**, 5106 (1983).

3. D. Krajnovich, Z. Zhang, L. Butler, and Y. T. Lee, J. Phys. Chem. **88**, 4561 (1984); T. K. Minton, G. N. Nathanson, and Y. T. Lee, J. Chem. Phys. **86**, 1991 (1987).

4. **Dynamics of Molecular Photofragmentation**, Chem. Soc., Faraday Disc. **82** (1986); M. N. R. Ashfold and J. E. Baggott, Eds., **Molecular Photodissociation Dynamics** (Royal Soc. of Chem., London, 1987).

5. R. G. W. Norrish and G. Porter, Nature **164**, 658 (1949); G. Porter, Proc. Royal Soc. (London) **A200**, 284, (1950).

6. J. G. Calvert and J. N. Pitts, Jr., **Photochemistry** (Wiley, New York, 1966), pp. 587-590, 599.

7. J. Solomon, J. Chem. Phys. **47**, 889 (1967); C. Jonah, P. Chandra, and R. Bersohn, J. Chem. Phys. **55**, 1903 (1971); J. Solomon, C. Jonah, P. Chandra, and R.

Bersohn, J. Chem. Phys. **55**, 1908 (1971).

8. E. H. Taylor and S. Datz, J. Chem. Phys. **23**, 1711 (1955); D. R. Herschbach, G. H. Kwei, and J. A. Norris, J. Chem. Phys. **34**, 1842 (1961).

9. G. E. Busch, J. R. Cornelius, R. T. Mahoney, R. I. Morse, D. W. Schlosser, and K. R. Wilson, Rev. Sci. Instrum. **41**, 1066 (1970); G. E. Busch, R. T. Mahoney, R. I. Morse, and K. R. Wilson, J. Chem. Phys. **51**, 449, 837 (1969); G. E. Busch and K. R. Wilson, J. Chem. Phys. **56**, 3626, 3638, 3655 (1972).

10. I.-C. Chen, W. H. Green, Jr., and C. B. Moore, J. Chem. Phys. **89**, 314 (1988).

11. L. R. Khundkar and A. H. Zewail, Chem. Phys. Lett. **142**, 426 (1987); R. Bersohn and A. H. Zewail, Ber. Bunsenges. Phys. Chem. **92**, 373 (1988).

12. X. Zhao, W. B. Miller, E. J. Hintsa, and Y. T. Lee, J. Chem. Phys., in press; X. Zhao, R. E. Continetti, A. Yokoyama, E. J. Hintsa, and Y. T. Lee, J. Chem. Phys., submitted.

13. L. J. Butler, E. J. Hintsa, and Y. T. Lee, J. Chem. Phys. **84**, 4104 (1986); L. J. Butler, E. J. Hintsa, S. F. Shane, and Y. T. Lee, J. Chem. Phys. **86**, 2051 (1987).

14. In the case of $ClNO_2$ photodissociation, the RSM was down for more than a week for consequent repairs, but the experiment still took less than a day.

15. A. Yokoyama, X. Zhao, R. E. Continetti, E. J. Hintsa, and Y. T. Lee, in preparation; M. S. Helfand and Y. T. Lee, in preparation.

16. Chapter 2 and A. M. Wodtke, E. J. Hintsa, and Y. T. Lee, J. Chem. Phys. **84**, 1044 (1986); A. M. Wodtke, E. J. Hintsa, and Y. T. Lee, J. Phys. Chem. **90**, 3549 (1986); E. J. Hintsa, A. M. Wodtke, and Y. T. Lee, J. Phys. Chem. **92**, 5379 (1988).

17. E. J. Hintsa, A. M. Wodtke, A. M. Schmoltner, and Y. T. Lee, unpublished results; D. F. McMillen, S. E. Nigenda, A. C. Gonzalez, and D. M. Golden, Spectrochim. Acta **A43**, 237 (1987); S. E. Nigenda, D. F. McMillen, and D. M. Golden, J. Phys. Chem. **93**, 1124 (1989); P. H. Stewart, J. B. Jeffries, J.-M. Zellweger, D. F. McMillen, and D. M. Golden, J. Phys. Chem., in press.

18. G. N. A. van Veen, T. Baller, and A. E. De Vries, Chem. Phys. **97**, 179 (1985); W. P. Hess, R. Naaman, and S. R. Leone, J. Phys. Chem. **91**, 6085 (1987); R. E. Continetti, B. A. Balko, and Y. T. Lee, J. Chem. Phys. **89**, 3383 (1988).

19. P. Andresen, G. S. Ondrey, B. Titze, and E. W. Rothe, J. Chem. Phys. **80**, 2548 (1984); P. Andresen, V. Beushausen, D. Häusler, H. W. Lülf, and E. W. Rothe, J. Chem. Phys. **83**, 1429 (1985); V. Engel, R. Schinke, and V. Staemmler, J. Chem. Phys. **88**, 129 (1988); D. Häusler, P. Andresen, and R. Schinke, J. Chem. Phys.

**87**, 3949 (1987). For a somewhat different interpretation, see J. Zhang and D. G. Imre, Chem. Phys. Lett. **149**, 233 (1988); N. E. Henriksen, J. Zhang, and D. G. Imre, J. Chem. Phys. **89**, 5607 (1988).

20. D. J. Bamford, S. V. Filseth, M. F. Foltz, J. W. Hepburn, and C. B. Moore, J. Chem. Phys. **82**, 3032 (1985).

21. Chapter 4 and E. J. Hintsa, X. Zhao, W. M. Jackson, W. B. Miller, A. M. Wodtke, and Y. T. Lee, in preparation.

22. A. M. Wodtke and Y. T. Lee, J. Phys. Chem. **89**, 4744 (1985).

23. Chapter 3 and E. J. Hintsa, X. Zhao, and Y. T. Lee, in preparation.

24. F. P. Tully, Chem. Phys. Lett. **96**, 148 (1983); **143**, 510 (1988).

25. D. Krajnovich, Ph.D. Thesis, University of California, Berkeley, 1983.

26. In an attempt to resolve the $CH_3$ fragment vibrational states following photolysis of $CH_3I$ at 248 nm, Professor Qihe Zhu built a 40 cm extension for region II.

27. R. K. Sparks, K. Shobatake, L. R. Carlson, and Y. T. Lee, J. Chem. Phys. **75**, 3838 (1981).

28. X. Zhao, Ph.D. Thesis, University of California, Berkeley, 1988.

29. A. M. Wodtke, Ph.D. Thesis, University of California, Berkeley, 1986.

**Figure Captions**

Fig. 1. Rotating Source Machine schematic: 1, source chamber; 2, heating wire and thermocouple; 3, cryocooled plate; 4, entrance lens and exit window for laser; 5, interaction region of laser and molecular beam; 6, liquid $N_2$ cooled panels; 7, detector slide valve; 8, externally retractable TOF wheel for beam velocity measurements; 9, 5000 l/s diffusion pump for main chamber; 10, one of two 6" diffusion pumps for source chamber; 11, electron-bombardment ionizer; 12, quadrupole mass filter; 13, magnetically suspended turbomolecular pump; 14, exit ion optics; 15, "doorknob" ion target; 16, scintillator; 17, conventional turbomolecular pump; 18, photomultiplier tube; 19, liquid $N_2$ reservoirs.

Fig. 2. "Newton" diagram for the photodissociation of 2-bromoethanol, showing the beam velocity ($v_b$) and Newton circles for the recoil of the Br and $C_2H_4OH$ fragments at the peak translational energy of 33 kcal/mol. The two c.m. velocity vectors for $C_2H_4OH$ and Br are related by the conservation of linear momentum, and the resultant vector of $v_b$ and $u_{Br}$ determines one particular laboratory velocity of Br at 40°.

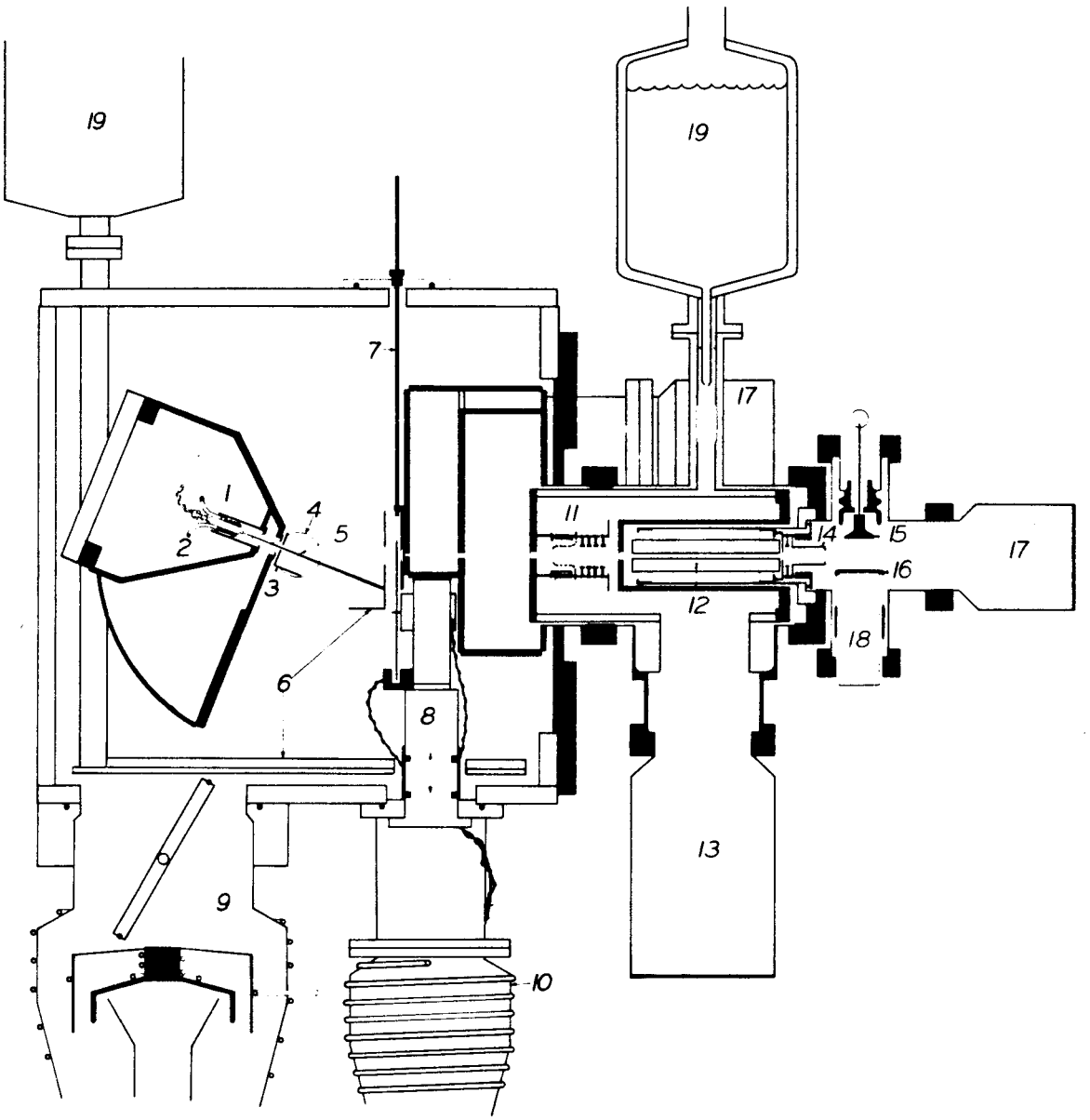


XBL 862-713

Figure 1

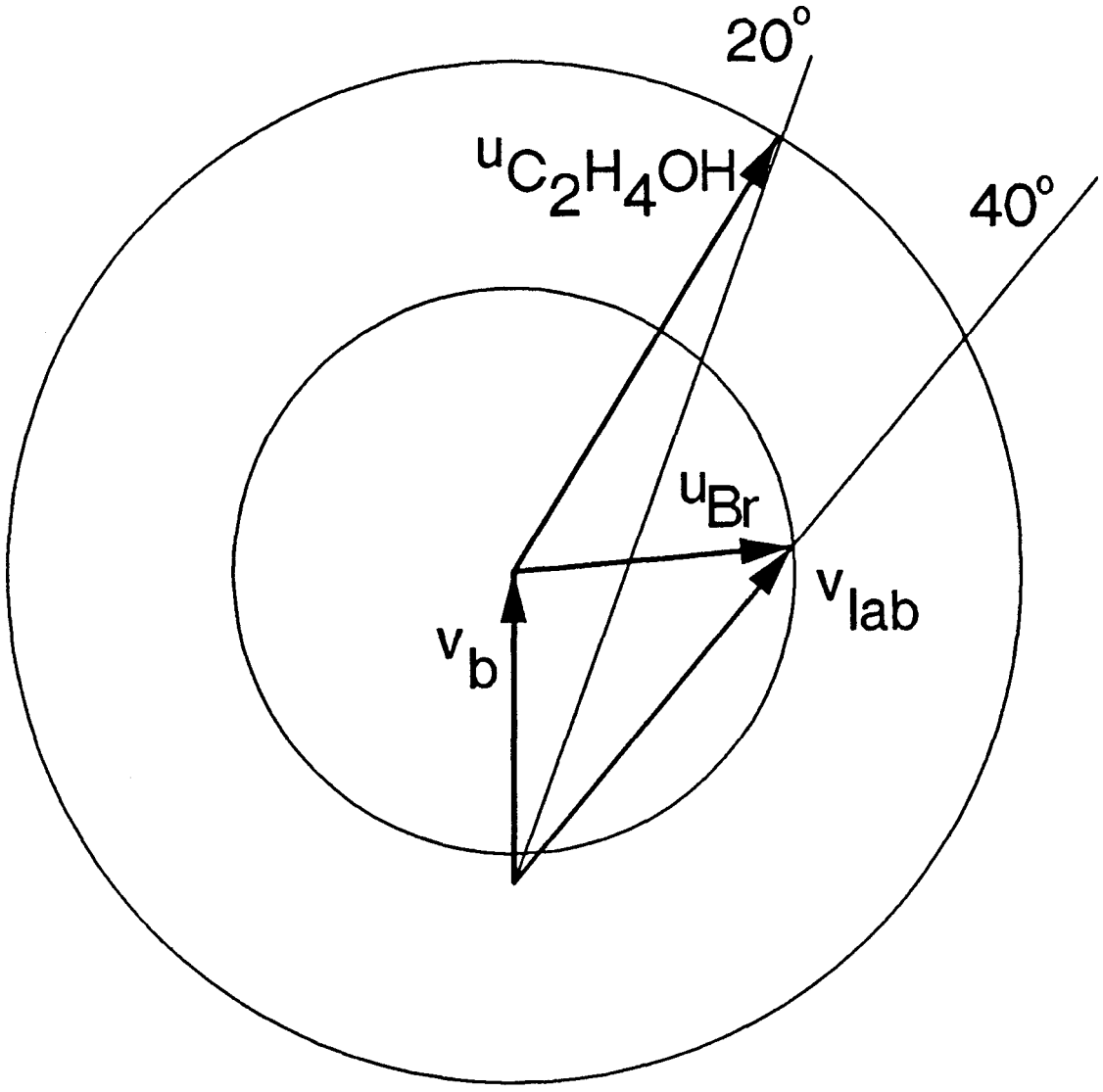


XBL 893-801

Figure 2

# Chapter II

# The Infrared Multiphoton Dissociation of Ethyl and Methyl Acetate

## Introduction

Since its discovery in the early 1970s, the phenomenon of multiphoton dissociation (MPD) has generated immense interest.[1] Much early work focused on isotope separation and on exploring the possibility of bond-selective chemistry by exciting a local mode in a polyatomic molecule. Although rapid intramolecular vibrational relaxation prevents true bond-selective fission,[2] this allows MPD to be used as a method for performing essentially "thermal" experiments in the collisionless environment of a molecular beam.[3,4]

The process of MPD can be roughly divided into three regions.[5] In the lowest region the molecules are excited through discrete rovibrational levels by intensity-dependent resonant absorption until the vibrational density of states becomes large enough for energy randomization to compete with absorption. In this "quasicontinuum" the molecules are pumped to higher and higher levels by stepwise incoherent excitation. Once the molecules are excited over the dissociation barrier, decomposition competes with continued up-pumping. The laser intensity determines how high the molecules are excited during the laser pulse before they dissociate, as long as the fluence is sufficient to dissoci-

ate most of the molecules in the quasicontinuum. If there is more than one possible decay channel at reasonably low energies, competition between the different pathways may be observed.[3,4] At high levels of excitation, vibrational energy is randomized on a very fast timescale, and statistical methods such as RRKM theory can be used to calculate the unimolecular rate constants. For simple bond rupture reactions, where there is no exit channel barrier, RRKM theory can be easily extended to predict the translational energy distribution of the products, allowing the average energy of the dissociating molecules to be determined. Using the translational energy distribution and the endoergicity of one channel, and the branching ratio between two competing channels, we have previously shown that it is possible to find the dissociation barrier of the other channel.[4]

This is especially relevant to cases where a concerted reaction competes with simple bond rupture. In a concerted reaction, bonds are broken and formed simultaneously, often through a cyclic transition state followed by a large release of translational energy. As part of an ongoing effort to understand the dynamics of translational energy release from different types of transition states, we have performed molecular beam IRMPD studies of various nitro compounds[4,6] and esters as well as other molecules.

Ethyl acetate is well-known to undergo reaction through

a six-membered transition state to form ethylene and acetic acid:

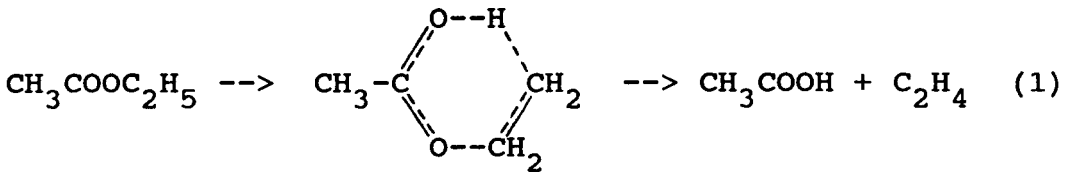


This reaction is endothermic by 12 kcal/mol, but the activation energy has been determined to be 48.0 kcal/mol,[7] leaving an exit channel barrier of about 36 kcal/mol. While a few MPD studies of ethyl acetate have been performed in gas cells[8,9] confirming the occurrence of reaction (1), there has been no determination of the fraction of energy released into translation or the internal degrees of freedom.

In comparison, there have been very few studies of methyl acetate thermolysis. Wolf and Rosie[10] examined methyl acetate decomposition using gas chromatography and interpreted the results with a radical reaction mechanism. Gil'burd and Moin[11] studied the reaction kinetics of methyl acetate in the gas phase from 1000 to 1150 K. They found that the principal products were methanol, CO, methane, and ketene, with a reaction order of 3/2, also suggesting that radical chain reactions were involved. Carlsen et al.[12] determined by isotope labeling and mass spectrometry that the major reaction at medium temperatures (~1000 K) was methyl group migration from one oxygen atom to the other, with ketene and methanol also produced in low yield. In a

recent high-temperature (1400-1800 K) reflected shock wave study, Sulzmann and coworkers found only $CO_2$ and methyl radicals, though they did not monitor other possible channels.[13] Energy level diagrams including possible decomposition products for ethyl and methyl acetate are shown in figures 1 and 2. The primary decomposition channels that we observed are indicated by dashed lines.

**Experimental**

The rotating source molecular beam translational energy spectrometer has been previously described in Chapter 1 and elsewhere.[14] Briefly, helium was bubbled through the liquid under study and passed through the 125 $\mu$m nozzle, creating a supersonic expansion with a mean velocity of $1.3 \times 10^5$ cm/sec (ethyl acetate) or $1.6 \times 10^5$ cm/sec (methyl acetate) and a full width at half maximum spread of about 10%. The acetates were held in a bubbler at 0 °C with a total backing pressure of 350 Torr. The nozzle was heated to 250 °C to eliminate cluster formation and improve absorption of IR radiation by the molecules. After passing through two collimating skimmers in differentially pumped regions which defined it to a 1.5° angular spread, the molecular beam was crossed with the focused output of a Gentec $CO_2$ laser operating on the P(22) line of the 9.6 $\mu$m branch (1045 $cm^{-1}$) with a fluence of about 40 $J/cm^2$. The source was rotated about the interaction region for data collection at differ-

ent source-to-detector angles. A small (~1.5°) angular fraction of the MPD fragments passed through two more regions of differential pumping and was detected by the quadrupole mass spectrometer using an electron impact ionizer and ion-counting techniques. The detector output was sampled by a multichannel scaler, triggered by the laser, for time-of-flight (TOF) measurements of product velocity distributions. Most of the data were taken at a source-to-detector angle of 20°, with 40,000 to 1,000,000 laser shots being required to achieve good signal-to-noise ratios at different masses.

**Results and Analysis**

The data were analyzed with forward convolution techniques to determine the translational energy release.[15] An assumed product translational energy probability distribution ($P(E_T)$) for a particular reaction channel is converted to a center of mass (c.m.) velocity flux distribution for one of the pair of products related by conservation of linear momentum. This c.m. velocity distribution is added vectorially to the beam velocity (obtained by beam TOF measurements using a spinning slotted disk) and transformed to a lab velocity flux distribution for a given source-to-detector angle using the appropriate Jacobian factor. Experimental parameters are averaged over, principally the beam velocity spread, but also the finite length of the

ionizer and the spread in beam angles. The resulting lab velocity distribution is converted to a theoretical TOF spectrum that can be compared to the experimental data. The $P(E_T)$ is then adjusted until the theoretical and experimental TOF spectra match. Secondary dissociation is modeled in an analogous way though with a more complicated algorithm.[16] Essentially, a primary c.m. flux distribution is converted to a density distribution in the primary reactant c.m. coordinates, then by using a second $P(E_T)$, a secondary flux distribution is calculated from the primary one. From this secondary distribution, the contributions at a given angle are calculated using the correct transformation factors.

A. Ethyl Acetate- Signal from MPD of ethyl acetate was observed at mass-to-charge ratios (m/e) of 13-18, 26-31, 42-45, and 59, but not at m/e = 60. A chart with all the detected ion masses, their corresponding neutral fragments, the reaction channel to which they have been assigned, and the relevant figure, is shown in Table I. As expected, reaction (1) producing acetic acid and ethylene was the dominant channel. The peaks in the m/e = 26 and 45 TOF spectra in figure 3 are from ethylene and the corresponding acetic acid fragment, respectively. Ethylene also appears as the parent ion (m/e = 28) and at several other masses, but the acetic acid produces no signal at m/e = 60 though it appears at almost all the lower daughter ion masses including m/e = 59. This absence of the parent ion is not

surprising, as it has been previously found that highly vibrationally excited species undergo extensive fragmentation in the electron bombardment ionizer and analysis must be based on the detection of daughter ions.[17]

The $P(E_T)$'s derived from the m/e = 26 and 45 spectra are shown in figure 4, and the fits to the data are shown in figure 3. The $P(E_T)$ of ethylene peaks at 19 kcal/mol and releases an average of 21.7 kcal/mol into translation. For a process producing two fragments, both of which are detected, the $P(E_T)$ derived from one should fit the other, but this is not the case for acetic acid recoiling from ethylene as can be seen in figure 3, bottom, with a dotted line showing the acetic acid data fit with the $P(E_T)$ derived from the ethylene data. The peak and the fast edge match (substantiating the identification of this channel), but the $P(E_T)$ derived from the ethylene data predicts considerably more slow acetic acid. The main difference between this $P(E_T)$ and that derived from the acetic acid data occurs at energies below 10 kcal/mol, as shown in figure 4.

An explanation of this comes from the fact that acetic acid may undergo secondary decomposition, with or without the absorption of more photons. Though not rigorously true for IRMPD, where the molecules dissociate from a considerable range of energy levels, molecules releasing a smaller amount of the energy of an exit channel barrier into translation should have, on the average, more internal energy and

thus be more likely to undergo secondary dissociation. A smaller effect is caused by the fact that molecules which dissociate early in the 650 nsec laser pulse and release little energy into translation literally spend more time in the interaction region and have longer to absorb more photons from the $CO_2$ laser than the fast products.

The secondary dissociation products of acetic acid are ketene and water produced by reaction (2) through a

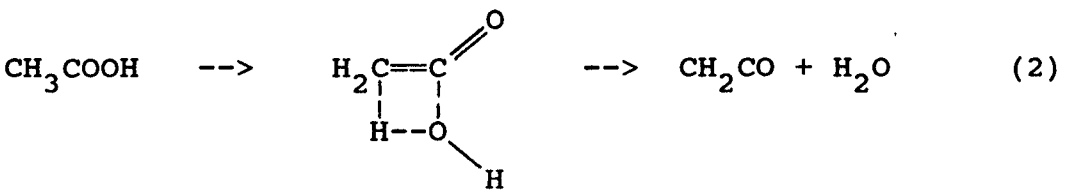


(2)

four-membered transition state, and their TOF spectra are shown in figure 5. These results were confirmed by MPD experiments on acetic acid[18] and are consistent with previous thermal studies.[7,19]

Since it was found that 67% of the acetic acid produced underwent secondary decomposition (vide infra), neither of the $P(E_T)$'s derived from ethylene or acetic acid was suitable for use as the primary $P(E_T)$ for acetic acid which eventually decomposed. This problem was resolved by taking the $P(E_T)$ for ethylene and subtracting 33% of the $P(E_T)$ for acetic acid (both initially normalized to unity), which represents the surviving acetic acid. The resulting primary $P(E_T)$ corresponds to the crosshatched area in figure 4. Though similar in shape to the $P(E_T)$ for ethylene, it is

shifted towards lower translational energies as these preferentially underwent secondary decomposition. The $P(E_T)$ for secondary dissociation is shown in figure 6 and the fits to the data are shown in figure 5. The peak of the $P(E_T)$ is at 25 kcal/mol with an average of 23.7 kcal/mol released to translation, though these numbers for secondary dissociation are inherently more uncertain. There was no evidence for any secondary dissociation of ethylene or any further dissociation of ketene.

In addition to the concerted reaction pathway there was evidence of another reaction occurring. Data at m/e = 15 and 44 (shown in figure 7) could not be fit with reactions (1) and (2). The mass 15 TOF spectrum shows extremely fast signal, and that at mass 44 is very broad, with signal appearing at faster and slower arrival times than would be expected from acetic acid. If the weakest bond in ethyl acetate, between an O atom and the ethyl group, broke to produce the acetoxyl radical ($CH_3CO_2$) and an ethyl radical through reaction (3), the acetoxyl could decompose via reaction (4) to give methyl radical and $CO_2$. Examination of

$$CH_3COOC_2H_5 \;\text{-->}\; CH_3COO^{\cdot} + C_2H_5^{\cdot} \qquad (3)$$

$$CH_3COO^{\cdot} \;\text{-->}\; CH_3^{\cdot} + CO_2 \qquad (4)$$

the mass 29 TOF spectrum (shown in figure 8, top) reveals a

slow component shown as a dotted line due to ethyl radical. The $P(E_T)$ for reaction (3) derived from the mass 29 data by using RRKM calculations described below is shown at the bottom of figure 8.

No trace of stable acetoxyl radical could be detected at any mass. Evidently this weakly bound species undergoes nearly complete secondary dissociation either by absorbing additional energy from the $CO_2$ laser or by being formed above its dissociation limit. The data at mass 15 (from methyl radical) and mass 44 (from $CO_2$) cannot be fit by a single secondary $P(E_T)$. The methyl radical signal is fit by a $P(E_T)$ averaging over 30 kcal/mol in translational energy and extending beyond 60 kcal/mol. The methyl radical <u>by itself</u> has an average of more than 21 kcal/mol in translation. $CO_2$ recoiling from methyl radical requires even more translational energy to reproduce the fastest signal (or a heavier particle than $CH_3$ to recoil from), indicating that a three-body dissociation process is occurring and accounts for at least some of the data. This is reasonable since dissociation of the acetoxyl radical to methyl radical and $CO_2$ is exothermic by almost 10 kcal/mol and cannot have too high a barrier since the C-C stretching surface has been calculated to be relatively flat.[20]

There was no evidence in the TOF spectra for any other reactions occurring. The results cannot be explained by primary loss of the methyl group, followed by decomposition

to give ethyl radical and $CO_2$ through reaction (5), as this

$$CH_3COOC_2H_5 \rightarrow CH_3^{\cdot} + {}^{\cdot}COOC_2H_5$$
$$\rightarrow CH_3^{\cdot} + CO_2 + C_2H_5^{\cdot} \qquad (5)$$

would produce much faster $C_2H_5$ product as well as slower methyl radicals. Simple bond rupture to give $CH_3$ and $CH_3COOCH_2$ is at least 5 kcal/mol more endothermic than reaction (3) and should not be important. A theoretical branching ratio calculation described below showed that less than 0.5% should react through this channel. Reactions (6) and (7) involving hydrogen atom transfer through a four-

$$CH_3COOC_2H_5 \rightarrow C_2H_5OH + CH_2CO \qquad (6)$$

$$CH_3COOC_2H_5 \rightarrow 2\ CH_3CHO \qquad (7)$$

membered transition state are expected to proceed only with very high barriers, thus limiting their contribution. A reaction analogous to (6) was observed in methyl acetate, with a barrier of 69 kcal/mol, but in that case there was no lower energy concerted reaction pathway such as reaction (1). Reaction (7) is a potential source of the m/e = 44 signal but should also produce signal at m/e = 43 ($C_2H_3O^+$).[21] Since the m/e = 43 data are identical to m/e = 45 and different from m/e = 44 this channel can be experi-

mentally ruled out.

Branching ratio calculations were carried out to determine the relative contribution from each channel. Using a slight modification of a method described by Krajnovich,[22] the branching ratio between channel A producing fragments of mass $m_1$ and $m_2$, and channel B with fragments $m_3$ and $m_4$, is

$$R\left(\frac{A}{B}\right) = \frac{N(m_1^+,\theta)}{N(m_3^+,\theta)} \cdot \frac{\sigma_{ion}(m_3)}{\sigma_{ion}(m_1)} \left(\frac{m_2 m_3}{m_1 m_4}\right) \frac{\int_o^\infty P_B(E_T) \frac{v_3}{u_3} dv_3}{\int_o^\infty P_A(E_T) \frac{v_1}{u_1} dv_1}$$

where $N(m_i^+,\theta)$ is the total number of detected ion counts per laser shot from fragment $m_i$ at angle $\theta$, $\sigma_{ion}(m_i)$ is the ionization cross section, $v_i$ is the lab velocity, and $u_i$ is the c.m. velocity of the neutral $m_i$. The ionization cross sections were calculated as recommended in ref. 22, using data from the literature.[23] The integrals represent the expected signal at angle $\theta$ and were calculated numerically. Because MPD is isotropic (and the laser was unpolarized), there are no corrections for anisotropy.

Since data were collected at almost every mass, $N(m_i^+,\theta)$ for each fragment was calculated by adding up the total number of ion counts per shot for that fragment at 20°. Minor corrections for the few undetected ions were made by comparison with the methyl acetate data ($O^+$, $CHCO^+$) or with known cracking patterns[21] ($C_2H^+$). All of the data

used were obtained under exactly the same experimental conditions, most on the same day, so variations due to laser power, beam intensity, etc., should be minimal.

The ratio between ethylene and acetic acid produced should be unity in the absence of secondary dissociation since these are the two momentum-matched fragments from the same dissociation channel. Experimentally these ratios have been within 15% of the expected value for cases with no secondary decomposition occurring.[22,24] In this experiment the ratio was 3.02, indicating that 67% of the acetic acid decomposes. Since so much of the acetic acid decomposes, it is not surprising that the $P(E_T)$ derived for the surviving acetic acid differs from that of ethylene. The branching ratio between reactions (1) and (3) was calculated to be 33.5 using the data from ethylene and ethyl radical, neither of which undergo secondary decomposition. The fact that 97% of the reaction occurs through the concerted mechanism and only 3% by simple bond rupture explains why the latter channel has not been previously observed and may occur only with the relatively high laser intensities in this experiment or at very high temperatures in thermal studies.

Power dependence measurements were performed for both ethyl and methyl acetate to determine the intensity dependence of the branching ratios. Unfortunately, the main effect observed was a drastic reduction of signal, and within a factor of 2.7 decrease in laser power there was

little change in the branching ratios. As expected, the amount of simple bond rupture and secondary dissociation through reaction (2) decreased relative to reaction (1), but the effect was small.

B. Methyl Acetate- Signal from methyl acetate was observed at m/e = 13-16, 28-31, 41, 42, and 44, but not at m/e = 17, 32, 43, or 59. The results are summarized in Table II. As with ethyl acetate, two competing dissociation channels were observed. The large peak at mass 42 (shown in figure 9) was assigned as the parent ion from ketene produced in reaction (8) proceeding through a four-membered

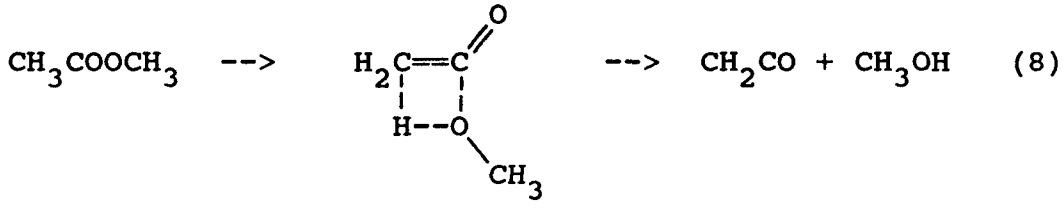


cyclic transition state. The momentum matched methanol fragment was measured at m/e = 31 and is also shown in figure 9. The absence of the parent ion of methanol is not surprising in light of the previous discussion. The $P(E_T)$ that fit both fragments peaks at 19 kcal/mol with an average translational energy release of 21.1 kcal/mol as shown in figure 10. There was no evidence for secondary dissociation of either fragment.

The signal at mass 44, shown in figure 11, top, was explained analogously to ethyl acetate using reactions (9) and (10). Primary decomposition occurs through the simple

$$CH_3COOCH_3 \rightarrow CH_3COO^{\cdot} + CH_3^{\cdot} \quad (9)$$

$$CH_3COO^{\cdot} \rightarrow CH_3^{\cdot} + CO_2 \quad (10)$$

bond rupture reaction to produce the acetoxyl radical and a methyl radical, then secondary dissociation produces $CO_2$ and a second methyl radical. The m/e = 14 TOF spectrum showing contributions from reactions (8), (9), and (10) is shown in figure 11, bottom.

In addition to the fast peaks from concerted dissociation observed at m/e = 31 and 42, there was a small amount of slower signal in both of these TOF spectra. This signal, which appears at roughly the same time in all the TOF spectra, may be due to dimers or a tiny fraction of the acetoxyl radicals which survive to the ionizer (as it is so attributed in figure 9). It could also be from another dissociation channel such as reaction (11) producing methoxy

$$CH_3COOCH_3 \rightarrow CH_3CO^{\cdot} + CH_3O^{\cdot} \quad (11)$$

and $CH_3CO$ radicals, as this channel is no more than 15 kcal/mol more endothermic than reaction (9) and could produce a small fraction of the total signal.[25] In any case this slow signal amounted to less than 1% of the total c.m. frame signal.

As with ethyl acetate, the methyl radical and $CO_2$ peaks

in the secondary dissociation data for the acetoxyl radical could be fit reasonably well by a single $P(E_T)$. However, signal from the fast methyl radical was noticeably narrower than would be predicted on the basis of the $CO_2$ data, indicating that simultaneous three-body dissociation is also occurring here. The RRKM-type $P(E_T)$ for reaction (9) peaks at zero and releases an average of 4.0 kcal/mol into translation. The $P(E_T)$ for reaction (10) peaks at 15 kcal/mol with an average release of 19 kcal/mol. Both $P(E_T)$'s are shown in figure 12. The fact that we observe essentially the same simple bond rupture channel followed by decomposition of the acetoxyl radical in both ethyl and methyl acetate is further evidence of the correct assignment of this channel.

Calculations similar to those for ethyl acetate were performed to determine the relative contributions of the two dissociation channels. The ratio between methanol and ketene produced in reaction (8) was very close to 1, as it should be since neither fragment undergoes secondary decomposition. In the decomposition of methyl acetate, the branching ratio between reaction (8) and simple bond rupture, reaction (9), determined from the slow methyl radical data, was 1.16, indicating that simple bond rupture accounts for almost half of the dissociation products, in sharp contrast to ethyl acetate. Since the energy release for reaction (9) is somewhat uncertain (a fairly wide range

of $P(E_T)$'s with the same general shape will fit the slow methyl radical data) the branching ratio was checked by using the signal from $CO_2$. The formula for the branching ratio changes slightly but is essentially the same as that used previously.[26] The advantage is that the shape of the c.m. $P(F_T)$ for the $CO_2$ alone is tightly constrained by the data and the TOF spectra used (at m/e = 16, 28, and 44) are largely uncontaminated by signal from other channels. The signal attributed to $CH_3CO_2$ was also included, but this affected the calculation by less than 1%. The results of this calculation gave a branching ratio of 1.12, in good agreement with the first calculation. The implications of this branching ratio on the barrier height for concerted reaction are discussed in the next section.

**Discussion**

A. Exit Barriers for Concerted Decomposition- RRKM theory is a widely used method for determining rate constants of unimolecular reactions.[27] Assuming randomization of internal energy, the unimolecular rate constant at an energy $E^*$ can be calculated as:

$$k(E^*) = L^{\ddagger} \frac{\sum_{E_{vr}^+=0}^{E^+} P(E_{vr}^+)}{hN^*(E^*)}$$

where the sum is over all rovibrational levels of the transition state up to $E^+$ (the excess energy over the

barrier) with some energy left in the reaction coordinate, $N^*(E^*)$ is the density of states of the molecule at a total energy $E^*$, and $L^\ddagger$ is the reaction path degeneracy. While this formula is valid for any reaction in the ground electronic state, for the case of reactions proceeding without an exit channel barrier (i.e., simple bond rupture reactions) it can be easily extended to predict the translational energy release of the two fragments at a given total energy. This is simply the amount of energy in the reaction coordinate at the transition state, and herein lies the reason that an "RRKM-type" $P(E_T)$ for simple bond rupture reactions peaks at zero and decreases roughly exponentially. Having a great deal of energy in one degree of freedom (the reaction coordinate) leaves little energy left over in the other degrees, and the number of possible rovibrational states at the transition state is low, thus the contribution to the sum of states is small. The largest contribution comes from those states with no energy in the reaction coordinate and quickly decreases with more energy partitioned into translation, as $P(E_{vr}^+)$ is a strongly increasing function of $E_{vr}^+$. In contrast, the $P(E_T)$ for concerted reactions is dominated by dynamical effects after the transition state, thus allowing the possibility of large translational energy releases.

We have previously used a further extension of RRKM theory to calculate dissociation barriers for concerted

reactions.[4] This method makes use of the RRKM rate constants for both channels, the branching ratio, and the $P(E_T)$ for the simple bond rupture channel. An MPD rate equation program[28] that models absorption, stimulated emission, and dissociation is used to integrate over the duration of the laser pulse and determine how high the molecules are pumped before they dissociate and the relative yield into competing dissociation channels. Since in reactions with no exit barrier, molecules dissociating from a higher level release a higher average amount of translational energy, the absorption cross-section (assumed constant with energy) is varied to match the predicted simple bond rupture $P(E_T)$ with the experimental one. This provides an internal measure of the energy in the ensemble of dissociating molecules. The barrier height for the competing concerted reaction channel is then varied to produce the correct branching ratio. This process is iterated until both the experimental $P(E_T)$ and the branching ratio are reproduced.

Rate constants and $P(E_T)$s were calculated with an RRKM program of Hase and Bunker.[29] The density of states was calculated from known vibrational frequencies of the ground state, obtained from the literature.[30] The transition state vibrational frequencies for calculating the sum of states were estimated by varying some of the ground state frequencies in the transition state in order to reproduce the correct Arrhenius preexponential A-factor. For the simple

bond fissions this was taken to be logA = 16, typical for such reactions,[7] for reaction (1) the literature value of 12.6 was used, and for reaction (8) we used logA = 13.9, in analogy to diethyl ether which also undergoes concerted decomposition through a $\overset{\frown}{C\text{-}C\text{-}O\text{-}H}$ four-center transition state to produce ethanol and ethylene.[31] All the kinetic parameters used and the calculated results are shown in Table III.

Using ethyl acetate as a test case with logA = 16.0 and a reaction barrier of 80.2 kcal/mol (simply the endothermicity of reaction) for simple bond rupture, logA = 12.6 for the concerted reaction (1), and a branching ratio of 33.5 in favor of reaction (1), an absorption cross-section of 7.0 x $10^{-20}$ $cm^2$ was required to give the $P(E_T)$ shown in figure 8. This leads to a reaction barrier of 50 kcal/mol for reaction (1). Converting this to an activation energy[4] gives a value of 49 kcal/mol at 900 K. This compares quite favorably with the recommended value of 48.0 kcal/mol in ref. 7 in that temperature range. An RRKM calculation by Beadle et al.,[32] using slightly different molecular parameters, gave almost identical rate constants for the concerted reaction. For methyl acetate, with logA = 16.0 and an activation barrier of 83.4 kcal/mol for the simple bond rupture reaction (9), logA = 13.9 for the concerted reaction (8), and a branching ratio of 1.16 in favor of concerted reaction, we derived a barrier height of 69 kcal/mol and an activation energy of 68 kcal/mol.

Although many approximations were made to derive this value, it is expected to be fairly accurate. This method worked well for ethyl acetate and two nitroalkanes.[4] The branching ratios here are well determined and should not contribute much error. The RRKM calculations are fortunately rather insensitive to the exact value of the vibrational frequencies as long as they reproduce the A-factors correctly. The main uncertainty lies in the kinetic data used, the value of the heat of formation of the acetoxyl radical and other species, and the exact shape of the simple bond rupture reaction $P(E_T)$. For the heat of formation of the acetoxyl radical, we used a value of -49.6 kcal/mol[33] with an uncertainty of ±1 kcal/mol. The slow methyl radical signal from reaction (8) merges into the signal from other channels near 220 μsec, so it is difficult to determine how far the $P(E_T)$ for the simple bond rupture channel in methyl acetate extends. The possible influence of three-body dissociation is another potential problem. The fact that the ethyl and methyl radical data from simple bond rupture can be fit with an RRKM type $P(E_T)$ and the fast methyl radicals and $CO_2$ can be fit reasonably well by assuming a sequential two-body dissociation mechanism argues that three-body effects are not very pronounced, but this point must be taken as an important caveat. We therefore assign a total uncertainty of ±3 kcal/mol to the value of 69 kcal/mol for the barrier to concerted decomposition in methyl

acetate. It is heartening to note however, that the activation energy for concerted decomposition of ethyl acetate (which suffers from the same problems) is well within this uncertainty when compared to ref. 7.

B. Dissociation Dynamics- In both ethyl and methyl acetate concerted reactions, a sizable amount of energy is released into translation as the two stable fragments repel each other. It is interesting to compare the translational energy release to the exit channel barrier (obtained by subtracting the endothermicity of the reaction from the activation barrier), which is the energy release after the transition state. For ethyl acetate, the exit barrier is 50.0 - 12.2 = 37.8 kcal/mol. With an average translational energy release of 21.7 kcal/mol for reaction (1), the fraction of the exit barrier appearing as product translational energy is 57%. Methyl acetate has an exit channel barrier of 69.0 - 37.6 = 31.4 kcal/mol and with an average energy release of 21.1 kcal/mol for reaction (8), 67% of the barrier appears in translation. In the secondary dissociation of acetic acid to give ketene and water through a four-center transition state, the exit barrier is about 35 kcal/mol, of which 68% becomes translational energy. The results of these and similar experiments have been tabulated elsewhere.[34]

Four- and six-center transition states with C, H, and O atoms typically have large translational energy releases,[34]

showing that the exit channel barrier couples strongly with translational rather than internal energy. The considerable excess internal energy above the activation barrier is distributed randomly and appears mostly as internal energy of the products as evidenced by the relatively small translational energy release in reactions (3) and (9) and other simple bond rupture reactions, which have no exit channel barrier. The large translational energy release from these four- and six-center transition states reflects the fact that the transition state occurs "late" on the potential energy surface, and strongly resembles the products. After the transition state, the closed-shell products, already close to their equilibrium geometries, experience a strong repulsion due to their overlapping electron clouds, giving rise to the large translational energy release. With a simple "soft fragment" impulse approximation[35] where energy is partitioned between translation and vibration, if an O and an H atom recoil off two C atoms (as occurs in the transition states of both reactions (1) and (8)), 52% of the exit channel barrier is predicted to appear in translation for the concerted dissociation of ethyl acetate, and 55% for methyl acetate. If the H atom is transferred far from its equilibrium geometry and feels little repulsion, so that the recoil is only between an O atom and a C atom, these numbers drop to 36% and 38% respectively. Including the effects of rotation (difficult

to model quantitatively as neither the transition state geometry nor the relative forces between the C-O and C-H pairs are known) would leave even less energy in translation. The fact that significantly more energy is released to translation is further evidence that the fragments are fairly "stiff" as they recoil down the exit channel, and behave as two closed-shell fragments which repel each other rather than only the nearest four atoms. In contrast, for an "early" barrier, the transition state more closely resembles the reactants, the products are formed far from their equilibrium geometries, and as they relax from the transition state this strain energy becomes product internal excitation, as apparently occurs with four-center HCl eliminations.[34]

One surprising result was the large amount of translational energy imparted to the dissociation products of the acetoxyl radical in reactions (4) and (10). Since the central carbon atom (which ends up in $CO_2$) changes its hybridization during the reaction, there should be some exit channel barrier, but ref. 20 suggests that it is not much greater than the exothermicity of ~10 kcal/mol. We can think of no convincing reason why more than twice this energy should end up in translation. Another question was why the ethyl or methyl radical from reaction (3) or (9) is so slow if three-body dissociation were occurring. A possible explanation is that in ethyl acetate, concerted

reaction occurs when the parent molecule has a geometry similar to the transition state for reaction (1). Simple bond rupture might occur only from geometries with the $C_2H_5$ and $CH_3$ moieties on the same side as shown here:

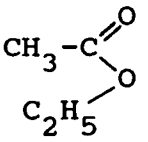

Then the $C_2H_5$ $P(E_T)$ would not be significantly altered from an RRKM-type exponentially decaying function, but the $CO_2$ would receive an added little "kick" that would account for its faster than expected translational energy distribution. An analogous process could also be occurring in methyl acetate.

C. Comparison with Previous Results- In both ethyl and methyl acetate decomposition, competition was observed between concerted reaction and simple bond rupture. The branching ratios between the channels shed new light on previous experiments. Concerted reaction (1) has long been known to be the dominant thermal decomposition pathway for ethyl acetate.[7] The competing simple bond rupture channel was probably too minor to have been observed before. The relatively high laser fluences used in these experiments favor simple bond rupture, and our higher sensitivity to slow products allowed us to detect this channel for the first time.

For methyl acetate, the concerted reaction has an activation barrier of ~69 kcal/mol, while simple bond

rupture is ~83 kcal/mol endothermic. Thus, at low temperatures the number of molecules with enough energy to react is small, and most of these have less than 83 kcal/mol, where they can only undergo concerted reaction. Much of Gil'burd and Moin's[11] reaction products are in fact due to unimolecular decomposition through reactions (8-10). Carlsen et al. observed only the concerted reaction,[12] finding no evidence for any $CH_3CO_2$ or $CO_2$ production. At high temperatures, the A-factors determine the relative rates of reaction, thus favoring simple bond rupture which proceeds through a loose transition state and consequently a high A-factor. In Sulzmann et al.'s shock tube experiments, which started at temperatures only slightly higher (1425 K) than the highest in ref. 12 (1404 K), only $CO_2$ and methyl radicals were observed.[13] There are two possible problems with this experiment. The initial (nonequilibrium) shock wave excitation may have produced molecules with an average energy far higher than a temperature of 1425 K would suggest, thus strongly favoring the radical channel. Also, though mass balance was claimed between methyl acetate and both $CH_3$ and $CO_2$, other channels were not explicitly monitored. With our kinetic parameters or those from ref. 13, the rates for the two channels should have been within a factor of 2 near 1400 K. At our intermediate to high energies we saw both channels in about equal amounts, indicating that methyl acetate is probably not a very good

source of methyl radicals except at very high temperatures. Furthermore, our experiments indicate that the radical channel is primarily a sequential reaction, with half the methyl radicals being produced translationally cold and half being produced translationally hot, so the use of methyl acetate as a source of methyl radicals for methyl radical reactions should be treated cautiously.

A recent MNDO and MNDO/CI calculation found a barrier of 93-96 kcal/mol for the concerted reaction of methyl acetate.[36] Since this would virtually eliminate any ketene and methanol formation compared to simple bond rupture, it is likely that the calculation overestimated the energy of the transition state.

**Conclusions**

We have observed competing primary and secondary dissociation channels in the IRMPD of ethyl and methyl acetate. In ethyl acetate, the dominant channel was concerted reaction to give acetic acid and ethylene, with small amounts of simple bond rupture producing acetoxyl and ethyl radicals. The acetic acid underwent significant secondary decomposition, producing ketene and water. Methyl acetate underwent concerted decomposition forming methanol and ketene, and simple bond rupture forming acetoxyl and methyl radicals, in about equal amounts. All the concerted reactions involved O and H atoms recoiling off of C atoms

and released an average of about 20 kcal/mol into translation. Essentially all the acetoxyl radicals underwent secondary decomposition to give $CH_3$ and $CO_2$ with a surprisingly large release of translational energy.

Using an MPD rate equation model, the activation barrier for the concerted reaction of methyl acetate was determined to be 69 ± 3 kcal/mol assuming an endothermicity of 83.4 kcal/mol for simple bond rupture. All of the concerted reactions (1, 2, and 8) where an H atom is transferred in a cyclic transition state released about 60% of the exit channel barrier into translational energy. This was interpreted in terms of a late transition state after which the closed-shell products, formed close to their equilibrium geometries, strongly repel each other.

**References**

1. D. S. King, "Infrared Multiphoton Excitation and Dissociation", in **Dynamics of the Excited State**, K. P. Lawley, Ed. (Wiley, New York, 1982); V. S. Letokhov, **Nonlinear Laser Chemistry** (Springer-Verlag, Berlin, 1983).

2. I. Oref and B. S. Rabinovitch, Acc. Chem. Res. **12**, 166 (1979); M. J. Coggiola, P. A. Schulz, Y. T. Lee, and Y. R. Shen, Phys. Rev. Lett. **38**, 17 (1977).

3. Aa. S. Sudbø, P. A. Schulz, Y. R. Shen, and Y. T. Lee, J. Chem. Phys. **69**, 2312 (1978); Aa. S. Sudbø, P. A. Schulz, E. R. Grant, Y. R. Shen, and Y. T. Lee, J. Chem. Phys. **70**, 912 (1979); F. Huisken, D. Krajnovich, Z. Zhang, Y. R. Shen, and Y. T. Lee, J. Chem. Phys. **78**, 3806 (1983).

4. A. M. Wodtke, E. J. Hintsa and Y. T. Lee, J. Phys. Chem. **90**, 3549 (1986).

5. P. A. Schulz, Aa. S. Sudbø, D. J. Krajnovich, H. S. Kwok, Y. R. Shen, and Y. T. Lee, Annu. Rev. Phys. Chem. **30**, 379 (1979).

6. A. M. Wodtke, E. J. Hintsa, and Y. T. Lee, J. Chem. Phys. **84**, 1044 (1986).

7. S. W. Benson and H. E. O'Neal, **Kinetic Data on Gas Phase Unimolecular Reactions** (NSRDS-NBS **21**, U. S. Dept. of Commerce, Washington, DC, 1970) and refs. therein.

8. W. C. Danen, W. D. Munslow, and D. W. Setser, J. Am. Chem. Soc. **99**, 6961 (1977); R. B. Knott and A. W. Pryor, J. Chem. Phys. **71**, 2946 (1979).

9. D. Gutman, W. Braun, and W. Tsang, J. Chem. Phys. **67**, 4291 (1977).

10. T. Wolf and D. M. Rosie, Anal. Chem. **39**, 725 (1967).

11. M. M. Gil'burd and F. B. Moin, Kinet. Katal. **13**, 836 (1972).

12. L. Carlsen, H. Egsgaard, and P. Pagsberg, J. Chem. Soc. Perkin Trans. II, 1256 (1981).

13. K. G. P. Sulzmann, D. E. Baxter, M. Khazra, and T. S. Lund, J. Phys. Chem. **89**, 3561 (1985).

14. A. M. Wodtke and Y. T. Lee, J. Phys. Chem. **89**, 4744 (1985).

15. A. M. Wodtke, Ph.D. Thesis, University of California, Berkeley, 1986.

16. X. Zhao, Ph.D. Thesis, University of California, Berkeley, 1988.

17. Y. T. Lee, "Reactive Scattering: Non-optical Methods", in **Atomic and Molecular Beam Methods**, G. Scoles and U. Buck, Eds. (Oxford University Press, New York, 1988) and refs. therein.

18. Unpublished results and A. J. Grimley and J. C. Stephenson, J. Chem. Phys. **74**, 447 (1981).

19. C. H. Bamford and M. J. S. Dewar, J. Chem. Soc., 2877 (1949).

20. S. D. Peyerimhoff, P. S. Skell, D. D. May, and R. J. Buenker, J. Am. Chem. Soc. **104**, 4515 (1982).

21. E. Stenhagen, S. Abrahamsson, and F. W. McLafferty, **Atlas of Mass Spectral Data** (Wiley, New York, 1969).

22. D. Krajnovich, F. Huisken, Z. Zhang, Y. R. Shen, and Y. T. Lee, J. Chem. Phys. **77**, 5977 (1982); D. Krajnovich, Ph.D. Thesis, University of California, Berkeley, 1983.

23. T. M. Miller and B. Bederson, Adv. At. Mol. Phys. **13**, 1 (1977).

24. L. J. Butler, Ph.D. Thesis, University of California, Berkeley, 1985, and unpublished results.

25. The difference between ethyl and methyl acetate is that methyl acetate has no low energy concerted reaction channel, almost half the molecules undergo simple bond rupture, and a "small fraction" of this signal in another channel should be easily visible. In contrast, for ethyl acetate only 3% of the molecules undergo simple bond rupture, and a small fraction of this will be virtually undetectable.

26. The mass weighting factor becomes $Mm_3/m_1m_4$ instead of $m_2m_3/m_1m_4$, where $m_1$ is the mass of the single fragment and M is the mass of the reactant molecule.

27. P. J. Robinson and K. A. Holbrook, **Unimolecular Reactions** (Wiley, New York, 1972).

28. P. A. Schulz, Ph.D. Thesis, University of California, Berkeley, 1979.

29. Available from Quantum Chemistry Program Exchange, Department of Chemistry, University of Indiana, # QCPE-234.

30. T. Shimanouchi, **Tables of Molecular Vibrational Frequencies** (NSRDS-NBS **39**, U. S. Dept. of Commerce, Washington, DC, 1972); B. Nolin and R. N. Jones, Can. J. Chem. **34**, 1392 (1956); J. J. Lucier and F. F. Bentley, Spectrochim. Acta **20**, 1 (1964); M. A. Raso, M. V. Garcia and J. Morcillo, J. Mol. Struct. **115**, 449 (1984).

31. L. J. Butler, R. J. Buss, R. J. Brudzynski, and Y. T. Lee, J. Phys. Chem. **87**, 5106 (1983); I. Seres and P. Huhn, Magy. Kem. Foly. **81**, 120 (1975).

32. P. C. Beadle, D. M. Golden, and S. W. Benson, Int. J. Chem. Kinet. **4**, 265 (1972).

33. D. F. McMillen and D. M. Golden, Annu. Rev. Phys. Chem. **33**, 493 (1982); H. E. O'Neal and S. W. Benson in **Free Radicals**, vol. II, J. Kochi, Ed. (Wiley, New York, 1973).

34. A. M. Wodtke and Y. T. Lee in **Advances in Gas Phase Photochemistry and Kinetics**, J. Baggott and M. Ashfold, Eds. (Royal Society of Chemistry, London, 1987).

35. G. E. Busch and K. R. Wilson, J. Chem. Phys. **56**, 3626 (1972).

36. C. B. Lebrilla and H. Schwarz, J. Chem. Soc. Perkin Trans. II, 237 (1987).

**Table I: MASS SPECTRUM OF IRMPD FRAGMENTS OF $CH_3COOC_2H_5$**

| Detected ion mass | Neutral fragment | Intensity[a] | Reaction channel | Figure |
|---|---|---|---|---|
| 59 | $CH_3COOH$ | 0.013 | 1 | |
| 45 | $CH_3COOH$ | 0.325 | 1 | 3 |
| 44 | $CH_3COOH$ | 0.049 | 1 | 7 |
| | $CO_2$ | 0.065 | 4 | |
| 43 | $CH_3COOH$ | 0.402 | 1 | |
| 42 | $CH_3COOH$ | 0.043 | 1 | 5 |
| | $CH_2CO$ | 0.068 | 2 | |
| 31 | $CH_3COOH$ | 0.030 | 1 | |
| 30 | $CH_3COOH$ | 0.001 | 1 | |
| 29 | $CH_3COOH$ | 0.193 | 1 | |
| | $CH_2CO$ | 0.059 | 2 | 8 |
| | $C_2H_5$ | 0.063 | 3 | |
| 28 | $CH_3COOH$ | 0.229 | 1 | |
| | $C_2H_4$ | 0.446 | 1 | |
| | $C_2H_5$ | 0.078 | 3 | |
| | $CO_2$ | 0.101 | 4 | |
| 27 | $C_2H_4$ | 0.680 | 1 | |
| | $C_2H_5$ | 0.015 | 3 | |
| 26 | $C_2H_4$ | 0.255 | 1 | 3 |
| | $C_2H_5$ | 0.014 | 3 | |
| 18 | $H_2O$ | 0.105 | 2 | 5 |

**Table I** (cont.)

| | | | | |
|---|---|---|---|---|
| 17 | $CH_3COOH$ | 0.063 | 1 | |
| | $H_2O$ | 0.027 | 2 | |
| 15 | $CH_3COOH$ | 0.748 | 1 | |
| | $C_2H_5$ | 0.050 | 3 | 7 |
| | $CH_3$ | 0.067 | 4 | |
| 14 | $CH_3COOH$ | 0.196 | 1 | |
| | $C_2H_4$ | 0.067 | 1 | |
| | $CH_2CO$ | 0.249 | 2 | |
| | $C_2H_5$ | 0.040 | 3 | |
| | $CH_3$ | 0.020 | 4 | |
| 13 | $CH_3COOH$ | 0.131 | 1 | |
| | $C_2H_4$ | 0.030 | 1 | |
| | $CH_2CO$ | 0.041 | 2 | |
| | $C_2H_5$ | 0.029 | 3 | |
| | $CH_3$ | 0.009 | 4 | |

[a]Ions/laser pulse at 20°.

**Table II: MASS SPECTRUM OF IRMPD FRAGMENTS OF $CH_3COOCH_3$**

| Detected ion mass | Neutral fragment | Intensity[a] | Reaction channel | Figure |
|---|---|---|---|---|
| 44 | $CO_2$ | 0.571 | 10 | 11 |
| 42 | $CH_2CO$ | 0.083 | 8 | 9 |
| 41 | $CH_2CO$ | 0.055 | 8 | |
| 31 | $CH_3OH$ | 0.104 | 8 | 9 |
| 30 | $CH_3OH$ | 0.015 | 8 | |
| 29 | $CH_2CO$ | 0.031 | 8 | |
| | $CH_3OH$ | 0.070 | 8 | |
| 28 | $CH_2CO$ | 0.080 | 8 | |
| | $CO_2$ | 0.297 | 10 | |
| 16 | $CO_2$ | 0.126 | 10 | |
| 15 | $CH_3OH$ | 0.109 | 8 | |
| | $CH_3$ (primary) | 0.339 | 9 | |
| | $CH_3$ (secondary) | 0.301 | 10 | |
| 14 | $CH_2CO$ | 0.281 | 8 | |
| | $CH_3OH$ | 0.012 | 8 | 11 |
| | $CH_3$ (primary) | 0.394 | 9 | |
| | $CH_3$ (secondary) | 0.159 | 10 | |
| 13 | $CH_2CO$ | 0.038 | 8 | |
| | $CH_3OH$ | 0.003 | 8 | |
| | $CH_3$ (primary) | 0.053 | 9 | |
| | $CH_3$ (secondary) | 0.023 | 10 | |

[a]Ions/laser pulse at 20°.

**Table III: DATA USED FOR REACTION BARRIER CALCULATIONS**

| Reaction channel | logA | $E_A$ (kcal/mol) | Simple bond rupture $P(E_T)$ used | Reaction barrier (kcal/mol) |
|---|---|---|---|---|
| Ethyl acetate | | | | |
| Simple bond rupture | 16[a] | | fig. 8 | 80.2[b] |
| Concerted | 12.6[a] | 49[c] | | 50[c] |
| Methyl acetate | | | | |
| Simple bond rupture | 16[a] | | fig. 12 | 83.4[b] |
| Concerted | 13.9[d] | 68[c] | | 69[c] |

[a]Ref. 7.

[b]Calculated using $\Delta H_f^o(CH_3COOC_2H_5)$ = -103.4 kcal/mol, $\Delta H_f^o(CH_3CO_2)$ = -49.7 kcal/mol, $\Delta H_f^o(C_2H_5)$ = 26.5 kcal/mol, $\Delta H_f^o(CH_3COOCH_3)$ = -98.0 kcal/mol, and $\Delta H_f^o(CH_3)$ = 35.1 kcal/mol, taken from refs. 7 and 33, and S. W. Benson, **Thermochemical Kinetics** (Wiley, New York, 1976).

[c]Determined in this study.

[d]In analogy to diethyl ether; see text.

**Figure Captions**

Fig. 1. Energy level diagram showing possible dissociation channels for ethyl acetate. The activation energy for the previously observed channel producing acetic acid and ethylene and all heats of formation were taken from refs. 7 and 33, and S. W. Benson, **Thermochemical Kinetics** (Wiley, New York, 1976). Both primary channels that we observed are shown as dashed lines.

Fig. 2. Energy level diagram for methyl acetate, similar to fig. 1.

Fig. 3. TOF spectra of products from reaction (1) at 20°. Data points are represented by open circles in the TOF spectra throughout this paper. Top: ethylene measured at m/e = 26. The large peak is fit by the corresponding $P(E_T)$ shown in fig. 4. The small, slow signal is from $C_2H_5$ produced in reaction (3). Bottom: acetic acid measured at m/e = 45, fit with a solid line using the lower $P(E_T)$ in fig. 4. The data points and the fit have been lowered to represent the extensive depletion of acetic acid through reaction (2). The dashed line shows an attempt to fit the m/e = 45 spectrum with the $P(E_T)$ derived from the ethylene data. The "missing" signal corresponds to acetic acid which has undergone secondary decomposition. Read the

text carefully.

Fig. 4. $P(E_T)$ for reaction (1) derived from the data in fig. 3. The solid line shows the $P(E_T)$ derived from the signal due to ethylene. The lower dashed line shows the $P(E_T)$ derived from acetic acid. The crosshatched area represents the acetic acid that underwent secondary decomposition, and was used as the primary $P(E_T)$ for reaction (2). See text.

Fig. 5. TOF spectra of products from reaction (2) at 20°. Top: $CH_2CO^+$ from ketene (-·-), and signal from acetic acid (---) from reaction (1). Bottom: $H_2O^+$ from water. Fits to the data are from the $P(E_T)$ shown in fig. 6.

Fig. 6. $P(E_T)$ for reaction (2), the secondary decomposition of acetic acid to give ketene and water, derived from the data shown in fig. 5.

Fig. 7. TOF spectra of m/e = 15 and 44 at 20°. Top: methyl radical from reaction (4) (-·-, fast), ethylene from reaction (1) (-···-), acetic acid from reaction (1) (---), and ethyl radical from reaction (3) (···, slow). Bottom: $CO_2$ from reaction (4) (-·-) and acetic acid (---).

Fig. 8. Top: TOF spectrum of m/e = 29 at 10° showing ketene from reaction (2) (-·-), acetic acid from reaction (1) (---), and ethyl radical from

reaction (3) (····) fit with the $P(E_T)$ shown below. Bottom: $P(E_T)$ for the simple bond rupture reaction (3).

Fig. 9. TOF spectra of the products of reaction (8) at 20°. The large peaks are from ketene (m/e = 42) and methanol (m/e = 31), fit with the $P(E_T)$ shown in fig. 10. The small, slow peaks may be due to surviving acetoxyl radical from reaction (9), and can be fit with the $P(E_T)$ shown in fig. 12, top.

Fig. 10. $P(E_T)$ for reaction (8), derived from the data shown in fig. 9.

Fig. 11. TOF spectra from MPD of methyl acetate at 20°. Top: $CO_2$ from reaction (10) (-··-) and possible surviving acetoxyl radical from reaction (9) (···). The fits to the data from reactions (9) and (10) are from the $P(E_T)$'s shown in fig. 12. Bottom, $CH_2^+$ due to fast methyl radical from reaction (10) (-··-), methanol (-····-) and ketene (---) from reaction (8), and slow methyl radical from reaction (9) (···).

Fig. 12. $P(E_T)$'s for reaction (9), (top), and (10), (bottom), derived in part from data shown in fig. 11.

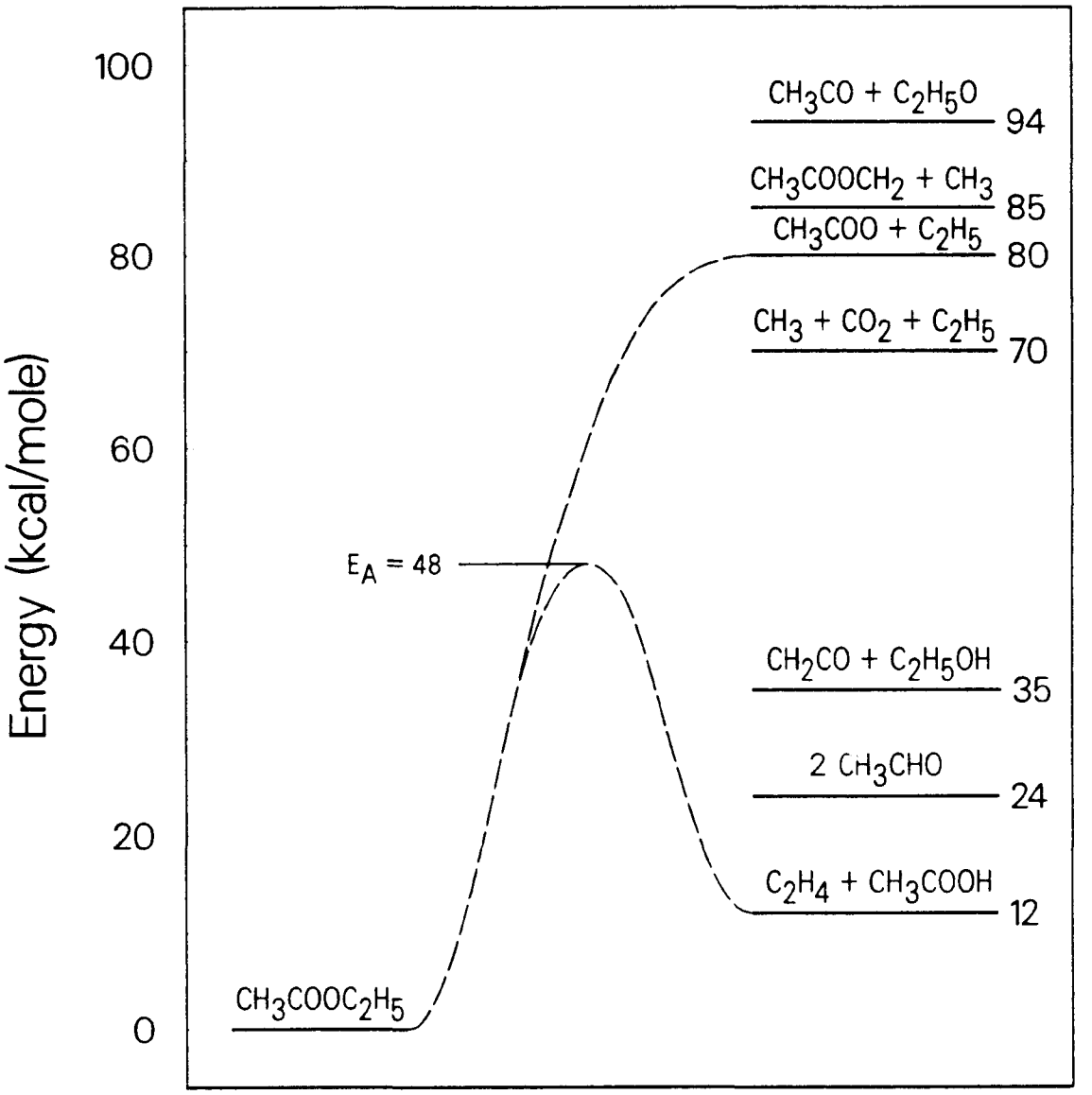


XBL 8711-4548

Figure 1

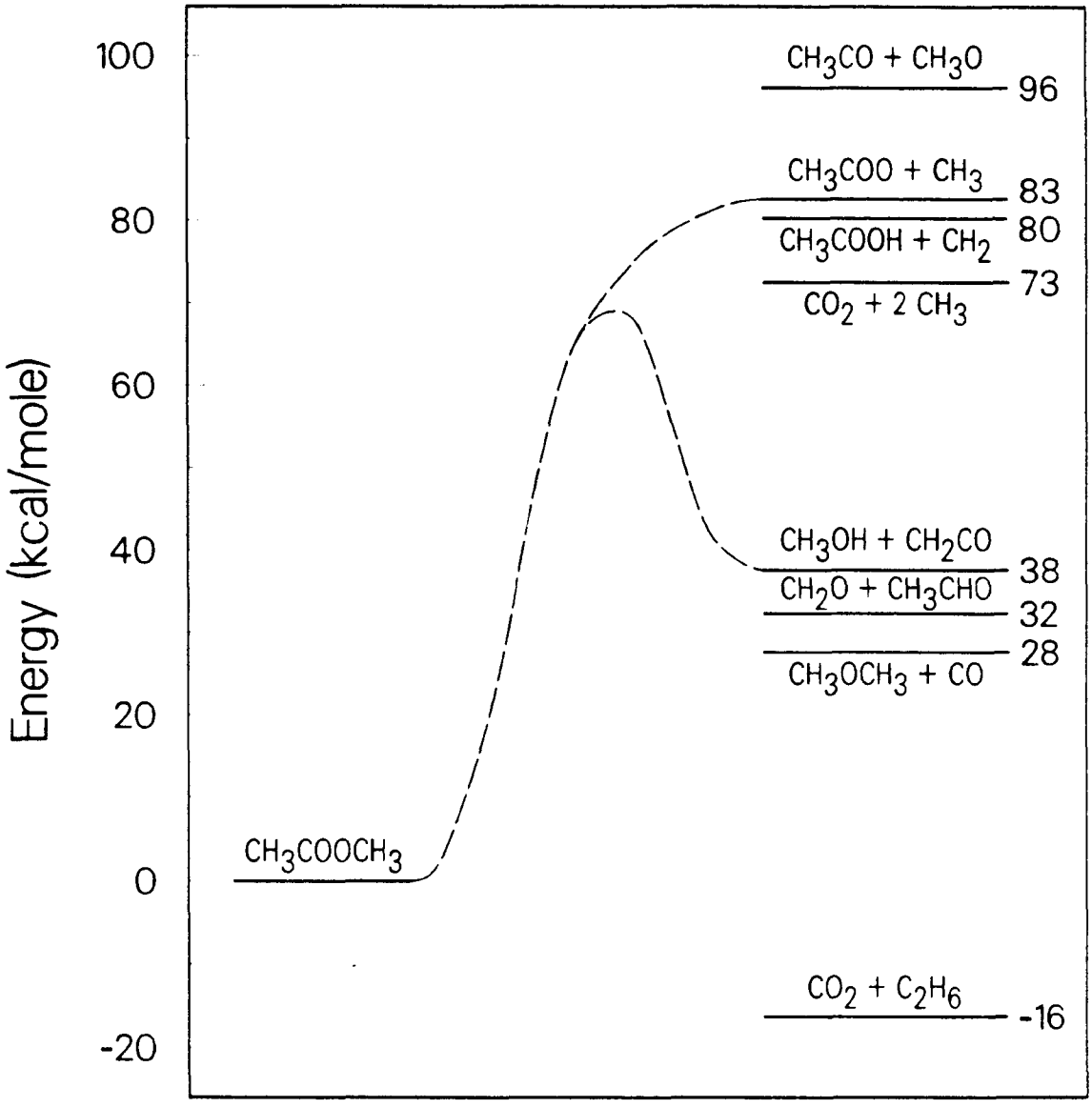
Energy (kcal/mole)
100
80
60
40
20
0
-20
$CH_3CO + CH_3O$
96
$CH_3COO + CH_3$
83
$CH_3COOH + CH_2$
80
$CO_2 + 2\ CH_3$
73
$CH_3OH + CH_2CO$
38
$CH_2O + CH_3CHO$
32
$CH_3OCH_3 + CO$
28
$CH_3COOCH_3$
$CO_2 + C_2H_6$
-16
XBL 8711-4549

Figure 2

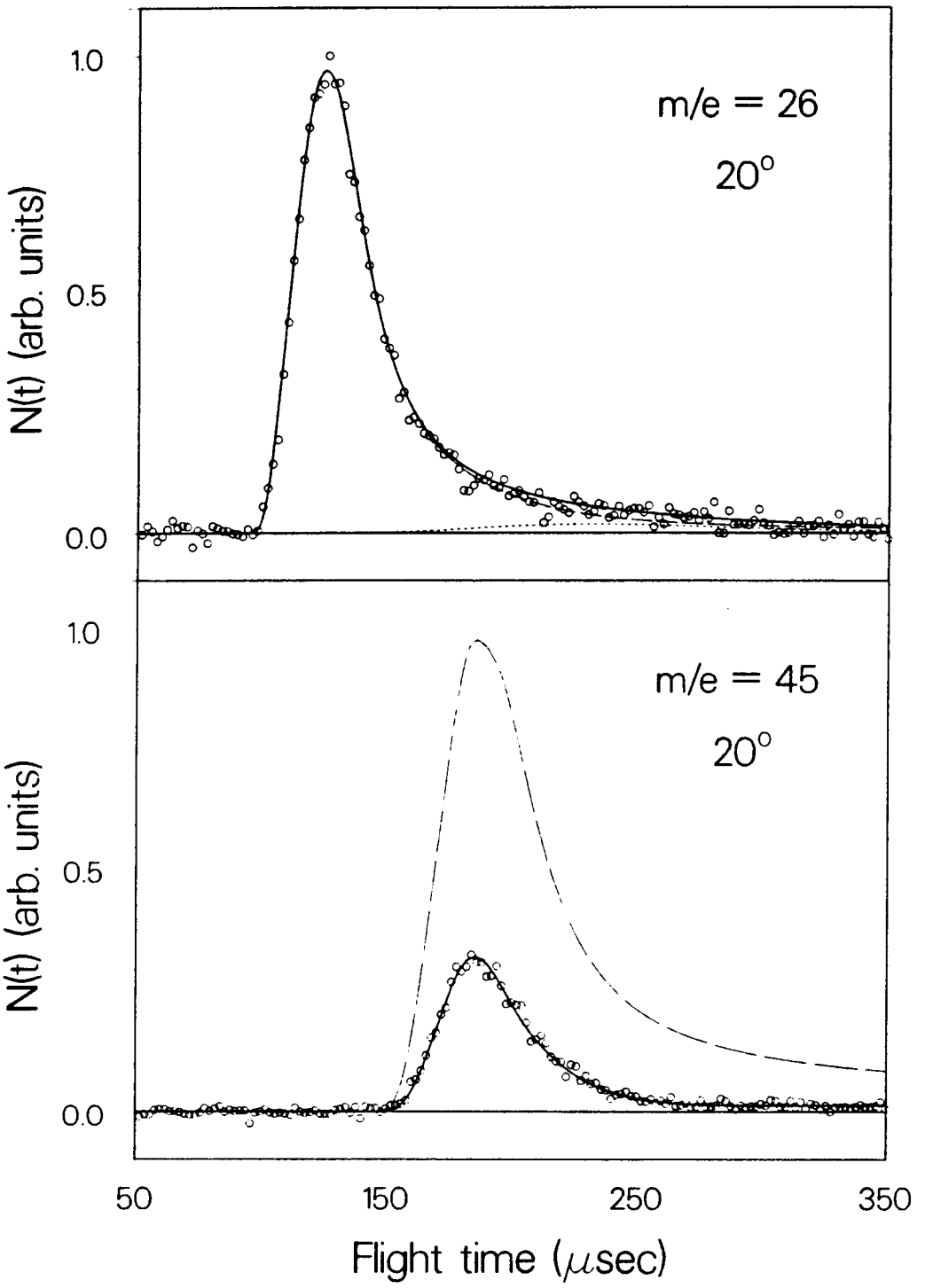


XBL 8711-4541

**Figure 3**

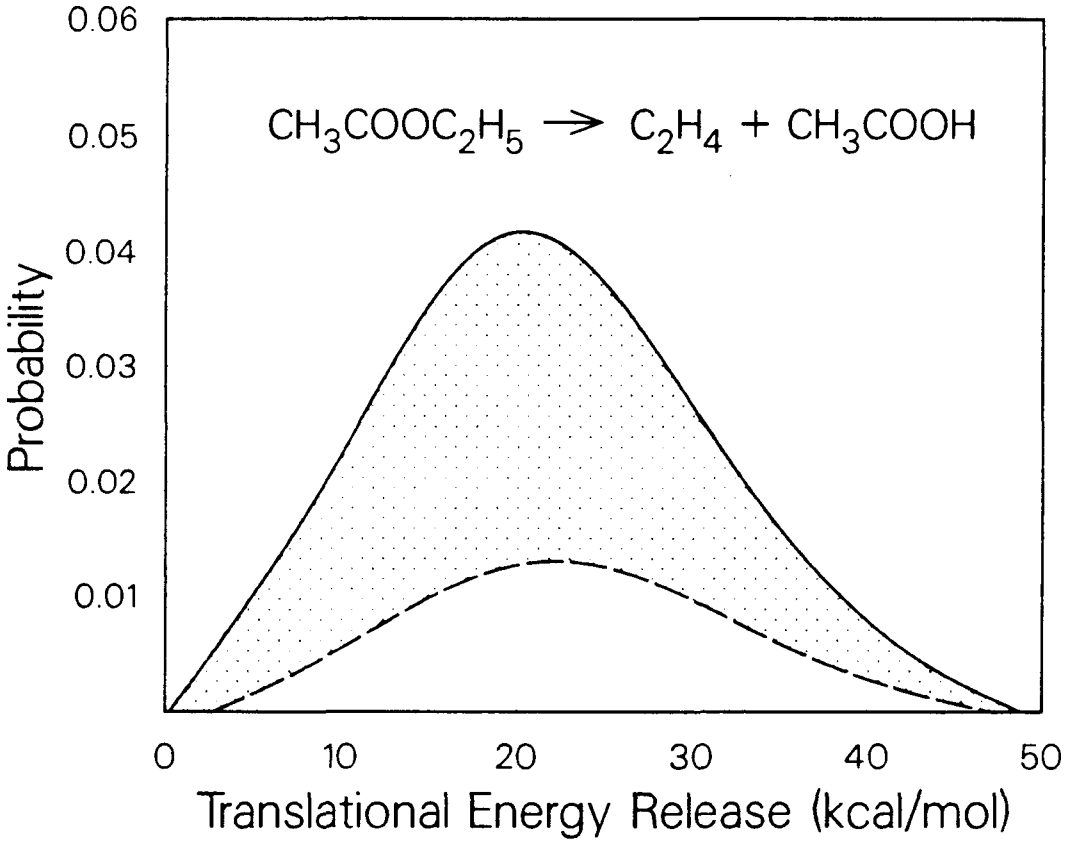
0.06
0.05
0.04
0.03
0.02
0.01
Probability
$CH_3COOC_2H_5 \rightarrow C_2H_4 + CH_3COOH$
0
10
20
30
40
50
Translational Energy Release (kcal/mol)
XBL 8711-4550

Figure 4

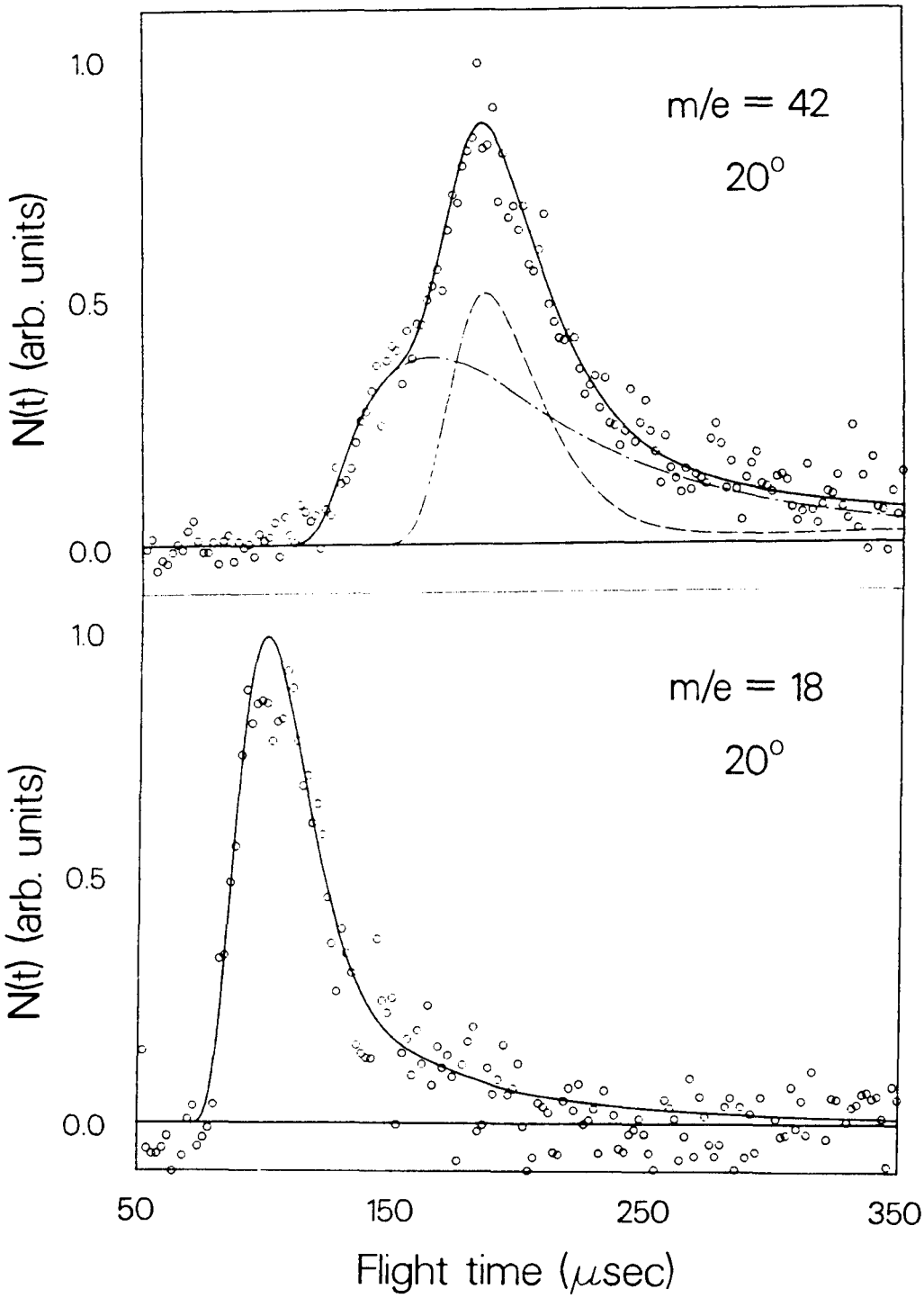


XBL 8711-4542

**Figure 5**

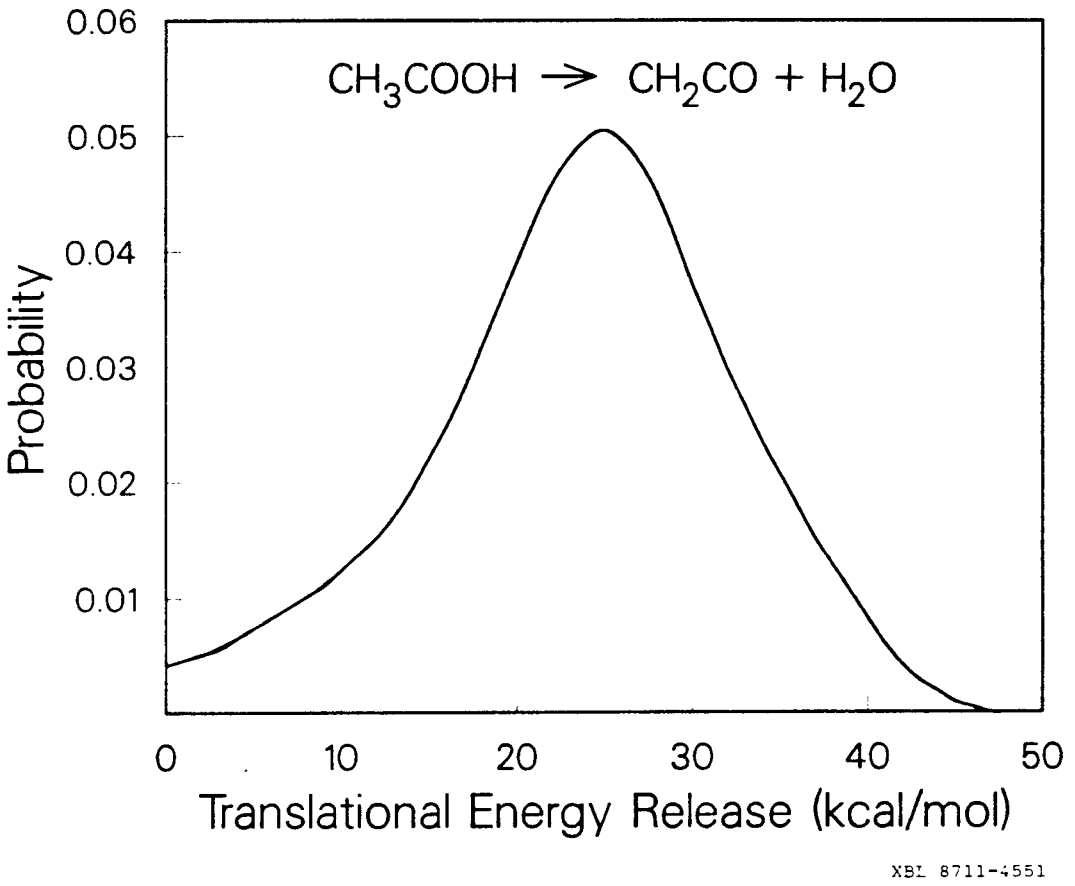
$CH_3COOH \rightarrow CH_2CO + H_2O$
Probability
0.06
0.05
0.04
0.03
0.02
0.01
0
10
20
30
40
50
Translational Energy Release (kcal/mol)
XBL 8711-4551

Figure 6

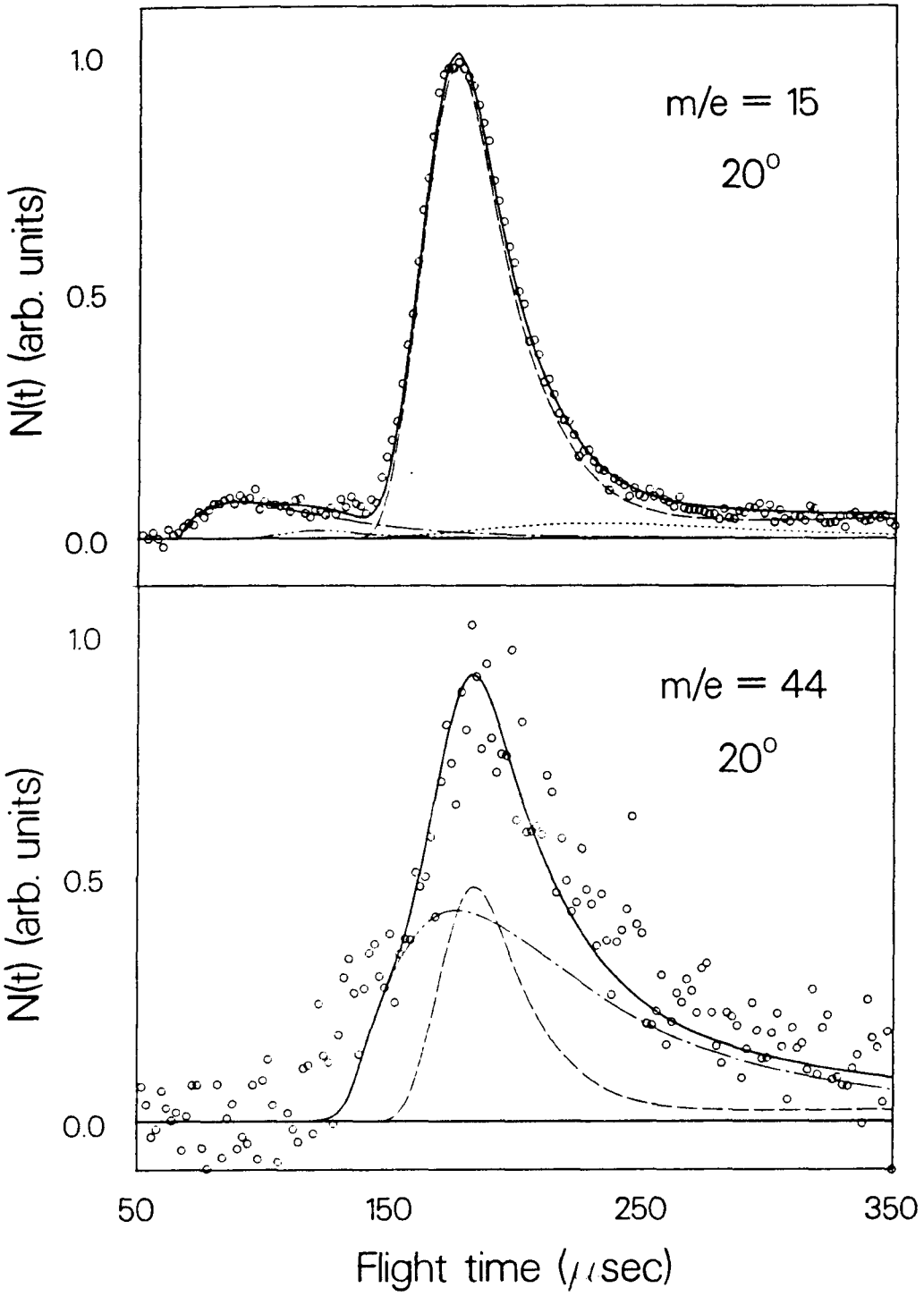
1.0
0.5
0.0
N(t) (arb. units)
m/e = 15
20°
1.0
0.5
0.0
N(t) (arb. units)
m/e = 44
20°
50
150
250
350
Flight time (μsec)
XBL 8711-4543

**Figure 7**

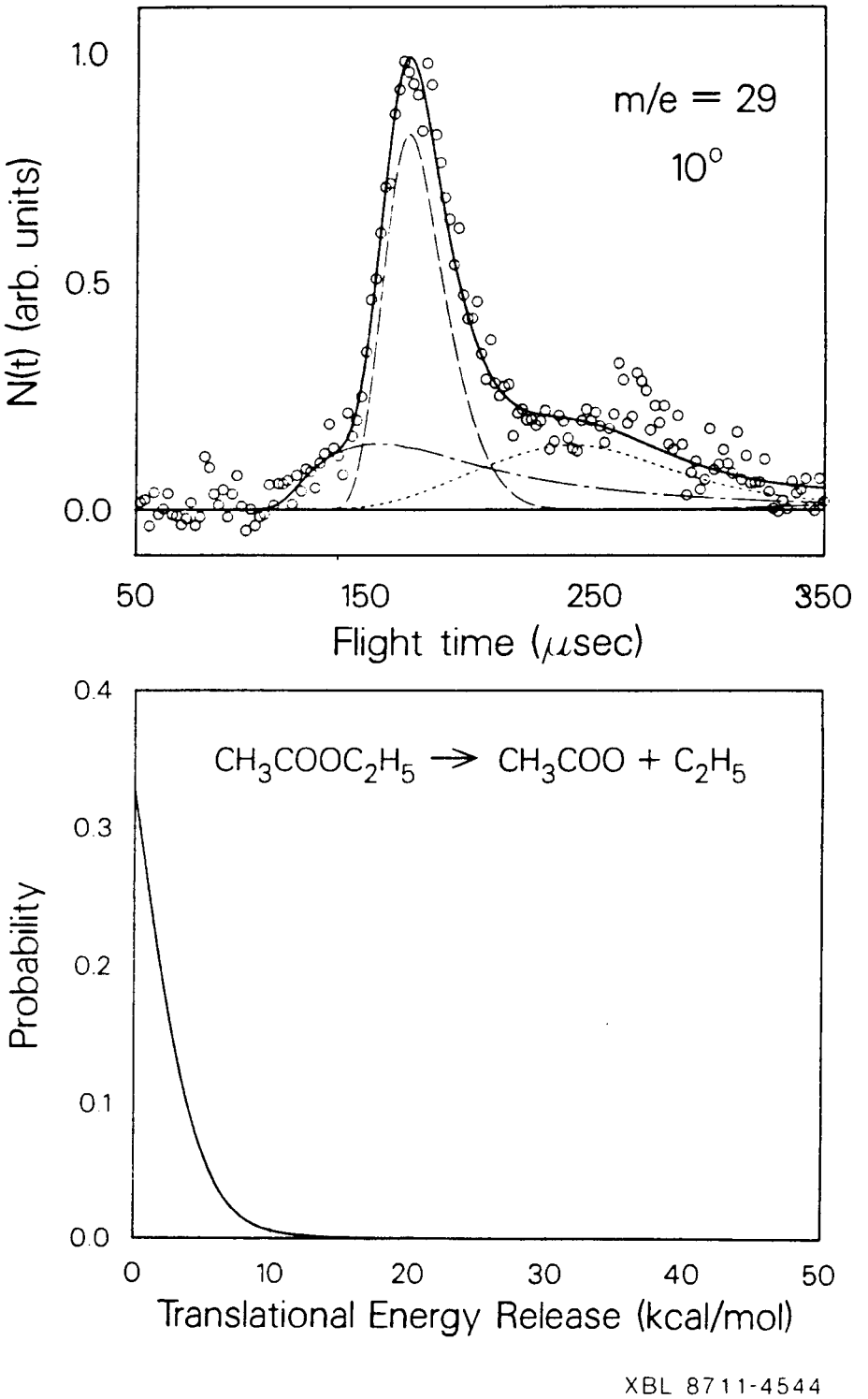
1.0
0.5
0.0
N(t) (arb. units)
m/e = 29
10°
50
150
250
350
Flight time (μsec)
0.4
0.3
0.2
0.1
0.0
Probability
CH3COOC2H5 → CH3COO + C2H5
0
10
20
30
40
50
Translational Energy Release (kcal/mol)
XBL 8711-4544

Figure 8

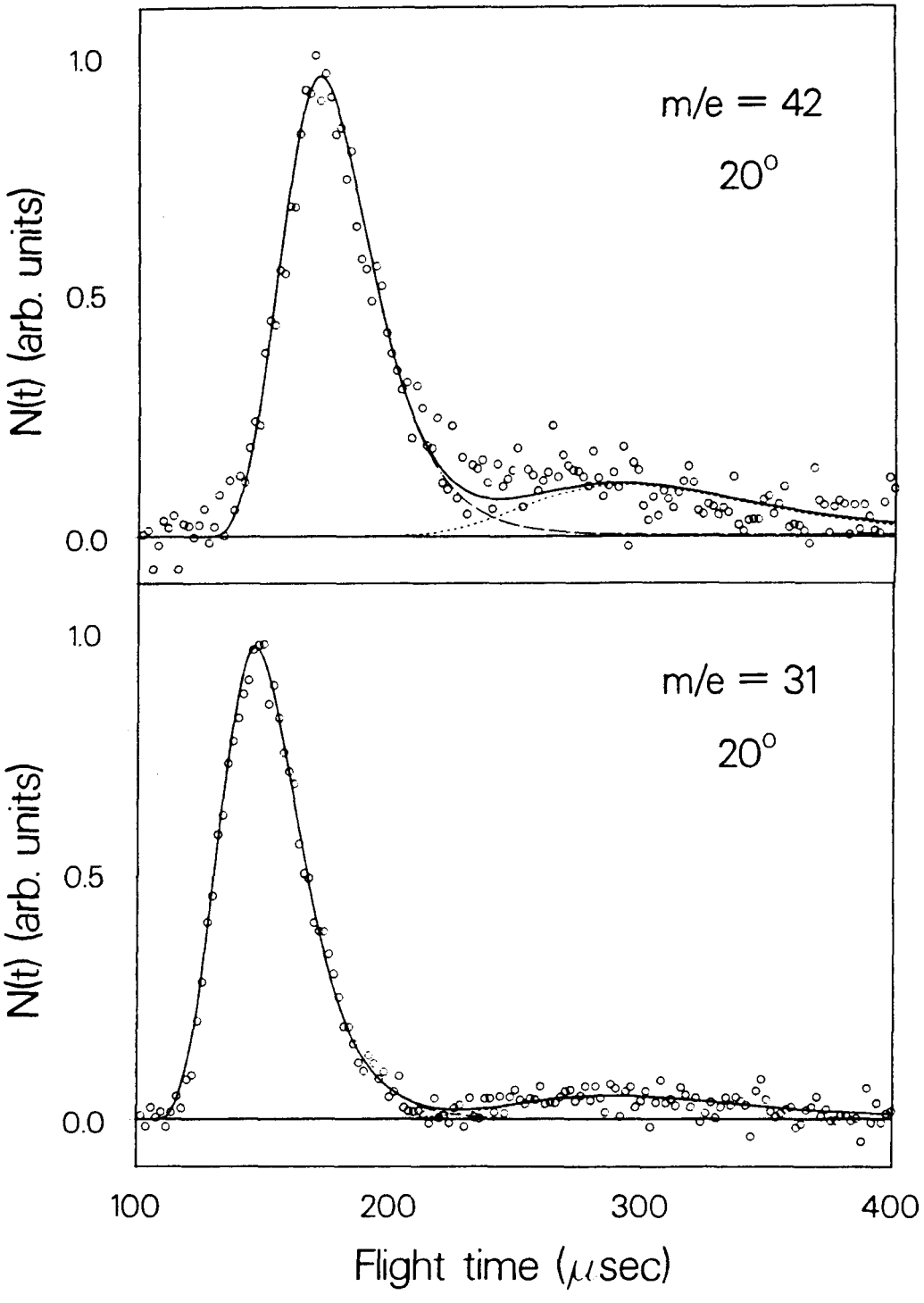
1.0
0.5
0.0
N(t) (arb. units)
m/e = 42
20°
1.0
0.5
0.0
N(t) (arb. units)
m/e = 31
20°
100
200
300
400
Flight time (μsec)
XBL 8711-4545

**Figure 9**

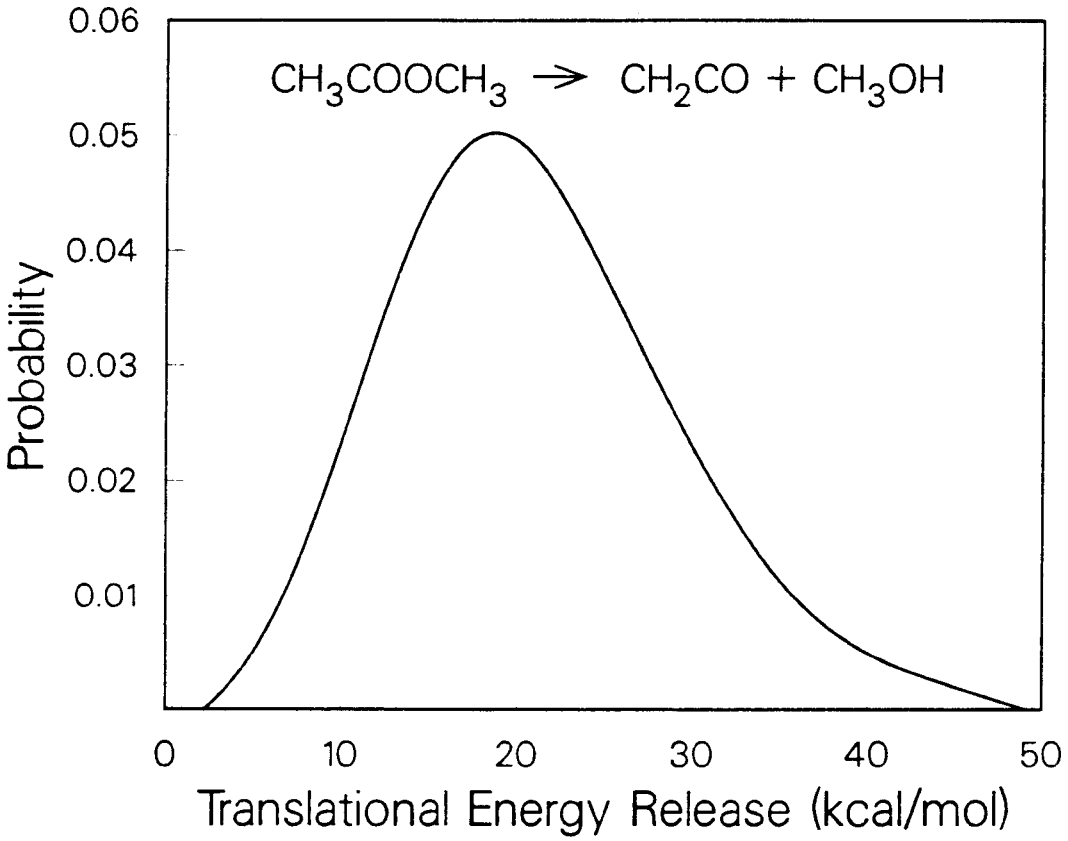
0.06
0.05
0.04
0.03
0.02
0.01
Probability
$CH_3COOCH_3 \rightarrow CH_2CO + CH_3OH$
0
10
20
30
40
50
Translational Energy Release (kcal/mol)
XBL 8711-4552

Figure 10

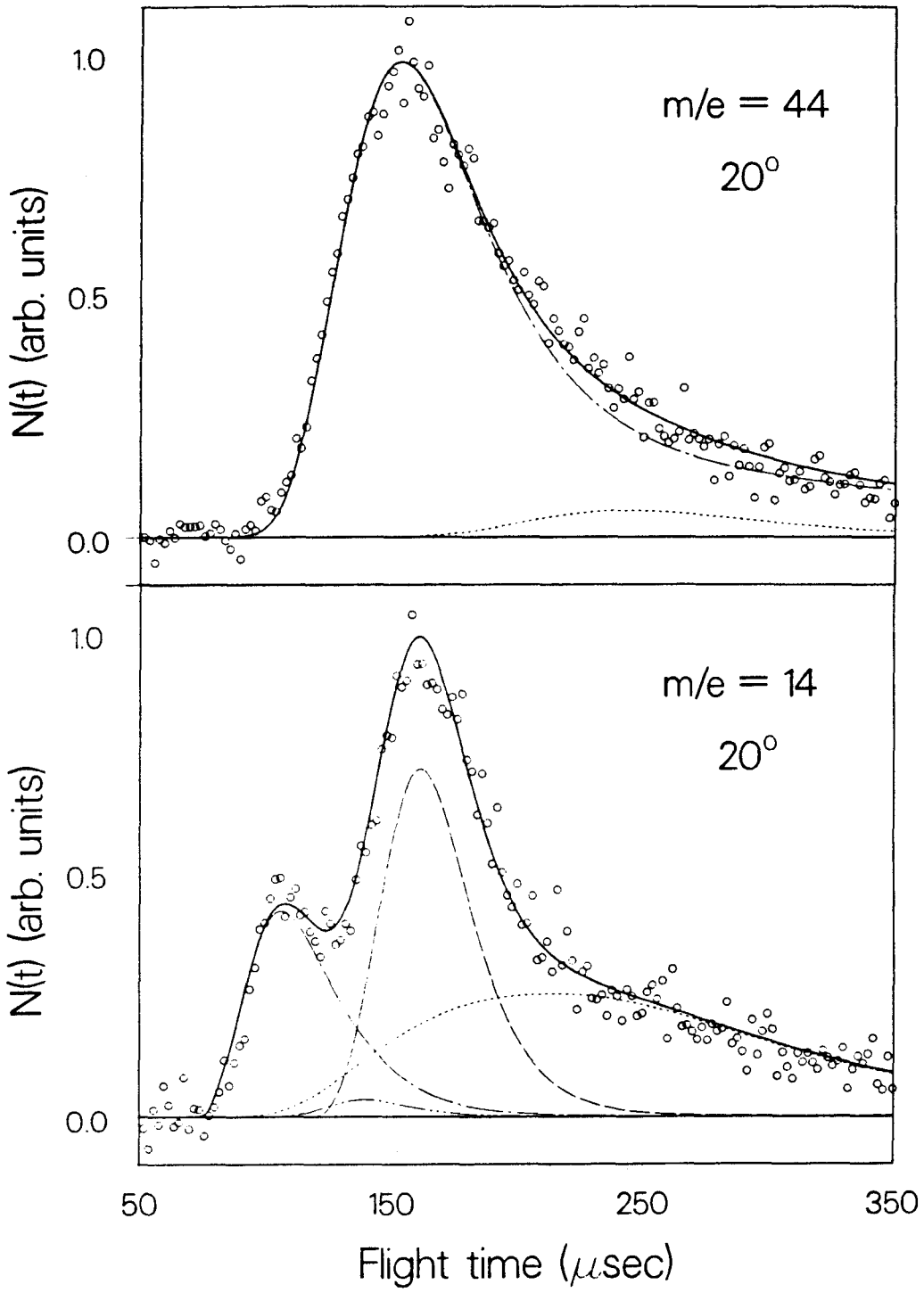


XBL 8711-4546

**Figure 11**

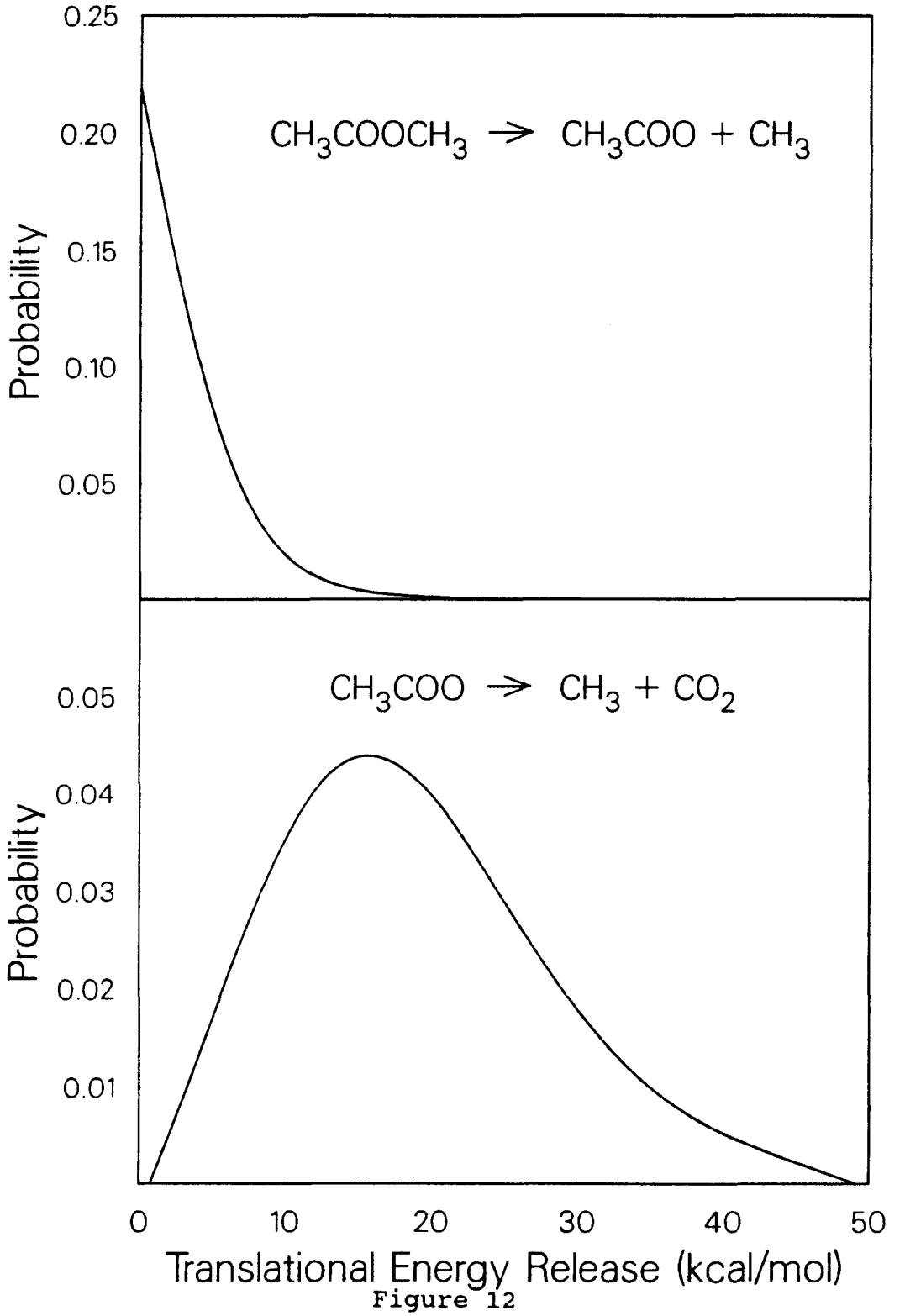


Figure 12

XBL 8711-4547

# Chapter III

# The Photodissociation of 2-Bromoethanol and 2-Chloroethanol at 193 nm

## Introduction

The experiments in this chapter were motivated by a talk by Frank Tully on the reactions of OH radicals with alkanes and alkenes.[1] Though he has studied many systems, one of the most interesting was the reaction of OH and ethylene.[2] At low temperatures (≤500 K), reaction (1) is

$$OH + C_2H_4 \longrightarrow C_2H_4 \cdot OH \qquad (1)$$

thought to be the only important channel leading to consumption of OH. The subsequent decay of this adduct occurs slowly and is not measured in his experiments. Between 500 and 650 K, equilibrium between the forward and reverse reactions is established on a millisecond timescale and the measured disappearance rate decreases by more than a factor of 15.[2] Only at higher temperatures does H atom abstraction begin to compete effectively with addition.

In an attempt to measure the kinetics of this reaction, he dissociated 2-chloroethanol at 193 nm, expecting to see reaction (2) which produces the "adduct" photolytically.

$$CH_2ClCH_2OH \xrightarrow{193\ nm} C_2H_4OH + Cl \qquad (2)$$

By using laser induced fluorescence (LIF) to monitor the OH, the approach to equilibrium could be observed. Unexpectedly, there was a large, immediate rise in the OH signal, which peaked at ~1.5 msec and then began to fall.[3] This could be from several sources, and did not appear to be from equilibration on a timescale almost as fast as the few hundred nsec resolution of the experiment. One possibility was that part of signal was due to the photodissociation of 2-chloroethanol in reaction (3) producing OH directly. This

$$CH_2ClCH_2OH \xrightarrow{193\ nm} CH_2ClCH_2 + OH \qquad (3)$$

is not implausible, as 193 nm is at the red edge of the first peak in the absorption spectrum of 2-chloroethanol. This transition is thought to be on the C-Cl bond, but the R-O-H group will be just starting to absorb there too. More likely is that the initial step in reaction (2) leaves enough energy in the $C_2H_4OH$ for it to fall apart through the reverse of reaction (1) before it has a chance to become thermalyzed. With a C-Cl bond energy of ~80 kcal/mol, a photon energy of 148 kcal/mol, and an adduct stability of ~28 kcal/mol with respect to ethylene and OH,[4] a substantial amount of energy must be released into translation for the $C_2H_4OH$ to be formed below its dissociation limit.

The Rotating Source Machine (RSM) is ideally suited for experiments to help resolve this matter. The primary photo-

chemical pathways and the translational energy release can be quickly determined, and secondary reaction pathways can be elucidated as well. This chapter describes the results of molecular beam photodissociation experiments on 2-chloroethanol and 2-bromoethanol at 193 nm. Because 2-chloroethanol absorbs very weakly, only reaction (2) could be observed and the only fragment which could be detected with good signal-to-noise (S/N) was $Cl^+$. This was sufficient to provide the translational energy distribution ($P(E_T)$) for reaction (2) and thus the internal energy of the $C_2H_4OH$ fragment.

In order to further investigate the reaction dynamics of this system, we photodissociated 2-bromoethanol under essentially the same conditions. The absorption cross-section is much larger, and all the fragments could be observed. The only primary channel occurring was reaction (4), analogous to the similar reaction with 2-chloroethanol.

$$CH_2BrCH_2OH \xrightarrow{193\ nm} C_2H_4OH + Br \qquad (4)$$

Some of the $C_2H_4OH$ adduct survived and some underwent secondary dissociation through reaction (5). The secondary

$$C_2H_4OH \longrightarrow C_2H_4 + OH \qquad (5)$$

angular distribution for this reaction was strongly forward-

backward peaked with respect to the primary $C_2H_4OH$ velocity vector, similar to that observed in the decay of a long-lived complex in crossed-beams reactive scattering experiments. Fitting all the data provided a stringent test of secondary dissociation data analysis formalisms and computer programs,[5] which they successfully passed.

**Experimental**

The photodissociation experiments were performed on the RSM, which is described in Chapter I. The beams were prepared by seeding 2-bromoethanol or 2-chloroethanol in helium and expanding the mixture into the source chamber through the .125 mm nozzle. The 2-bromoethanol was held in a bubbler at 46 °C, where it has a vapor pressure of about 4 Torr, with a total pressure of 145 Torr. The entire beam line from the bubbler to the nozzle was heated to 60 °C with heating tapes and the nozzle was heated to 180 °C with a coaxial wire soldered to the nozzle body. Great care was taken to eliminate dimers, by increasing the nozzle temperature and lowering the amount of 2-bromoethanol in the beam. Dimers were found to readily occur at lower nozzle temperatures, no doubt from the pair of intermolecular hydrogen bonds which can form. The mean velocity of the beam was 1.2 x $10^5$ cm/sec with a FWHM spread of 10%. The 2-chloroethanol was kept at 40 °C (P = 16 Torr) in the bubbler, with a total stagnation pressure of 130 Torr. The nozzle was heated to

115 °C to give a beam velocity of $1.1 \times 10^5$ cm/sec with a spread of 12%. It is expected that there were some dimers in the 2-chloroethanol beam, but they did not obscure the single fast peak observed in the TOF spectra.

A Lambda-Physik 103 MSC excimer laser was used with ArF at 193 nm, and focused to a 2 x 5 mm spot at the intersection of the laser and the molecular beam. Approximately 97% polarized light was obtained with a pile-of-plates polarizer consisting of 10 UV-grade quartz plates at Brewster's angle. The direction of polarization could be changed by rotating the polarizer during the experiment.

UV spectra of 2-bromo and 2-chloroethanol were taken on a commercial UV-vis spectrometer in dilute $H_2O$ solution. At approximately 193 nm, $\sigma(CH_2BrCH_2OH) = 5.2 \times 10^{-19}$ cm$^2$ while $\sigma(CH_2ClCH_2OH) = 2.2 \times 10^{-20}$ cm$^2$. These will be different in the gas phase, though our results suggested that the ratio of the cross-sections remained at least that large.

**Results and Analysis**

Very strong signal was detected at a mass-to-charge ratio (m/e) of 79 and 81 in the photodissociation of 2-bromoethanol. As shown in fig. 1, there was only a single relatively fast peak in the m/e = 79 TOF spectra, which is due to Br atoms produced in reaction (4). The data were fit using forward convolution techniques[5,6] to find the $P(E_T)$ for this channel, which is shown in fig. 2. The $P(E_T)$ peaks

at 33 kcal/mol and releases an average of 33.8 kcal/mol into translation.

The partner fragment from reaction (4), $C_2H_4OH$, was detected at m/e = 17, 25-27, 29, 31, 43, and 45. The fast edge of the $C_2H_4OH$ signal, shown in fig. 3, can be fit with the same $P(E_T)$, showing that these two fragments are both from reaction (4). However, there is considerable signal missing from the slow side of the m/e = 31 spectra in fig. 3, based on the $P(E_T)$ for reaction (4). This is just from the fact that some of the slower $C_2H_4OH$ was formed above its dissociation limit and underwent secondary dissociation through reaction (5). The $P(E_T)$ which fit the surviving $C_2H_4OH$ is shown as the lower curve in fig. 2, and peaks at 36 kcal/mol with an average translational energy release of 36.1 kcal/mol.

The $P(E_T)$ derived from the Br atoms is the true $P(E_T)$ for reaction (4), since Br cannot undergo any kind of secondary process. The difference between the two $P(E_T)$'s in fig. 2 represents the primary $P(E_T)$ for those $C_2H_4OH$ radicals which undergo secondary dissociation. The two $P(E_T)$'s are identical on their fast sides, but begin to diverge at 39 kcal/mol. The $P(E_T)$ for surviving $C_2H_4OH$ does not drop to zero until 27 kcal/mol, indicating that some of the $C_2H_4OH$ survives and some dissociates over a range of 12 kcal/mol. This is strong evidence that both the $^2P_{1/2}$ and $^2P_{3/2}$ states (hereafter referred to as $Br^*$ and Br, respec-

tively) of Br are formed, since the spin-orbit splitting in Br is about 11 kcal/mol.

The m/e = 29, 31, 43, and 45 data were all identical (the best S/N was at m/e = 31), showing a single peak, but at lower masses there was evidence of the secondary dissociation products of $C_2H_4OH$. TOF spectra with signal from reactions (4) and (5) at m/e = 26 and 17 are shown in fig. 4. A simple 2-dimensional Newton diagram analysis showed that these were consistent through momentum conservation with OH and $C_2H_4$ from reaction (5).[7] Actually fitting these data was considerably more difficult, however. The primary $P(E_T)$ used corresponded to the difference between the two $P(E_T)$'s in fig. 2. It was quickly found that no simple secondary $P(E_T)$ could match the peaks in the TOF spectra, especially those at longer times than the primary photodissociation signal. This is a consequence of the extensive "smearing out" in secondary dissociation, where all combinations of primary and secondary c.m. velocities and angles (in plane as well as out-of-plane) are averaged over. The molecular beam and detector direction form a plane, and any primary dissociation out of that plane is not detected. For secondary dissociation, however, the primary step can be out-of-plane and the secondary step can bring the fragment back into the plane; only the resultant c.m. velocity vector need be in the plane. Thus, any structure in the simulated data is easily wiped out.

The data strongly suggested forward-backward peaking with respect to the initial primary c.m. velocity vector, since it is otherwise impossible to get a secondary peak at longer times than the primary peak. With an isotropic angular distribution, the calculated secondary signal has only a single peak, occurring at faster times than the primary signal. The data were fit by using a strongly forward-backward peaked secondary angular distribution to fit the data, as shown in fig. 5. This peaking in the secondary angular distribution is due to the fact that the Br departs with a large exit impact parameter and the $C_2H_4OH$ is left highly rotationally excited, as will be discussed later.

Since the $C_2H_4OH$ dissociated with a ~20 kcal/mol range of internal energies and released a large amount of energy into translation, the primary and secondary $P(E_T)$'s are correlated. Using a single $P(E_T)$ for secondary dissociation, both fragments could not be fit simultaneously. This was resolved by using a secondary "RRK" $P(E_T)$ of the form

$$P(E_T) = (E_T - b)^r (E_{tot} - E_T)^w \qquad (6)$$

where b, r, and w are fitting parameters corresponding physically in an ideal case to a barrier height, the dimensionality of the reaction coordinate, and the number of active modes, respectively.[8] In practice, except for b, it

is doubtful that they have much physical significance at all. $E_{tot}$ is the total energy available for translation (in the secondary reaction), calculated from the equation

$$E_{tot} = h\nu - \Delta H_1 - \Delta H_2 - E_T(1) \qquad (7)$$

where $\Delta H_1$ and $\Delta H_2$ are the endothermicities of the primary and secondary reactions, and $E_T(1)$ is the energy released into translation in the primary reaction. The data analysis program steps along $E_T(1)$ and creates a new secondary $P(E_T)$ at each available energy. This conserves energy properly and correctly normalizes the $P(E_T)$'s. In theory, r and w should perhaps change as function of $E_{tot}$, but this was not done. With a total available energy for translation in reactions (4) and (5) of 54 kcal/mol, the data could be fit reasonably well with b = 6, r = 1, and w = 1.5. This released a peak energy of between 9 and 18 kcal/mol into translation in the secondary step, depending on the energy release of the primary process.

At very fast times in the m/e = 17 and 26 TOF spectra there is signal which cannot be from the secondary dissociation of $C_2H_4OH$ with only one photon. It is likely from the secondary photodissociation of $C_2H_4OH$ in reaction (8), where

$$C_2H_4OH^{\ddagger} \xrightarrow{193\ nm} C_2H_4 + OH \qquad (8)$$

the $C_2H_4OH^{\ddagger}$ from reaction (4) has a wide range of internal energies. Power dependence measurements showed that the $Br^+$ signal was linear with laser power and that the primary reaction is a one-photon process. Little power dependence data were taken at m/e = 17 and 26, but they seemed to show that the fastest signal changed in relative size with respect to the main peaks, consistent with what one would expect for reaction (8).

There was no evidence of any other reactions. No signal was observed at m/e = 93 ($CH_2Br^+$) or any higher mass, showing that there was no reaction analogous to (3) occur-

$$CH_2BrCH_2OH \xrightarrow{193\ nm} CH_2CH_2Br + OH \qquad (9)$$

ring. Signal from HOBr was also checked for to ensure that there was no contribution from reaction (10). The strongest

$$CH_2BrCH_2OH \xrightarrow{193\ nm} C_2H_4 + HOBr \qquad (10)$$

evidence, however, is the single, momentum-matched peaks in the m/e = 29, 31, 43, 45, 79, and 81 TOF spectra. If any other primary reaction were occurring it would certainly produce additional signal at one or more of these fragments.

Polarization measurements were taken of the signal from Br, since it provides a complete picture of the primary photodissociation reaction. Data were taken with the laser

horizontally and vertically polarized (with respect to the detector) at 20° and 40°. These laboratory angles include a wide range of c.m. recoil angles and any anisotropy effects should be obvious. Between horizontal and vertical polarization, the signal levels changed less than 1%, and the shapes of the TOF spectra were identical. This indicates that reaction (4) is completely isotropic, and that either dissociation is very long with respect to a rotational period, that the transition dipole contains a mixture of parallel and perpendicular components, or that the geometry changes upon dissociation are so severe that all anisotropy is wiped out. A combination of these effects is also possible.

Signal from the photodissociation of 2-chloroethanol could only be observed at m/e = 35 ($Cl^+$). The shape of the peak, shown in fig. 6 (top), is quite similar to that of $Br^+$, and is likely to be solely from reaction (2). The $P(E_T)$ which fits this data also peaks at 33 kcal/mol and is shown in fig. 6 (bottom). Very weak signal could be observed at a few masses corresponding to the $C_2H_4OH$ fragment, but it was insufficient for any kind of analysis.

**Discussion**

A. Translational energy release- In the photodissociation of 2-bromoethanol, only one primary reaction channel was observed, loss of Br through reaction (4). A large

amount of the available energy was released into translation and the $P(E_T)$ peaked far from zero. The photon energy at 193 nm is 148 kcal/mol and assuming a C-Br bond energy of 68 kcal/mol,[9] the total available energy is about 81 kcal/mol, including 1 or 2 kcal/mol from vibrational energy unrelaxed in the supersonic expansion. Of this, an average of 33.8 kcal/mol or 42% appears in translation. In comparison, in the photodissociation of 1,2-$C_2F_4BrI$ at 193 nm, where one reaction channel involved breaking a C-Br bond of approximately equal strength, an average of only 25 kcal/mol was released into translation.[10] Presumably this is due to the greater number of low frequency vibrational modes in the $C_2F_4I$ product.

In neither case could the production of different spin-orbit states of Br ($Br^*$ is higher than Br by 10.54 kcal/mol) be distinguished. The translational energy distributions are too broad to resolve the two states, unlike in the photodissociation of similar molecules containing C-I bonds, where the much higher spin-orbit splitting of the I atoms (21.7 kcal/mol) allowed the two different states to be resolved in the TOF spectra.[11]

The large release of translational energy reflected in the $P(E_T)$ is suggestive of a direct dissociation from a repulsive excited electronic state. This is consistent with previous interpretations of excitation at 193 nm as being an ($\sigma^* \leftarrow n$) transition on the C-Br bond,[10] which is directly

repulsive and has a lifetime of less than a picosecond. Therefore it is surprising that no anisotropy effects were observed in dissociation with polarized light. The photodissociation of 1,2-$C_2F_4BrI$ was found to have a strongly parallel polarization dependence,[10] with an anisotropy parameter of 1.85, close to the limiting value of 2 for a purely parallel dissociation.[12] It is unlikely that this lack of anisotropy in the photodissociation of 2-bromoethanol is due to a long dissociation lifetime since the initial excitation should still be a directly repulsive transition localized on the C-Br bond. Rather, as the molecule dissociates, the $C_2H_4OH$ fragment may undergo large geometrical rearrangements, and dissociate with a wide range of impact parameters, thus wiping out any observed anisotropy. It is also possible that the initial transition may have both parallel and perpendicular components.

B. Rotational excitation- 2-bromoethanol and 2-chloroethanol exist in the gas phase as intramolecularly hydrogen-bonded monomers in the gauche conformation.[13] The XCCO dihedral angles (X = Cl, Br) are both close to 64°, with the hydroxyl proton-X bond lengths both about .5 Å less than the sum of the atomic van der Waals radii,[13] indicating a strong interaction. Experimental studies and theoretical calculations have indicated that this structure is about 2 kcal/mol more stable than the trans configuration,[14] where the halogen and the OH are on opposite sides. In a supersonic

expansion, essentially all the molecules should be in the gauche conformation, though there is also the possibility of forming dimers with two intermolecular hydrogen bonds.

In the dissociation of 2-bromoethanol, if the Br atom departs along the direction of the C-Br bond, the exit impact parameter will be about 1.36 Å.[13] Since the molecules initially have little rotational energy, the final orbital angular momentum must be approximately equal (and opposite) to the rotational angular momentum of the $C_2H_4OH$,

$$\mathbf{L} = \mu v b = -\mathbf{J} \tag{11}$$

where $\mu$ is the reduced mass between the two fragments, v is the relative velocity vector and b is the exit impact parameter. The peak energy release for reaction (4) is 33 kcal/mol, which corresponds to a relative velocity of $3.1 \times 10^5$ cm/sec. With a reduced mass $\mu$ = 28.8 a.m.u., the most probable value of J will be 190. The moment of inertia of $C_2H_4OH$ (about the axis perpendicular to the CCO plane) is $7.60 \times 10^{-23}$ g·Å$^2$ which leads to a rotational energy of 38 kcal/mol. This corresponds to 89% of the available energy in rotation and translation for the production of Br, and all the energy in rotation and translation if $Br^*$ is produced. For higher translational energies, energy conservation would be violated with an exit impact parameter of 1.36 Å. Therefore the CCBr angle must become wider than

110° during dissociation, giving a smaller value of b and less energy in rotation. The main point is that a large fraction of the available energy is channeled into translation and rotation, and comparatively little energy can remain as vibration in the $C_2H_4OH$ product.

With this information, the lack of measurable anisotropy becomes more understandable. Since the 2-bromoethanol must dissociate from a range of geometries with different amounts of energy in translation and rotation in order to conserve energy and angular momentum, the anisotropy will be sharply reduced from that expected from a single dissociation geometry. The effect of the hydrogen-bonded proton is unclear, but it could exert additional torque between the Br and $C_2H_4OH$ fragments during dissociation which would further smear out the anisotropy. The hydrogen-bonding interaction between the O-H and the Br atom could also perturb the electronic transitions on the C-Br bond, and induce additional parallel or perpendicular components.

C. Secondary dissociation- The spontaneous secondary dissociation of the $C_2H_4OH$ fragment showed very interesting dynamics. With reaction (5) endothermic by 28 kcal/mol,[4] unless $Br^*$ was produced and at least 42 kcal/mol went into translation (or 53 kcal/mol in translation with Br produced) the $C_2H_4OH$ product should be unstable with respect to $C_2H_4$ and OH. As expected, this secondary reaction channel was observed. It was hoped that by observing the threshold for

surviving $C_2H_4OH$, a better value for the endothermicity of reaction (5) could be obtained, similar to the work of Minton *et al.* on $C_2H_4Cl$.[11] However, $C_2H_4OH$ with translational energies as low as 27 kcal/mol survived the ~100 $\mu$sec flight time to the ionizer. It is possible that this implies a binding energy of 81 - 27 - 11 = 43 kcal/mol for $C_2H_4OH$, but unlikely. A much more plausible explanation is that the high rotational energy of the $C_2H_4OH$ fragment creates the polyatomic analogue of a centrifugal barrier to dissociation. The rotational energy cannot all be used to break the C-O bond, allowing the detection of some metastable $C_2H_4OH$. An alternative, more physical argument is that highly rotationally excited $C_2H_4OH$ cannot dissociate without leaving some energy in $C_2H_4$ (or OH) rotation in order to match the orbital angular momentum produced and thus conserve total angular momentum. A simple calculation assuming a 4 Å C-O bond length at the transition state showed that 7.2 kcal/mol remained in overall rotation with J = 190. Of this, the $C_2H_4$ accounted for 3 kcal/mol. In addition, since the primary dissociation event does not occur in a plane, some of the rotational energy will be in "prolate" motion of the $C_2H_4OH$ (K > 0) and unable to participate in the dissociation to $C_2H_4$ and OH. Finally, there may be a slight electronic barrier to dissociation as the C=C double bond forms. This is consistent with the 5-7 kcal/mol barrier in the secondary $P(E_T)$.

The secondary dissociation products of $C_2H_4OH$ showed a high degree of anisotropy in their angular distribution. The $C_2H_4$ and OH were peaked strongly forward and backward with respect to the initial C-Br recoil direction. This would be expected for the secondary dissociation of a primary photoproduct with large amounts of rotational and translational energy, but to our knowledge has not been previously observed. The initial angular momentum of the 2-bromoethanol is close to zero. As has been described, the primary reaction occurs with a large exit impact parameter, leading to high rotational excitation of the $C_2H_4OH$ fragment. Though the primary dissociation does not occur within a planar OCCBr framework, the initial torque will be in the CCBr plane, and should lead to the rotational angular momentum being approximately perpendicular to this plane, or in other words $\mathbf{v} \perp \mathbf{J}$. Secondary dissociation then occurs preferentially along a "pinwheel" perpendicular to **J**. Since all azimuthal orientations of J perpendicular to **v** are equally likely in a beam of isotropically oriented molecules, this causes secondary signal intensity to build up preferentially along the poles, parallel and antiparallel to **v**. This is just the photodissociation analog to the angular distribution of long-lived complexes in reactive scattering experiments first observed by Miller, Safron, and Herschbach.[15]

In order to observe this forward-backward peaking, the

$C_2H_4OH$ must be long-lived with respect to the rotational period (.24 psec with J = 190). Since we observed metastable $C_2H_4OH$ which survived for over 100 μsec, some of these complexes are long-lived indeed! There is one important difference between the secondary dissociation of $C_2H_4OH$ in this experiment and the long-lived complexes observed in crossed-beams scattering experiments. In a crossed-beams experiment, the initial beam velocities are oriented in the laboratory frame. The initial orbital angular momentum **L** is perpendicular to the relative velocity vector and the forward-backward scattering appears in the c.m. and laboratory angular distributions. In the photodissociation of 2-bromoethanol, the primary reaction producing $C_2H_4OH$ is isotropic, and therefore any secondary angular distribution of $C_2H_4$ and OH with respect to the initial $C_2H_4OH$ velocity vector will still leave an isotropic c.m. angular distribution. The forward-backward peaking will instead manifest itself in the TOF spectra, with slight effects possible in the laboratory angular distribution. Instead of the broad, featureless peaks typical of isotropic secondary dissociation,[10,16] the signal peaks at longer and shorter times (slower and faster lab velocities) than the primary peak from $C_2H_4OH$. This is because the secondary products are preferentially scattered parallel and antiparallel (forward/backward) to the initial primary recoil velocity.

D. Comparison with bulk-phase kinetic studies- It is now clear that in the photodissociation of 2-bromoethanol, some of the initially formed $C_2H_4OH$ will quickly fall apart to $C_2H_4$ and OH. In this experiment, about 2/3 of the $C_2H_4OH$ adduct decomposed. Actually, if $C_2H_4OH$ is only bound by 28 kcal/mol, there should have been much more secondary decomposition, but some of the $C_2H_4OH$ is metastable due to its high rotational energy. In a gas cell experiment, some of this rotational energy could be transformed into vibrational energy by collisions, but the nascent $C_2H_4OH$ radicals are much more likely to simply lose energy to the bath gas. It is quite possible that the $C_2H_4OH$ requires a significant amount of time to become thermalyzed, and the initial secondary dissociation occurs from a nonequilibrium distribution of internal energies. It is important to note that no OH was formed in the primary photodissociation of 2-bromoethanol, but that a small amount of $C_2H_4OH$ underwent secondary photodissociation to produce $C_2H_4$ and OH.

Among the surviving $C_2H_4OH$, the relative amounts of stable and metastable products are difficult to estimate as it is not known how much corresponds to Br and how much to spin-orbit excited $Br^*$, and the stability of $C_2H_4OH$ may be incorrect. Since the difference in energy at which $C_2H_4OH$ starts dissociating to that where it all dissociates is approximately the spin-orbit splitting, it is likely that both states of Br are produced. For those primary dissocia-

tion events producing Br, all of the $C_2H_4OH$ should undergo secondary dissociation since about 53 kcal/mol must go into translation for the adduct to be stable. Because of the two problems just mentioned, it is difficult to reach a definite conclusion.

In the photodissociation of 2-chloroethanol to produce Cl and $C_2H_4OH$ through reaction (2), the $P(E_T)$ was almost identical to that for 2-bromoethanol. For Cl atoms, however, the spin-orbit splitting is only 2 kcal/mol and can almost be neglected. Assuming a C-Cl bond energy of 80 kcal/mol, the minimum translational energy for stable $C_2H_4OH$ would be 148 - 80 - 28 = 40 kcal/mol, or 38 kcal/mol for $Cl^*$ formation. Therefore, the part of the $P(E_T)$ corresponding to Cl atom production with more than 40 kcal/mol in translation must yield stable $C_2H_4OH$. Below 40 (or 38) kcal/mol the $C_2H_4OH$ must be either be metastable or dissociate, unless $C_2H_4OH$ is more strongly bound than is currently believed. Unfortunately, no partner $C_2H_4OH$ or any secondary dissociation fragments were detected, which could have shed light on this problem. Since the absorption cross-section of 2-chloroethanol at 193 nm (at least in aqueous solution) is approximately 20 times less than that of 2-bromoethanol, one would have to signal average for between 20 and 400 times longer to achieve comparable S/N for equal molecular beam intensities. Substantially raising the amount of 2-chloroethanol in the beam is risky since the background at

daughter ions of $C_2H_4OH$ would likely go up and dimer formation would become much more probable.

**Conclusions**

In the photodissociation of 2-bromoethanol and 2-chloroethanol at 193 nm, only one primary channel, halogen atom elimination, was observed, with a translational energy distribution peaking near 33 kcal/mol. Substantial rotational excitation is expected in both cases due to the large exit impact parameters and high recoil velocities. In the photodissociation of 2-bromoethanol, the observation of stable $C_2H_4OH$ with as little as 27 kcal/mol in translation indicates that $C_2H_4OH$ may be bound by up to 43 kcal/mol, or much more likely that some of the $C_2H_4OH$ is metastable as a result of some of its internal energy being tied up in rotation. The $C_2H_4OH$ which underwent secondary dissociation producing $C_2H_4$ and OH was found to have a strongly forward-backward peaked secondary angular distribution as a result of angular momentum constraints. This was compared to previous crossed molecular beams studies of long-lived complexes.

**References**

1. F. P. Tully, invited talk, Berkeley-Sandia seminar series, Berkeley, 1987.

2. F. P. Tully, Chem. Phys. Lett. **96**, 148 (1983); **143**, 510 (1988).

3. F. P. Tully, private communication.

4. C. Melius, unpublished results; this can also be calculated assuming a $\beta$ C-H bond energy of 99 kcal/mol in ethanol, and using the heats of formation in H. M. Rosenstock, K. Draxl, B. W. Steiner, and J. T. Herron, J. Phys. Chem. Ref. Data **6**, suppl. 1, I-774 (1977).

5. X. Zhao, Ph.D. Thesis, University of California, Berkeley, 1988; X. Zhao, G. M. Nathanson, and Y. T. Lee, in preparation.

6. R. K. Sparks, K. Shobatake, L. R. Carlson, and Y. T. Lee, J. Chem. Phys. **75**, 3838 (1981).

7. Starting with the primary circle for $C_2H_4OH$ in the Newton diagram shown as fig. 2 in chapter I and drawing secondary circles centered along its circumference, the secondary peak positions in the TOF spectra in fig. 4 could be predicted. The peaks at faster times than the primary peak were clearly due to forward scattering (in the direction of the molecular beam) in both the primary and secondary events. The slower peaks have contributions from both forward scattering in the primary reaction (4) and backward scattering in the

secondary reaction (5), and vice versa. This 2-dimensional picture is a simplification of the real situation, however, since out-of-plane contributions play a very important role in the shape of the observed secondary peaks.

8. This is not a rigorous use of RRK theory, but it has been used previously within the group as a functional form for $P(E_T)$'s in reactive scattering experiments.

9. Estimated by taking the C-Br bond energy of $C_2H_5Br$ and adding 1.2 kcal/mol for the added stability of the intramolecular hydrogen bond.

10. D. Krajnovich, L. J. Butler, and Y. T. Lee, J. Chem. Phys. **81**, 3031 (1984).

11. T. K. Minton, P. Felder, R. J. Brudzynski, and Y. T. Lee, J. Chem. Phys. **81**, 1759 (1984); T. K. Minton, G. M. Nathanson, and Y. T. Lee, J. Chem. Phys. **86**, 1991 (1987).

12. R. N. Zare, Mol. Photochem. **4**, 1 (1972).

13. R. G. Azrak and E. B. Wilson, J. Chem. Phys. **52**, 5299 (1970).

14. P. Buckley, P. A. Giguère, and M. Schneider, Can. J. Chem. **47**, 901 (1969); A. Almenningen, O. Bastiansen, L. Fernholt, and K. Hedberg, Acta Chem. Scand. **25**, 1946 (1971); K. B. Wiberg and M. A. Murcko, J. Mol. Struct. (Theochem) **163**, 1 (1988).

15. W. B. Miller, S. A. Safron, and D. R. Herschbach, Chem. Soc., Faraday Disc. **44**, 108, 292 (1967); J. Chem. Phys. **56**, 3581 (1972).

16. E. J. Hintsa, A. M. Wodtke, and Y. T. Lee, J. Phys. Chem. **92**, 5379 (1988).

**Figure Captions**

Fig. 1. TOF spectra of Br atoms from reaction (4) at 20° and 50° from the molecular beam. The scattered circles are the experimental data and the lines are the fits using the $P(E_T)$ shown as the upper curve in fig. 2.

Fig. 2. The upper curve is the $P(E_T)$ for reaction (4), derived from the Br data shown in fig. 1. The lower curve, starting at 27 kcal/mol, represents the $P(E_T)$ for $C_2H_4OH$ from reaction (4) which survives to the detector. The cross-hatched area corresponds to $C_2H_4OH$ which underwent secondary dissociation.

Fig. 3. TOF spectra of $C_2H_4OH$ from reaction (4) at m/e = 31, detected at 20° and 50° and fit with the $P(E_T)$ shown as the lower curve in fig. 2.

Fig. 4. TOF spectra of the secondary dissociation products of reaction (5). Top: m/e = 26 from $C_2H_4$ at 20°. Bottom: m/e = 17 from OH at 20°. The narrow peaks near 130 $\mu$sec are the contribution of surviving $C_2H_4OH$ from reaction (4). The broader peaks are products of the secondary reaction (5), fit with the RRK $P(E_T)$ as described in the text.

Fig. 5. Secondary angular distribution used to fit the data shown in fig. 4 from reaction (5). 0° corresponds to the secondary fragment velocity being parallel to the velocity of the primary fragment which produced it.

Fig. 6. Top: TOF spectrum at m/e = 35 of Cl atoms from reaction (2) at 20°. The data are fit with the $P(E_T)$ shown below. Bottom: $P(E_T)$ for reaction (2) derived from the m/e = 35 data above.

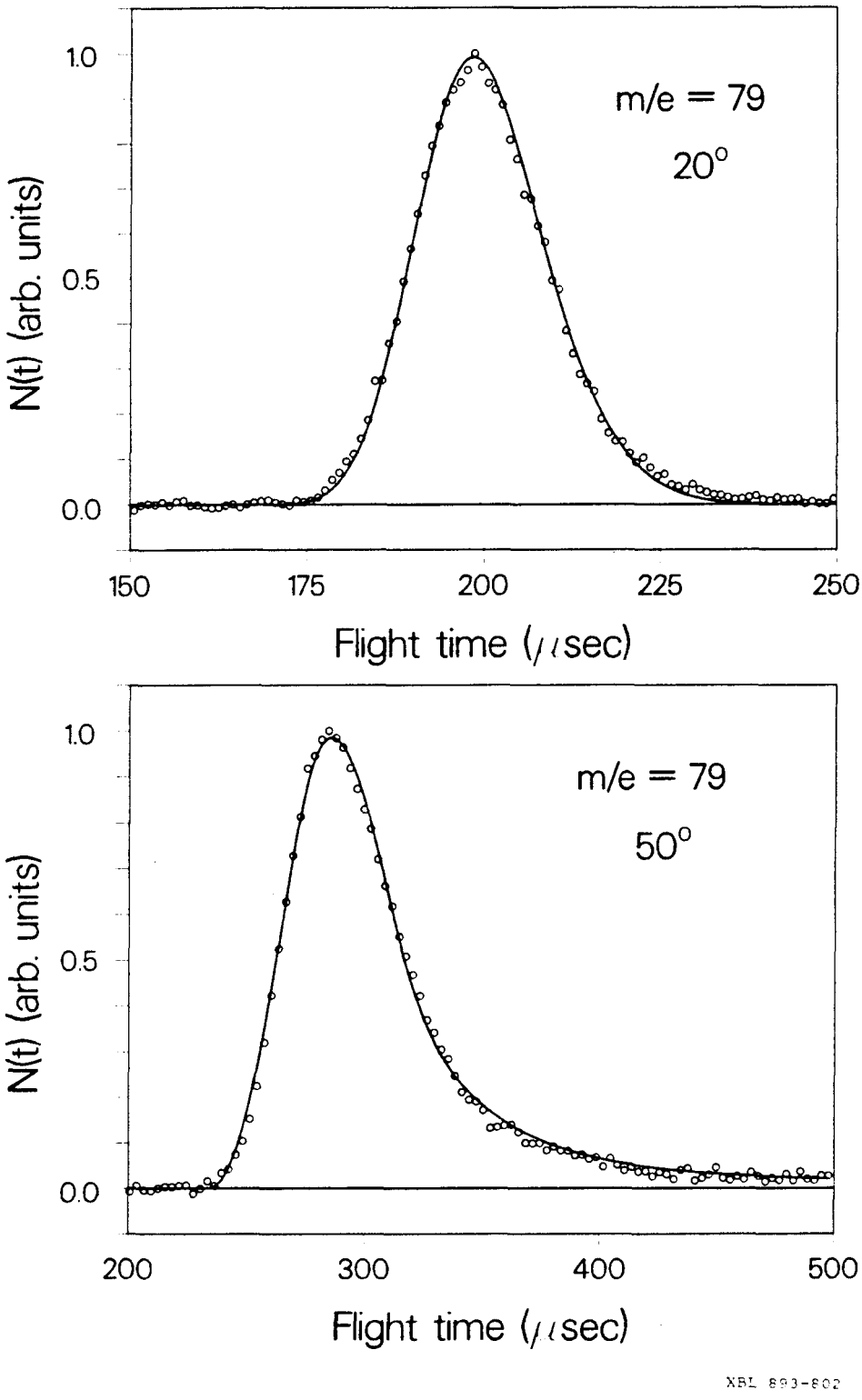
1.0
0.5
0.0
N(t) (arb. units)
m/e = 79
20°
150
175
200
225
250
Flight time (μsec)
1.0
0.5
0.0
N(t) (arb. units)
m/e = 79
50°
200
300
400
500
Flight time (μsec)
XBL 893-802

Figure 1

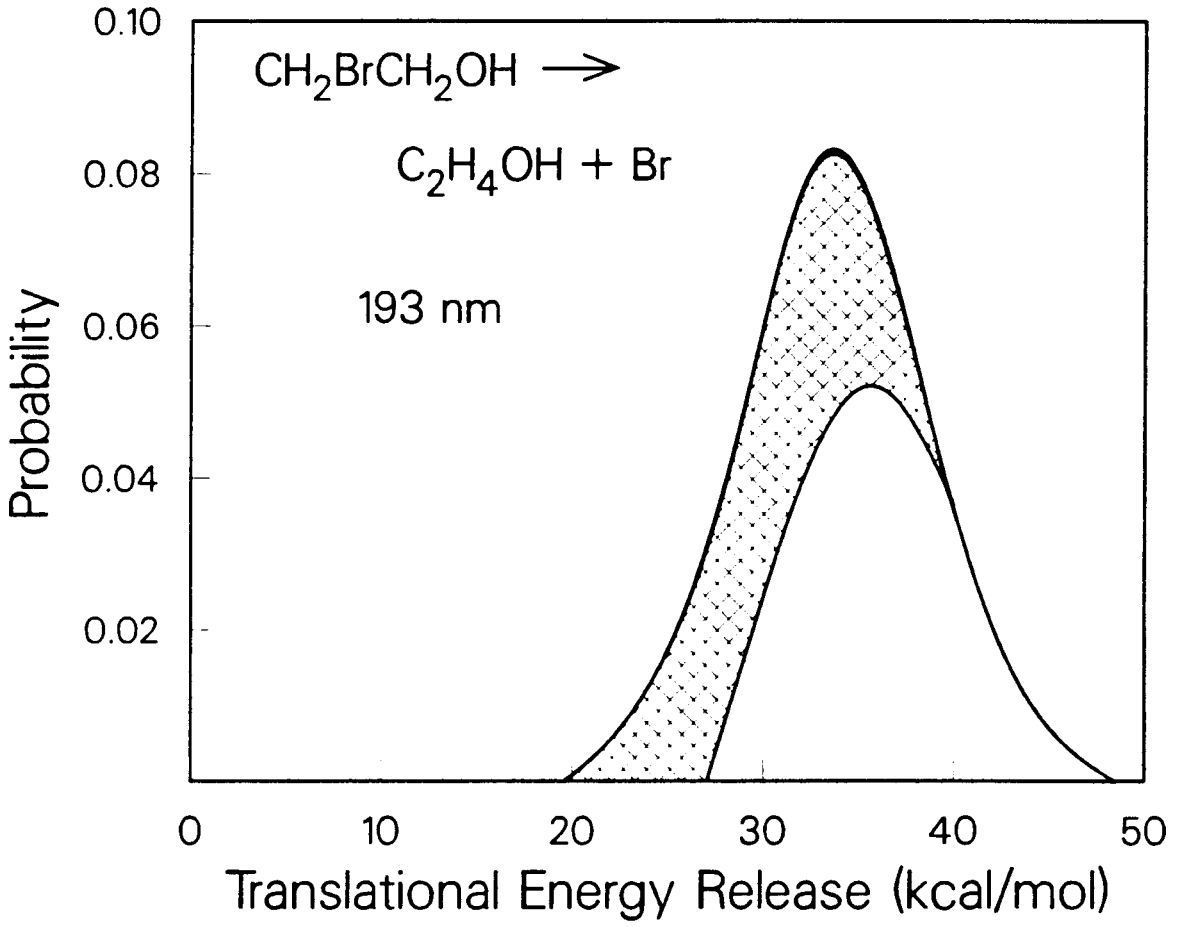
0.10
0.08
0.06
0.04
0.02
Probability
$CH_2BrCH_2OH \rightarrow$
$C_2H_4OH + Br$
193 nm
0
10
20
30
40
50
Translational Energy Release (kcal/mol)
XBL 893-803

Figure 2

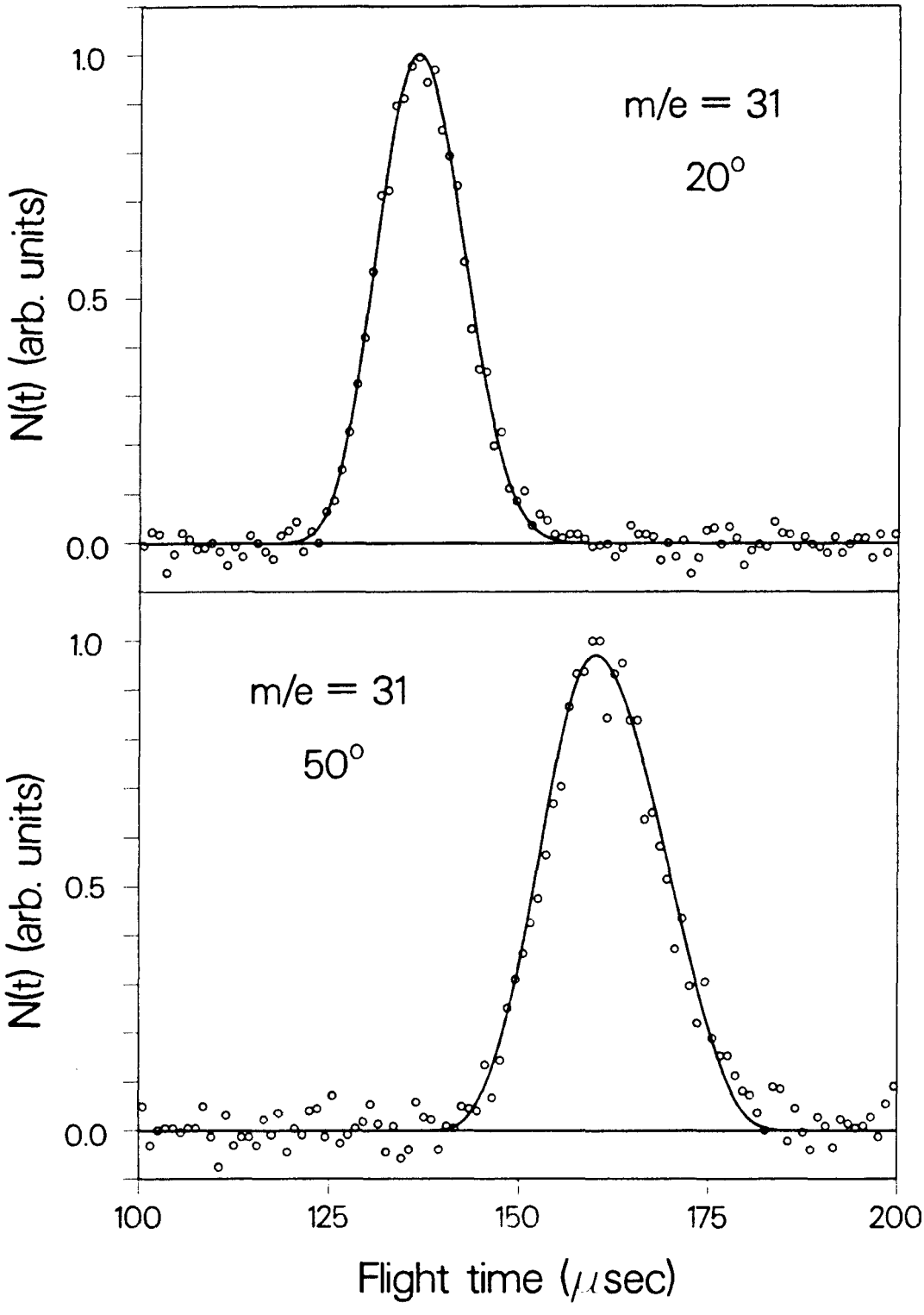


Figure 3

XBL 893-804

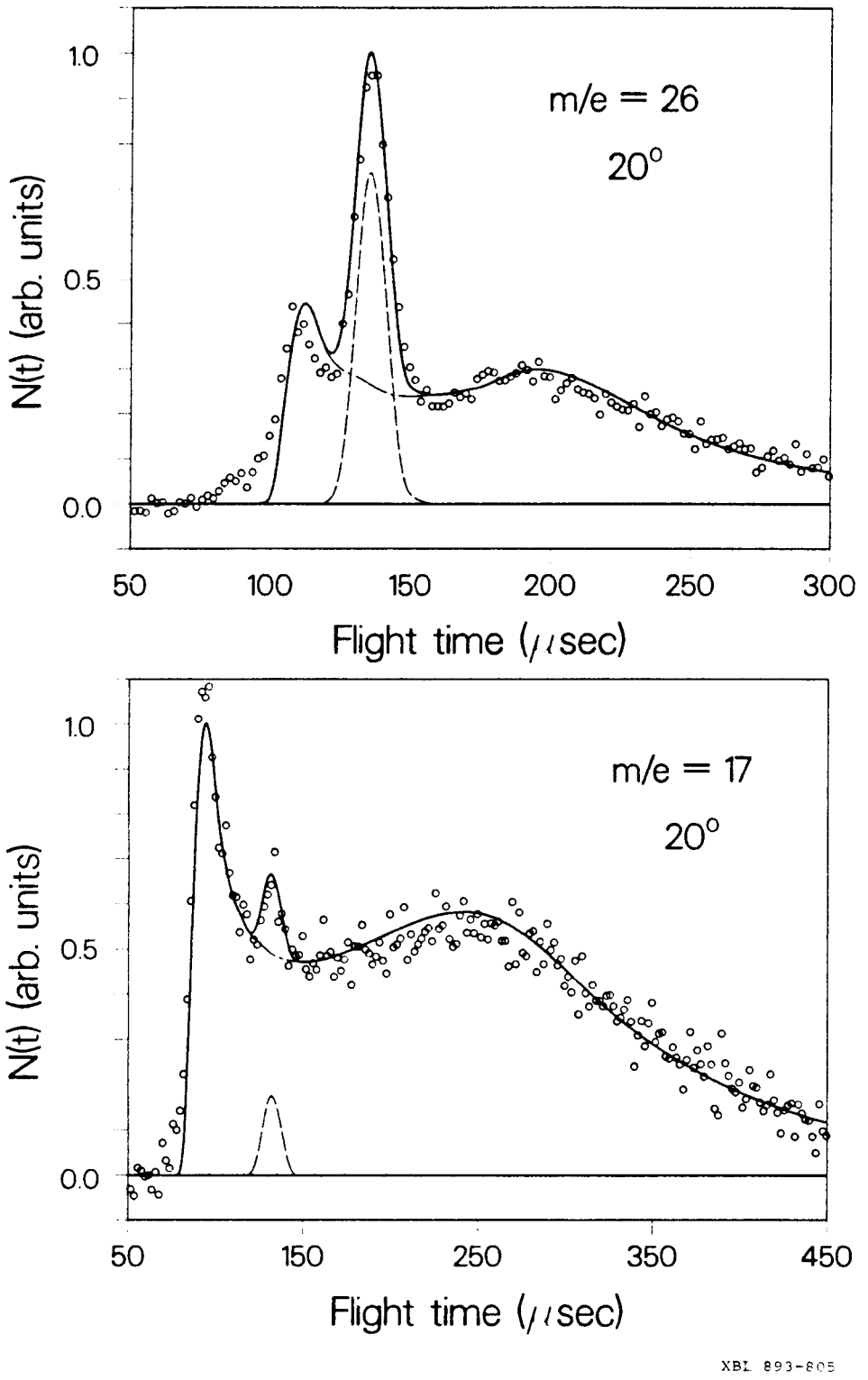
m/e = 26
20°
N(t) (arb. units)
1.0
0.5
0.0
50
100
150
200
250
300
Flight time (μsec)
m/e = 17
20°
N(t) (arb. units)
1.0
0.5
0.0
50
150
250
350
450
Flight time (μsec)
XBL 893-805

Figure 4

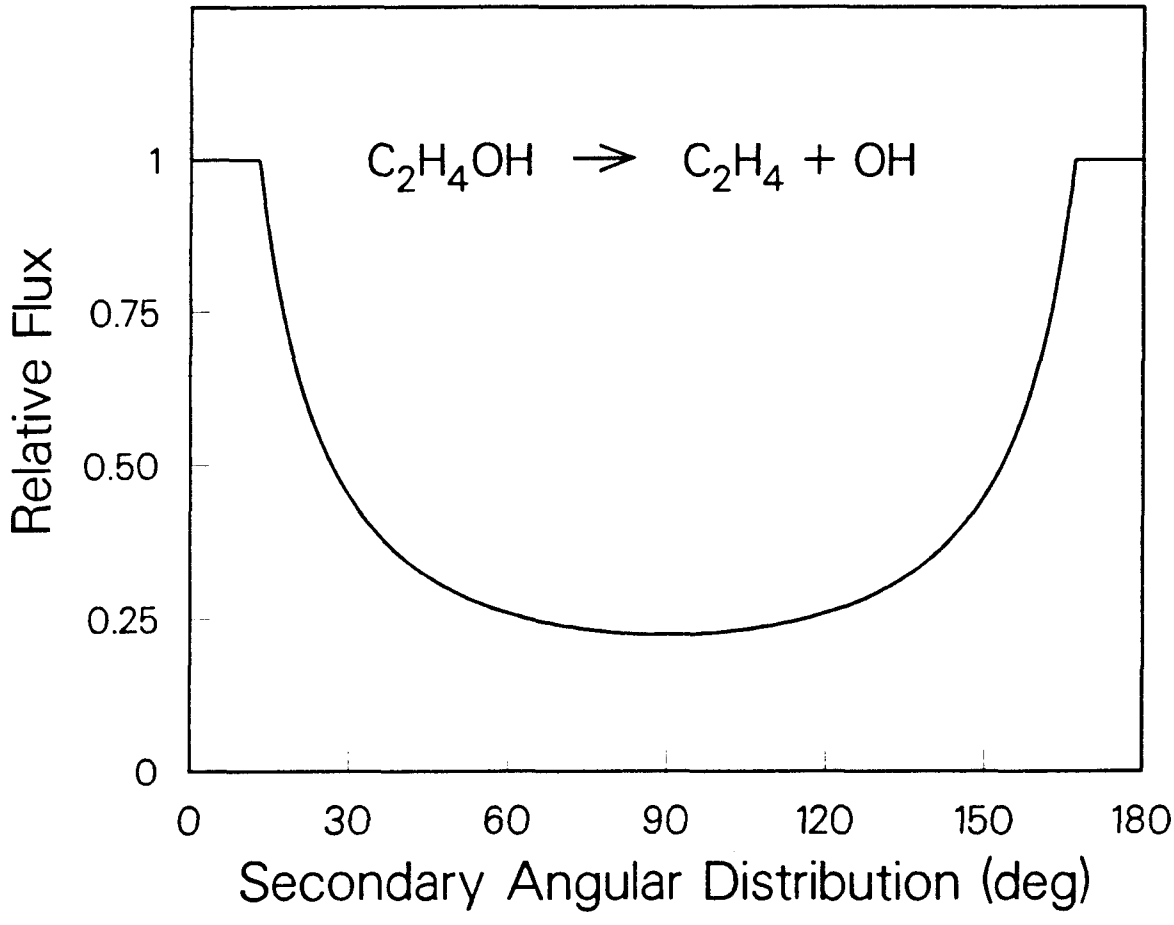
$C_2H_4OH \rightarrow C_2H_4 + OH$
Relative Flux
1
0.75
0.50
0.25
0
0
30
60
90
120
150
180
Secondary Angular Distribution (deg)
XBL 893-606

Figure 5

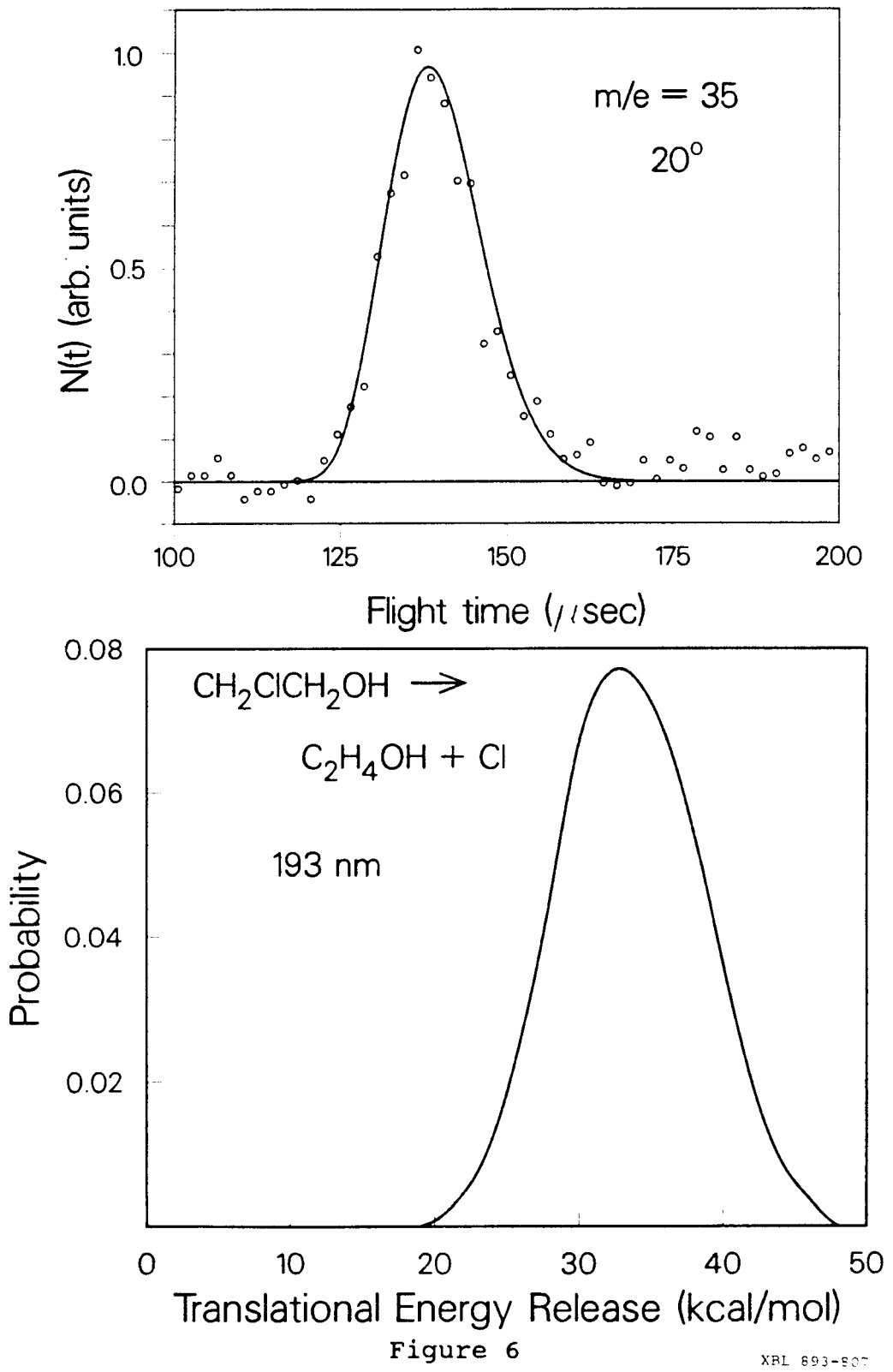


Figure 6

XBL 893-807

# Chapter IV

# Production and Photodissociation of $CCl_3$ Radicals in a Molecular Beam

## Introduction

There has long been a great deal of interest in the properties and reactions of polyatomic radicals.[1] These open-shell species are key intermediates in combustion, atmospheric chemistry and many other reactions. They are generally quite reactive and readily form more stable products. Because of this high reactivity they must usually be produced directly prior to study since they tend to be transient species.

Enormous amounts of effort have been directed towards producing radicals,[2] in order to study their structures, thermochemistry, reactivities, and other properties. The experiments described in this chapter grew out of an idea of Alec Wodtke's that we could make a pulsed beam of cold polyatomic radicals and then study them by photodissociation. We intended to produce the radicals in much the same way that Peter Andresen was generating OH radicals.[3] Andresen's radical source consists of a quartz tube attached to the end of a pulsed valve. At a fixed delay after the valve opens, a UV laser beam crosses the quartz tube transversely, producing OH from a precursor molecule ($HNO_3$ or $H_2O$). The OH is confined within the tube where it is

rapidly thermalyzed by collisions with buffer gas, then cooled in the resulting supersonic expansion out the end of the tube. The OH radicals are used to characterize the supersonic expansion process and for inelastic scattering experiments.[4] They are detected with laser induced fluorescence (LIF), which allows the internal state distributions to be monitored and is very sensitive for OH. However, LIF is limited to very small fragments, mostly atoms and diatomics.

Smalley et al. have also produced radicals inside a source mounted at the end of a pulsed valve.[5] Unlike Andresen's, this had a transverse hole cut through the source which allowed some of the gas to escape out the sides, but Smalley estimated that this was not a great loss and may have actually helped by preventing turbulence from rapid heating due to the laser pulse.[6] Their source was made out of teflon, presumably to avoid creating a plasma of reactive metal atoms. They published two papers on the spectroscopy of radicals,[5] then switched to the investigation of metal clusters using a similar approach and never went back. Our final source design was essentially the same as theirs but with a better pulsed valve. Jim Weisshar's group did some spectroscopy of radicals using an Andresen-type source but found it difficult to produce polyatomic radicals. It was actually Alec who suggested that they use a quartz tube, as is acknowledged in their paper.[7] Terry Miller and coworkers

also produced radicals (mostly ions) in a jet, by crossing a supersonic expansion with an electron beam from a hot filament, then probed them with spectroscopy.[8]

In our molecular beam photofragmentation experiments, we had had previous experience with the secondary photodissociation of primary fragments, such as $C_2H$ (from acetylene) $\rightarrow C_2 + H$,[9] CS (from $CS_2$) $\rightarrow C + S$,[10] and some of the bromo-iodo compounds, i.e. $CH_2BrI$.[11] Because the initial radical fragment usually has a wide range of angles, velocities, and internal energies (in sharp contrast to a well-collimated molecular beam) the information obtainable on the secondary dissociation dynamics is limited. In fact, a great deal of effort in recent years has gone into the correct interpretation and analysis of secondary dissociation (with or without the absorption of more photons) and it is only recently that Xinsheng Zhao and Gil Nathanson have succeeded in fully analyzing the problem.[12]

It would be a considerable improvement to dissociate internally cold radicals directly in a molecular beam, where they would start with a narrow (and measured) velocity and angular distribution. In addition to photodissociation, this source could be used for spectroscopy of radicals, crossed-beam scattering experiments, and even the Grand Plan.[13] Because radicals are highly reactive intermediates involved in combustion and atmospheric chemistry and are a sort of "new frontier" for gas-phase physical chemists,

there is much interest in their study, both for the vitally important role they play in chemical transformations and their tendency to exert a "para-magnetic" attraction on those who work with them. The Lee group in particular is moving towards more and more work on radicals, and it was hoped that this set of experiments would lead to a simple, versatile source of cold polyatomic radicals which could be used in other experiments.

While not everything worked out as well as expected, we were finally able to produce large quantities of trichloromethyl radicals in a molecular beam, photodissociate them at 308 nm, and observe the products. This chapter contains a rather long experimental section, including details of all the experimental setups and a discussion of their strengths and shortcomings, then a much shorter section on the results of $CCl_3$ photodissociation, and finally a discussion of those results.

**Experimental**

A. 1986- When we first began these experiments, the only apparatus available was the Rotating Source Machine (RSM), which we had been working on and which is described in Chapter I. It was less than ideal for the radical experiments since the source is hard to get to and is not fixed (the main reason it is known as the Rotating Source Machine). The plan was to bring another laser beam into the

source region, from the same side as the laser beam going into the main chamber. It would cross a quartz tube epoxied to the end of a pulsed valve, at an appropriate time after the valve was opened, and produce radicals by photodissociating a suitable precursor molecule seeded in buffer gas. The radicals would be quickly thermalyzed in the high pressure environment of the quartz tube and channelled towards the open end, where they would be rotationally cooled in the supersonic expansion. After passing through the two skimmers, the radicals would be crossed with a second laser beam (again delayed appropriately) and the dissociation products would be detected.

Alec built a rotating back flange, with two lens ports, one down the centerline just as usual, the other mounted off-center to allow another laser to irradiate the source. This lens made a seal from atmosphere directly into the source, and quickly became dirty from DP oil forming a thin layer on the inner (vacuum) surface of the lens and then being photolyzed. We had anticipated this problem, and replaced the old Varian VHS-6 diffusion pumps with Edwards Diffstaks, which are much cleaner and allowed the source laser lens to be used for long periods of time (weeks) without cleaning. The other major innovation was the installation of a Lasertechnics pulsed valve in the source region. It was mounted in a cage attached to the wall separating the source from the differential region. This

allowed the valve to be keyed into the skimmer assembly but also allowed for gas molecules to be quickly pumped away from the first skimmer area. The original skimmer was replaced by an electroformed 1 mm skimmer from Beam Dynamics. A 1 cm long, 1 mm i.d. quartz tube was epoxied to the end of the valve, and the source laser could be focused onto the tube or right at the end.

The first molecule we tried was vinyl bromide ($C_2H_3Br$), in an attempt to photodissociate the vinyl radical. We had already probed the photodissociation of vinyl bromide at 193 nm,[14] where it undergoes Br and HBr elimination in a ratio of about 1.3 to 1. The vinyl radical has been found to absorb between 400 and 500 nm,[15] with the spectrum showing discrete bands. We used a Lambda-Physik excimer laser at 193 nm in the source, and for the second laser (into the main chamber) we used a Lambda-Physik FL 2002 dye laser, pumped by a second Lambda-Physik excimer at 308 nm.

This experiment was unsuccessful for several reasons, the most important being that we had no diagnostic technique to determine whether we were producing radicals. We typically rely on mass spectrometric detection of both the molecular beam (to characterize its velocity distribution) and the photodissociation products. Simply pointing the source straight into the detector (through the small hole) is not a good way of determining whether radicals are being produced, because the parent ion of the radical is usually a

large crack (prominent daughter ion) of the precursor. For example, the vinyl radical parent ion, $C_2H_3^+$ (as well as $C_2H_2^+$, $C_2H^+$, etc.) is also produced by electron bombardment of vinyl bromide. Because there is so much more precursor in the beam, the signal from radicals is swamped by background from the precursor. In fact, what is usually observed by looking at the beam profile with the source laser on and without the time-of-flight (TOF) wheel is a dip at the radical parent and daughter ion masses due to depletion of the precursor.

A more ingenious method, suggested by Yuan, was to monitor, for example, $Br^{4+}$, under the assumption that $C_2H_3Br$ will give lots of $Br^+$, some $Br^{2+}$, but essentially no $Br^{4+}$, while Br atoms will give proportionally much more $Br^{4+}$. By monitoring $Br^{4+}$ one can see where the free Br atoms are, and the $C_2H_3$ radicals as well, provided they have been translationally thermalyzed as efficiently as the Br atoms (a fairly good assumption at the high pressures in the quartz tube) and have not undergone any secondary chemistry (a much more tenuous assumption). Unfortunately, the amount of $Br^{4+}$ was extremely small, and most of it seemed to be from $C_2H_3Br$ anyway, but by looking at the depletion at least we were able to get an idea of the correct timing between the pulsed valve and the source laser.

To determine the correct delay between the source laser and the second laser was a little more tricky. Naively, one

could choose a delay for the source laser such that it fired in the middle of the strongest part of the gas pulse (about 200 μsec wide at the maximum intensity, with a fairly sharp rise time and a long tail, at least by the time the gas arrived at the detector, 36.75 cm away) and then scan the delay for the second laser in the general vicinity of where the gas pulse should arrive at the interaction region, based on a rough idea of the beam velocity. We started out doing just that, but never saw any signal so we switched to a more sophisticated method. With the source set off-axis from the detector we dissociated a molecule in the interaction region with only the second laser, and measured the photodissociation signal as a function of the delay time between the valve trigger pulse and the laser. Then we repeated the experiment with the source laser firing at a fixed delay after the valve. By comparing the two sets of data, we could see where maximum depletion of the parent molecule was occurring. This "hole burning" experiment proved to be a good method for finding the proper delays, as we could reproducibly burn a 20-30% hole about 30 μsec wide.

Vinyl bromide was not the best choice for the first experiment, since even though the room temperature spectrum has been reported, the jet-cooled spectrum may be considerably narrower.[16] Thus we had to scan the dye laser (by hand!) at the same time as we were trying out everything else for the first time. Even worse, the fate of any vinyl

radicals we did manage to excite was still unknown. We only detect photofragments, so if the fluorescence quantum yield is close to unity, there would be no signal. Finally, if the molecule underwent internal conversion (IC) and then dissociation, the translational energy release might not be large enough to kick the $C_2H_2$ (the expected product along with an H atom) out to 10°. With time-dependent background from the pulsed valve everywhere, but especially severe at small angles, the experiment was close to impossible, at least as a warm up.

We then switched to $CH_2ClI$, making $CH_2Cl$ radicals in the source with the reaction:

$$CH_2ClI \xrightarrow{248\ nm} CH_2Cl + I \qquad (1)$$

The idea was to dissociate the $CH_2Cl$ radicals in the interaction region where they might undergo the following reactions:

$$CH_2Cl \xrightarrow{193\ nm} CH_2 + Cl \qquad (2)$$

$$\xrightarrow{193\ nm} CH + HCl \qquad (3)$$

One new problem was that now the second laser could dissociate the parent molecule, and any radical dissociation was swamped by signal from $CH_2ClI$ at 193 nm. Even though we

were probably close to saturating the 3 mm long or 5-10 μsec wide "hole" with the source laser (based on the absorption cross-section and the laser intensity), by the time the gas pulse reached the interaction region 9 cm away, the hole had mostly filled in, either through diffusion or recombination, so we saw only about 35% depletion.

$CH_2ClI$ is an interesting molecule which should be pursued further in one-laser experiments, as it seems to be undergoing bs photochemistry similar to $CH_2BrI$.[11,17] At 248 nm, the dominant channel is C-I fission (the only one at 308 nm), and at 193 nm it appears to be mostly C-Cl fission, though there is clearly much more going on than that.

We later tried $CH_2I_2$ as well, as that should have more favorable kinematics, but were still unable to see any signal definitely from radicals produced in the source. When the detector mechanical pump failed, venting the detector in a particularly nasty way, we terminated the experiment. The lessons learned seemed to be that we needed some way of determining whether we were making radicals in the source and how many were reaching the interaction region, and that trying to dissociate radicals at a wavelength where the parent molecule also absorbs would add a lot of difficulty in seeing the dissociation products of the cold radicals. Along the way, we also found that the source laser had a tendency to destroy the quartz tube after awhile, and that the correlated background from the pulsed

valve made it very difficult to detect slow products (those with close to the beam velocity) in either one-laser or two-laser experiments.

B. 1987- About half a year later, after we had moved down to campus and set up the RSM, the radicals project reared its head again. It was decided that we would systematically solve all the problems of the previous summer and get the experiment to work. My biggest complaint was that we had been unable to determine whether we were producing radicals and how much they were spreading out in time. To look at a pulsed beam with the single-shot TOF wheel you must have the pulsed valve firing synchronously with the wheel, otherwise all you see is an average over the varying velocity profile of the gas pulse. (Actually, you see very little signal at all, because most of the time the valve is closed, and is typically only open for ~200 $\mu$sec at ~100 Hz.) This is especially important in the pulsed radicals experiment, where you only want to look at the tiny section which the source laser has intersected, and nothing else. Walter Miller built a nice little dividing circuit to decrease the frequency (normally 1200 Hz since the wheel spins at 300 Hz and has 4 equally spaced slots) of the output pulses from the TOF wheel to $\leq$100 Hz and then trigger the pulsed valve. Since the wheel is now driving the valve, but obviously the valve must fire first before the gas molecules can reach an open slot on the wheel, we delayed the

valve almost as long as the period (frequency$^{-1}$) of the valve repetition rate. Thus the $n^{th}$ gas pulse from the valve went through the $(n + 1)^{th}$ (divided) open slot in the TOF wheel. This was not a problem as the jitter was much less than the ~50 $\mu$sec open time of the slot.

Unfortunately, the design of the RSM made data obtained with this method much more difficult to interpret than would have been desirable. Because the TOF wheel is permanently mounted inside the main chamber and can be raised into position and lowered by an external screw (Beam TOF anytime, no venting required!), it has to stay clear of the rotating source. It is mounted 14 cm from the interaction region, right next to the detector wall. This is unimportant in a cw beam experiment where the beam velocity distribution is constant at all distances from the nozzle, but in a pulsed beam experiment the instantaneous velocity distribution changes as the pulse spreads out. What you would like to measure is the velocity distribution at the interaction region, 9 cm from the nozzle, but what you end up measuring is the distribution 14 cm further downstream. This is especially serious for short times between the valve and the wheel (long set delay times) where you can measure an anomalously fast and narrow distribution due to the fastest molecules, which have "outrun" the rest of the pulse, but it will affect the results for all delay times, especially on the RSM where the distances are so great. In fact, this was

never a problem because we again failed to see signal, but it must be considered for all crossed-beam and one-laser photodissociation experiments using a pulsed valve. By measuring the velocity distribution at a range of delay times one can, in principle, reconstruct the velocity distribution at the interaction region, but this has not yet been done.

Yuan had the idea that the quartz tube might be acting as a very tight focusing lens, and that we were only irradiating a very small section in the center. Since the laser intensity would be very strong there, we might even be destroying the few radicals produced, by secondary photodissociation or photoionization. Therefore we designed a holder for parallel quartz plates that would make a 1 x 1 mm square channel where the precursor would be irradiated. Two 1/16" plates were held apart by two pieces of 1 mm thick microscope slide (also quartz) spaced 1 mm apart to create the channel. They were glued into a transverse slot along the face of the nozzle and kept in place by the holder at the other end. During mounting and gluing they were kept at the appropriate distance from each other by a 1 mm dia. removable dowel pin.

We started out by testing several molecules ($CH_2BrI$, $CH_2ClI$, 1,2-$C_2H_4ClI$), first with a YAG laser at 266 nm, then with an excimer at 308 and 248 nm. We again settled on $CH_2ClI$ as the most hopeful choice, breaking the C-I bond in

the source, then trying to dissociate the $CH_2Cl$ radical in the interaction region. Taking synchronous beam TOF with the source laser on we saw a tiny fast peak at $I^{3+}$ corresponding to where we thought the I atoms might be. At $CH_2Cl^+$ there was a similarly fast but much larger peak, with a second, slower peak corresponding to the main part of the beam. Unfortunately we saw the same two peaks when tuned to $CH_2ClI^+$, though the relative size of the faster peak was smaller. We were almost certainly making radicals, but the entire irradiated section of gas was heating up and had a higher velocity as it emerged from the end of the quartz plates assembly. It then partially overtook the slower parent molecules, perhaps picking up some of them on the way, at least in the early stages of the supersonic expansion. Thus there was no way to keep the radicals apart from the parent molecules, and we would be always irradiating both in the interaction region. A chopper wheel close to the nozzle (perhaps between the two skimmers) would be able to let only the pulse of radicals through, but that is not feasible on the RSM. We went ahead anyway, thinking that we would fit the signal from dissociation of parent molecules, subtract it out, and be left with the signal from the dissociation of radicals.

The most frustrating aspect of the experiment was the tendency of the source (either quartz plates or tube) to be destroyed within hours, even at moderate laser powers. A

black deposit would build up just at the edge of where the laser passed through the quartz, the irradiated section sometimes became opaque, and then a hole was drilled through. The exact mechanism was somewhat uncertain and the subject of much inconclusive discussion as to whether it was thermal shock, absorption by the black deposit, heating from the gas, or multiphoton absorption. This had been a problem before, but as we gradually solved the others this became the most serious. Attenuating the source laser power so much that the quartz lasted for a long time would produce very few radicals and leave most of the parent molecules intact. Other materials ($CaF_2$, $MgF_2$, etc.) have better transmission in the UV, but much worse thermal shock properties. In the TOF spectra, we often thought there was a small bump on top of the signal from dissociation of parent molecules, but it would disappear after 20 minutes, and when we vented it was always time to replace the quartz tube or plates.

All we ever saw was dissociation of parent molecules. Even the small signal we briefly observed was suggested by Peter Weber to be from dissociation of SiCl (Si from the quartz) rather than $CH_2Cl$. This would explain why we only saw it at m/e = 35 ($Cl^+$) and why it disappeared as soon as the quartz was blown away. (Andy Sappey from Jim Weisshar's group told me that there was less than a factor of 2 difference in signal whether they used a quartz tube, a tube

with a hole in the side, or excitation just beyond the tip of the nozzle. The intact tube was best.) Another problem was that we had no idea where the radicals might absorb, other than based on the absorption spectra of similar closed-shell molecules. We tried $CH_2Cl$ at 248 and 193 nm, then gave up since other molecules didn't look any more promising. In addition we had destroyed most of the quartz tubes and plates, and that part of the setup clearly needed revision.

C. 1988- To make a successful attempt at the photodissociation of radicals we had to solve two final problems. The first was to develop a source that could be used for long periods of time without replacement. The second was to isolate the signal from radicals, given that the second laser could often dissociate the parent molecule as well. I had already come to the conclusion that shining a focused laser beam through any optical material was going to be a perpetual problem, whether it was a tube, plate, or more exotic (and expensive) form such as a prism dye cell. A "Smalley-type" source with a transverse hole cut through the side of the nozzle seemed more and more attractive, but the question remained, how much of the gas pulse (and the radicals) would just leak out the side? Smalley's experiments had used LIF detection, typically much more sensitive (but yielding different information) than our photodissociation technique, at least for molecules with good fluores-

cence quantum yields. For our experiment, we needed as many radicals as we could get, and it would still be difficult. When I talked to Rick Smalley, he estimated that relatively few of the radicals escaped out the side, and that the transverse holes might actually be helpful, by cutting down turbulence (and mixing) inside the nozzle after the laser pulse. This was exactly what I wanted to hear, and I decided to go with a similar design.

How to actually see signal was more subtle, and we attacked this problem along two fronts. My feeling was that we should choose the right chemical system and find a radical that would absorb at a wavelength where its precursor wouldn't. Since there has been so little spectroscopy of radicals involving valence states, I made up a list of potential precursors and the radicals they could generate. This included the usual suspects (dihalocompounds) but also nitrites, esters, peroxides, and ketones. Especially intriguing was the possibility of making $C_2F_3$ from $C_2F_3Br$ or $C_2F_3I$. $C_2F_3$ would be chemically interesting (being similar to the oft-studied vinyl radical), it has been observed in matrix studies,[18] and the absorption spectrum should be similar to $C_2H_3$, which has already been observed at low resolution. $C_2F_3Br$ and $C_2F_3I$ are readily available,[19] have a high vapor pressure ($C_2F_3Br$ is a gas at room temperature), and should absorb strongly at 193 and 248 nm respectively, producing lots of $C_2F_3$. $C_2F_3$ should absorb around 400 nm,

perhaps down as low as 308 nm, and both fragments should recoil out to wide angles, far from the beam.

Another molecule in the back of my mind was $CCl_4$. Rick Brudzynski asked me to check it out on the RSM at 193 nm, since he was seeing some very interesting behavior in its resonance Raman spectrum at nearby wavelengths while a postdoc in Bruce Hudson's lab. I had always thought of $CCl_4$ as being inert, but there was lots of signal at 193 nm. This is because the four identical C-Cl bonding and antibonding orbitals mix and split, pushing one of the electronic transitions to lower energies. The only primary channel seemed to be

$$CCl_4 \xrightarrow{193\ nm} CCl_3 + Cl, \qquad (4)$$

but there was evidence of some secondary dissociation as well, probably due to the absorption of a second photon. Although the IR spectrum of $CCl_3$ has been observed,[20] there has been only a preliminary report on its electronic spectroscopy.[21] However, it can be produced at 193 nm and should absorb at longer wavelengths than 216 nm, where $CH_3$ absorbs,[22] since the absorption of $CCl_4$ is red-shifted from that of $CH_4$. An added bonus is that there is essentially no absorption by $CCl_4$ at 248 nm or longer wavelengths.[23]

Yuan was much more interested in improving the technology, so we could produce any radical without having to

worry about the chemistry. One easy improvement was to use a fixed source, rotating detector machine so that going from one angle to another would not require realignment of the source. Therefore we switched over to the B-Machine, which Pam Chu had equipped with a laser going into the source to excite molecules for collisional energy transfer experiments. We also implemented the new Physik-Instrumente pulsed valve which Tom Trickl and coworkers at the Max Planck Institut in Garching had developed.[24] It can put out up to 10 times as much gas as the Lasertechnics valve since its poppet translates both farther and faster. The only drawback is that it requires two fast HV power supplies to drive it, making the cost a lot higher.

A schematic of the experiment is shown in fig. 1. The pulsed valve was mounted from below, attached to an aluminum block normally used for mounting a chopper wheel velocity selector. We now had the option of chopping the gas pulse immediately after the nozzle, to let only the radicals through. An old differential wall from the 35" Machine was used, since it could accommodate the aluminum block (and the velocity selector). The source laser entered through a lens mounted in the main chamber door, and passed into the source region through a 3/8" tube welded to the differential wall. No reducer cone was used so there was only one region of differential pumping. The beam passed through a .060" skimmer, giving it a nominally 5° angular divergence. The

second laser entered through the secondary source and was focused into the interaction region. We were restricted to detector angles of 0° to 60°, since beyond that, the back of the detector began to block the source laser.

The source, shown in fig. 2, was constructed out of teflon and fit over the end of the pulsed valve "snout" where it was held in place by two set screws. It was quite similar in design to that of Smalley et al.,[5] with minor modifications. A 1.5 mm channel was drilled out along the axis for the gas from the pulsed valve to flow through. A 1 x 3 mm transverse slot, ending 2 mm from the front of the nozzle, was cut through the nozzle to allow the focused excimer laser to irradiate the gas pulse. The source was aligned by first moving and shimming the valve and mounting plate so that the snout was pointing straight through the skimmer, towards the interaction region. Then the teflon nozzle was installed such that the slot was horizontal (parallel to the source laser beam). Finally, the laser beam was focused through the slot. An aperture was placed on the differential wall to partially collimate the laser, since it was easily capable of drilling right through the teflon. The end of the teflon nozzle was about .50" away from the skimmer. This distance was somewhat constrained, since the laser had to pass through the (fixed) 3/8" hole in the differential wall.

Throughout the experiments we used two Lambda-Physik EMG 103 MSC excimer lasers, with ArF (193 nm), KrF (248 nm), and XeCl (308 nm) gas mixtures. The source laser was focused to a 1 x 3 mm spot to maximize the power through the slot, and the second laser in the interaction region was focused to a slightly larger spot, both with UV grade quartz lenses. The B-Machine has been described in detail elsewhere,[25] and its detector is quite similar to that of the RSM.

For data taking, the Lasertechnics valve driver was used to generate a train of 200 μsec TTL pulses, which would trigger the Physik-Instrumente power supply to open and close the valve. The gas pulse was also about 200 μsec long, with a reasonably flat plateau falling off at the edges. The trigger pulse was then delayed (typically 200-300 μsec) and sent to the source laser, then delayed again (50-100 μsec) before triggering the second laser. The multichannel scaler (MCS) was also triggered at the same time as the second laser and recorded the TOF spectra. For beam TOF, the valve (and source laser) could be triggered synchronously or asynchronously as has already been described. In Machine B, the TOF wheel is only 3 cm from the interaction region, and the velocity distribution should be nearly unchanged over that distance.

**Results and Analysis**

A. One laser experiments- In a continuous beam experiment at 248 nm, $C_2F_3I$ showed only one dissociation channel, producing $C_2F_3$ and I with about half the excess energy released into translation. When the $C_2F_3Br$ (~10% in a tank mixed with He) was tested at 193 nm, it quickly clogged the .004" hole in the continuous beam source, probably by polymerization, so we switched to the pulsed valve. Again there was evidence for only one channel, producing $C_2F_3$ and Br with about half the available energy in translation. At neither wavelength was there any sign of secondary dissociation of $C_2F_3$.

$CCl_4$ dissociation at 193 nm had already been observed on the RSM with large quantities of $CCl_3$ produced. There was also some secondary dissociation of $CCl_3$, likely with the absorption of another photon. The TOF spectrum of m/e = 117 ($CCl_3^+$) is shown in fig. 3 (top) and is fit by the translational energy distribution ($P(E_T)$) shown in fig. 4. The m/e = 35 ($Cl^+$) spectrum in fig. 3 (bottom) shows both momentum-matched fragments from reaction (4). The remaining signal is due to further dissociation of the $CCl_3$. It is estimated that much of the $CCl_3$ produced survived to the ionizer. There was no evidence for any $Cl_2$ production from reactions such as:

$$CCl_4 \xrightarrow{193\ nm} CCl_2 + Cl_2 \qquad (5)$$

B. Two laser experiments- As in the past, the plan was to first measure depletion of the precursor molecule with just the source laser on, find the correct delay time for the second laser, and then attempt to see signal from the dissociation of radicals. With $C_2F_3Br$, the source laser was used at 193 nm and the arrival time of the gas pulse was monitored at 0°. Almost 70% depletion of the parent molecule was observed over a ~30 μsec interval. Much less depletion (about 1/3) was found at $C_2F_3^+$, suggesting that large quantities of $C_2F_3$ radicals were being produced. With the laser through the interaction region at 308 nm, no signal from the photodissociation of radicals could be detected. The $C_2F_3$ likely absorbs at longer wavelengths, as does $C_2H_3$,[15] though it may fluoresce rather than dissociate.

The next molecule tried was $CH_2ClI$, with the source laser at 193 nm and the second laser at 308 nm. There was similar evidence for the conversion of a large fraction of the precursor molecules into $CH_2I$ radicals (and also some $CH_2Cl$ radicals) in a short section of the gas pulse. However, no signal could be detected from the photodissociation of $CH_2I$ at 308 nm, because signal from reaction (1), producing $CH_2Cl$ and I, was so strong. Even under conditions close to saturation of the transition at 193 nm, enough parent molecules either survived or diffused in to mask any signal from $CH_2I$ photodissociation.

The final molecule to be tried was $CCl_4$, with the same configuration of lasers. We expected that $CCl_3$ should absorb closer to 248 nm but wanted to try it at 308 nm before switching the second laser to fluorine. $CCl_4$ produces almost no parent ion in the mass spectrometer,[26] so depletion of the precursor molecule with only the source laser on was difficult to measure. With the detector set at 0°, monitoring $CCl_3^+$ or $CCl_2^+$, some depletion (~30%) was observed, but we had no way of even estimating how much of this was from the production of $CCl_3$ radicals. The correct delay time between the two lasers was found by dissociating $CH_2ClI$ (accidentally) left in the source, either adsorbed onto the gas inlet tubing or the pulsed valve walls. This hole-burning experiment showed that a delay of 50-70 $\mu$sec was required for the gas pulse to travel approximately 5 cm from the nozzle to the interaction region in the main chamber.

With the source moved away from 0° and the last traces of $CH_2ClI$ removed, the dissociation of $CCl_3$ radicals at 308 nm was observed. The raw data at m/e = 35 ($Cl^+$) with the second laser on and off is shown in fig. 5. The large time-dependent background at longer times is from the gas pulse and had to be subtracted away to obtain the true TOF spectra shown in figs. 6 and 8. Much of this background appeared to be coming directly from the nozzle through the skimmer and into the detector, which is quite plausible with only one

differential pumping region and a large (nominally 5°) beam angular divergence. Unfortunately this prevented any data collection at beam-to-detector angles of less than 25°, and the best signal-to-noise was obtained at 35°. Any future experiments should certainly use a smaller skimmer, since the raw signal level was actually quite high. If a second differential pumping region is not added, then much greater care should be taken to eliminate holes between the source and the main chamber, to prevent the main chamber pressure from rising to $6 \times 10^{-7}$ Torr as it did in this experiment.

The background peak (data with only the source laser on) was fit to a sum of polynomials using a version of the program PAN,[27] with any oscillations in the baseline before the rise manually set to a constant value. This was scaled up or down a few percent if necessary, then subtracted from data taken with both lasers on. The intention was to make the peaks near the end of the TOF spectra approximately match and cancel out, while the signal appears at shorter times. Because of this, the signal at times longer than about 400 $\mu$sec is fairly uncertain, and has high statistical fluctuations as well.

Signal was observed at m/e = 35, 47, and 83, corresponding to $Cl^+$, $CCl^+$, and $CCl_2^+$, respectively. No signal was observed at m/e = 70 ($Cl_2^+$) even though the background was much lower at this mass. The m/e = 83 TOF spectrum shown in fig. 6 contains a single peak from $CCl_2$ from the reaction

$$CCl_3 \xrightarrow{308\ nm} CCl_2 + Cl \qquad (6)$$

The following evidence indicates that $CCl_3$ was the reactant in reaction (6): 1) $CCl_4$ produces abundant $CCl_3$ radicals at 193 nm, 2) $CCl_4$ does not absorb at 308 nm and there was no dissociation signal with the source laser off, and 3) No evidence for any larger $C_xCl_y$ species was found by monitoring the molecular beam at 0°. Therefore the reactant was produced in the source and can only be $CCl_3$.

The $P(E_T)$ for reaction (6) is shown in fig. 7 and peaks at 10 kcal/mol with an average release of 13 kcal/mol into translation. In a rotating detector experiment, there are always effects from the dissociation anisotropy, even with the laser unpolarized. The anisotropy can be expressed as

$$P(\theta) \sim (1 + \beta P_2(\cos\theta)) \qquad (7)$$

where $\beta$ is the anisotropy parameter and $P_2(x)$ is the second Legendre polynomial.[28] $\beta$ ranges from -1 (perpendicular transition), with the fragments scattered in a $\sin^2\theta$ distribution with respect to the laser polarization direction in the c.m. frame, to 2 (parallel transition), with a $\cos^2\theta$ distribution. Since no data were taken with the laser polarized, the effects of anisotropy are small, but a value of $\beta = 1.0 \pm .2$ seemed to fit the data best.

The m/e = 47 TOF spectrum contains two peaks, as shown in fig. 8 (top). The area under the slower peak depended linearly on the laser power while the faster peak had a quadratic power dependence. The slower peak is just from the fragmentation of $CCl_2$ from reaction (6) in the ionizer, while the faster peak must be from the secondary photodissociation of the product $CCl_2$ in the reaction

$$CCl_2 \xrightarrow{308\ nm} CCl + Cl \qquad (8)$$

The production of CCl requires two photons and apparently neither step is strongly saturated. Since the $CCl_2$ is the product of photodissociation after the supersonic expansion, it has a broad distribution of internal energies, exactly what we were trying to avoid in this experiment. The $P(E_T)$ for reaction (8) released an average of about 13 kcal/mol into translation and this energy comes from both the second photon absorbed and the initial internal energy.

The m/e = 35 TOF spectrum, shown in fig. 8 (bottom), should be able to be fit with contributions from $CCl_2$, CCl, and primary and secondary Cl atoms, using the $P(E_T)$'s for reactions (6) and (8). There was also a sharp spike in the TOF spectrum at about 100 $\mu$sec, from the photodissociation of $Cl_2$ in the reaction

$$Cl_2 \xrightarrow{308\ nm} 2Cl \qquad (9)$$

Since the initial photolysis reaction in the source produces Cl atoms, they can recombine to form $Cl_2$. It is also possible that a Cl atom could abstract another Cl from either $CCl_4$ or $CCl_3$. The $P(E_T)$ for reaction (9) can be calculated by simply subtracting the $Cl_2$ bond energy (57 kcal/mol)[29] from the photon energy (93 kcal/mol). A very narrow $P(E_T)$ centered around 36 kcal/mol fit the fast spike, indicating that it is from the photodissociation of $Cl_2$ and that our measured beam velocity is correct. The m/e = 35 TOF spectrum can be fit reasonably well assuming reactions 6, 8, and 9. The $P(E_T)$'s are already determined so the only adjustable parameters are the relative heights of each curve.

**Discussion**

It is now clear that a pulsed photolysis source of radicals can be created with sufficient intensity for molecular beams experiments. However, there will also be other species present in the beam, chiefly undissociated precursor molecules, but also potentially products of further chemical reactions of the dissociated fragments. In the photodissociation of $CCl_4$ at 193 nm in the source, the predominant species was $CCl_3$ radicals, with some $Cl_2$ produced as well. Though difficult to measure since $CCl_4$ produces essentially no parent ions in an electron bombardment ionizer, there was also almost certainly a large amount

of undissociated $CCl_4$ in the pulse. This residual precursor molecule is from two sources, the $CCl_4$ undissociated by the source laser pulse and either $CCl_4$ "diffusing" in from before and after the laser pulse or faster $CCl_3$ radicals overtaking slower $CCl_4$. With a strongly absorbing precursor molecule, a high buffer gas pressure (to prevent diffusion between the initial photolysis step and the supersonic expansion), and an experimental geometry with the two laser beams spatially as close as possible, it is expected that the amount of residual precursor molecule could be reduced to a low value but never completely eliminated.

A simple estimate can be made of the number density of radicals available from this technique. With the Physik-Instrumente pulsed valve, number densities of greater than $10^{13}$/cc can be obtained at the interaction region in the main chamber.[30] Assuming a 10% mixture of precursor in buffer gas, that half the precursor molecules are dissociated in the source to produce radicals, and that 80% of the gas in the nozzle goes out the end rather than the sides gives ~4 x $10^{11}$ radicals/cc in the interaction region. However, the radical pulse is only about 4 mm long, or 4-10 $\mu$sec in time. This is not a problem for photodissociation or multiple laser pump-probe experiments where the laser beam is typically focused to a few mm dia. and the pulse duration is 20 nsec or less, but would not be suitable for crossed-beams reactive scattering experiments. We actually

observed the pulse of radicals to have spread out to 10-20 μsec in time, indicating substantial diffusion or turbulent mixing, but presumably this could be corrected by increasing the buffer gas pressure or optimizing the source-interaction region distance and geometry.

In the photodissociation of $CCl_3$ at 308 nm, there was only one primary channel observed, reaction (6) producing $CCl_2$ and Cl. The primary chemistry was not unexpected but the fact that $CCl_3$ absorbed at 308 nm was. The preliminary report of the electronic spectrum of $CCl_3$ showed an absorption band at 365 nm,[21] but this has been suggested to be incorrect.[31] It is unlikely that the $CCl_3$ absorption at 308 nm is from vibrational hot bands, since other researchers have observed strong vibrational cooling following photolysis in the high pressure region of a supersonic expansion.[32]

Reaction (6) released an average of 12-13 kcal/mol into translation, less than 30% of the available energy of 44-54 kcal/mol.[29,33] In contrast, $CCl_4$ dissociation at 193 nm released 41% of the available energy into translation. $CCl_3$ has a non-planar $C_{3v}$ structure, similar to $CF_3$, with a Cl-C-Cl bond angle of 116°.[20,34] Even considering the rotational excitation from dissociation with a non-zero exit impact parameter, the translational energy release is rather low and suggests three possibilities: 1) The thermochemistry is incorrect, and the C-Cl bond energy in $CCl_3$ is higher than 40-50 kcal/mol, 2) An excited electronic state of $CCl_2$ is

produced, or 3) The dynamics of radical photodissociation are qualitatively different than for closed-shell molecules. The first explanation is possible, since it is unclear why the C-Cl bond energy in $CCl_3$ is so low when the C-H bond in $CH_3$ is actually stronger than in $CH_4$, and the stated uncertainties in the heats of formation of many of the $C_xCl_y$ compounds are rather high. However, the C-F bond energy in $CF_3$ is also comparatively low.[29] The ground state of $CCl_2$ is the singlet,[35] analogously to $CF_2$, with a small singlet-triplet splitting. It is likely that the singlet ground state is produced, though there is no reason why the triplet state could not be produced, or some combination of the two. The last possibility clearly requires more study to explore how the dissociation dynamics of polyatomic radicals differ from those of stable molecules.

In the secondary photodissociation of $CCl_2$ radicals, reaction (8), an average of 13 kcal/mol was also released into translation. This is slightly more than the available energy for reaction (8) at 308 nm starting from cold $CCl_2$ radicals, and presumably this extra energy comes from internal energy already present in the nascent $CCl_2$. Since the $CCl_2$ starts with a wide range of internal energies, little can be said about its dissociation dynamics, but it appears to release a large fraction of its available energy into translation.

**Summary**

We have built a pulsed radical beam source capable of generating high number densities of cold polyatomic radicals, suitable for photodissociation, spectroscopy, and pump-probe dynamics experiments. The source was used to generate $CCl_3$ radicals by photolysis of $CCl_4$ at 193 nm, and the $CCl_3$ was then dissociated at 308 nm. The only primary reaction channel observed was the production of $CCl_2$ and Cl with a relatively low translational energy release. Some of the $CCl_2$ absorbed a second photon and dissociated to produce CCl and Cl. In addition to $CCl_3$ radicals and undissociated $CCl_4$ in the beam, $Cl_2$ was also produced, presumably from the recombination of Cl atoms in the supersonic expansion. There was no evidence for any other species produced in the source in quantities detectable with a mass spectrometer.

**References**

1. G. Herzberg, **The Spectra and Structure of Simple Free Radicals** (Cornell University Press, Ithaca, NY, 1971); J. K. Kochi, Ed., **Free Radicals**, vols. I and II (Wiley, New York, 1973); J. M. Hay, **Reactive Free Radicals** (Academic Press, London, 1974); T. A. Miller, Science **223**, 545 (1984) and refs. therein.

2. F. A. Paneth and W. Hofeditz, Chem. Ber. **62B**, 1335 (1929); E. W. R. Steacie, **Atomic and Free Radical Reactions** (Reinhold, New York, 1954); J. G. Calvert and J. N. Pitts, Jr., **Photochemistry** (Wiley, New York, 1966); J. W. Hudgens, Progress in Resonance Enhanced Multiphoton Ionization Spectroscopy of Transient Free Radicals, in **Advances in Multi-photon Processes and Spectroscopy**, S. H. Lin, Ed. (World Scientific Press, Singapore, 1987).

3. P. Andresen, D. Häusler, and H. W. Lülf, J. Chem. Phys. **81**, 571 (1984).

4. P. Andresen, D. Häusler, H. W. Lülf, and W. H. Kegel, Astron. Astrophys. **138**, L17 (1984).

5. D. L. Monts, T. G. Dietz, M. A. Duncan, and R. E. Smalley, Chem. Phys. **45**, 133 (1980); D. E. Powers, J. B. Hopkins, and R. E. Smalley, J. Phys. Chem. **85**, 2711, (1981).

6. R. E. Smalley, private communication.

7. A. D. Sappey and J. C. Weisshar, J. Phys. Chem. **91**,

3731 (1987).

8. T. A. Miller, B. R. Zegarski, T. J. Sears, and V. E. Bondybey, J. Phys. Chem. **84**, 3154 (1980); B. M. DeKoven, D. H. Levy, H. H. Harris, B. R. Zegarski, and T. A. Miller, J. Chem. Phys. **74**, 5659 (1981); M. I. Lester, B. R. Zegarski, and T. A. Miller, J. Phys. Chem. **87**, 5228 (1983); M. Heaven, L. DiMauro, and T. A. Miller, Chem. Phys. Lett. **95**, 347 (1983).

9. A. M. Wodtke and Y. T. Lee, J. Phys. Chem. **89**, 4744 (1985).

10. J. G. Frey, A. M. Wodtke, and Y. T. Lee, unpublished results.

11. L. J. Butler, E. J. Hintsa, S. F. Shane, and Y. T. Lee, J. Chem. Phys. **86**, 2051 (1987).

12. X. Zhao, Ph.D. Thesis, University of California, Berkeley, 1988; X. Zhao, G. M. Nathanson, and Y. T. Lee, in preparation.

13. J. D. Myers, Ph.D. Thesis, in preparation.

14. A. M. Wodtke, E. J. Hintsa, J. Somorjai, and Y. T. Lee, Isr. J. Chem., submitted.

15. H. E. Hunziker, H. Kneppe, A. D. McLean, P. Siegbahn, and H. R. Wendt, Can. J. Chem. **61**, 993 (1983).

16. R. E. Smalley, L. Wharton, and D. H. Levy, Acc. Chem. Res. **10**, 139 (1977); R. E. Smalley, L. Wharton, D. H. Levy, and D. W. Chandler, J. Mol. Spectrosc. **66**, 375 (1977).

17. L. J. Butler, E. J. Hintsa, and Y. T. Lee, J. Chem. Phys. **84**, 4104 (1986).

18. P. H. Kasai, J. Phys. Chem. **90**, 5034 (1986).

19. We obtained $C_2F_3Br$ and $C_2F_3I$ from PCR, but Pfaltz & Bauer, SCM, and others are also suppliers.

20. L. Andrews, J. Phys. Chem. **71**, 2761 (1967); J. Chem. Phys. **48**, 972 (1968); J. H. Current and J. K. Burdett, J. Phys. Chem. **73**, 3504 (1969); E. E. Rogers, S. Abramowitz, M. E. Jacox, and D. E. Milligan, J. Chem. Phys. **52**, 2198 (1970).

21. J. P. Suwalski and J. Kroh, Nukleonika **24**, 253 (1979).

22. G. Herzberg and J. Shoosmith, Can. J. Phys. **34**, 523 (1956); G. Herzberg, **Electronic Structure and Electronic Spectra of Polyatomic Molecules** (Van Nostrand Reinhold, New York, 1966).

23. C. Hubrich and F. Stuhl, J. Photochem. **12**, 93 (1980).

24. D. Proch and T. Trickl, Rev. Sci. Instrum., in press.

25. Y. T. Lee, J. D. McDonald, P. R. LeBreton, and D. R. Herschbach, Rev. Sci. Instrum. **40**, 1402, (1969).

26. E. Stenhagen, S. Abrahamsson, and F. W. McLafferty, **Atlas of Mass Spectral Data** (Wiley, New York, 1969).

27. R. E. Continetti, private communication.

28. R. N. Zare, Mol. Photochem. **4**, 1 (1972).

29. H. M. Rosenstock, K. Draxl, B. W. Steiner, and J. T. Herron, J. Phys. Chem. Ref. Data **6**, suppl. 1, I-774, (1977).

30. The Physik-Instrumente valve has an output 5 to 10 times higher than previous nozzles, which can generate number densities of ~2 x $10^{12}$/cc in the interaction region.

31. N. V. Klassen and C. K. Ross, J. Phys. Chem. **91**, 3668 (1987).

32. L. F. DiMauro, M. Heaven, and T. A. Miller, J. Chem. Phys. **81**, 2339 (1984).

33. S. G. Lias, Z. Karpas, and J. F. Liebman, J. Am. Chem. Soc. **107**, 6089 (1985).

34. C. Hesse, N. Leray, and J. Roncin, Mol. Phys. **22**, 137 (1971); J. Moc, Z. Latajka, and H. Ratajczak, Z. Phys. D **4**, 185 (1986).

35. F. X. Powell and D. R. Lide, Jr., J. Chem. Phys. **45**, 1067 (1966); C. W. Mathews, J. Chem. Phys, **45**, 1068 (1966).

**Figure Captions**

Fig. 1. Experimental arrangement for radical photodissociation on the B-Machine, showing the pulsed valve in the singly differentially pumped source region, the two laser beams, and the detector. The detector could be rotated from 0° to approximately 60° in this experiment.

Fig. 2. Teflon nozzle used to produce radicals, shown fitting over the end of the pulsed valve snout. The gas pulse travels down the 1.5 mm channel and is intersected by the laser beam through a 1 x 3 mm slot. The radicals are thermalyzed as they travel the 2-5 mm to the end of the nozzle.

Fig. 3. Top: TOF spectrum of m/e = 117 from $CCl_3$ from reaction (4) taken on the RSM. The circles are the experimental points and the line shows the fit using the $P(E_T)$ in fig. 4. Bottom: m/e = 35 TOF spectrum at 20°. The slower peak is from $CCl_3$ and the faster one from Cl, both from reaction (4), fit with the $P(E_T)$ in fig. 4.

Fig. 4. $P(E_T)$ for reaction (4), the photodissociation of $CCl_4$, derived from the data shown in fig. 3.

Fig. 5. Raw data from the photodissociation of $CCl_3$ on the B-Machine at m/e = 35, 35° from the beam. The solid circles show the signal with both lasers on and the open circles show the signal with only the

source laser. With the pulsed valve in a singly differentially pumped source chamber, there was always a rising background after the valve opened. The small shoulder in the lower curve near 250 $\mu$sec appeared to be due to heating of the gas pulse by the source laser.

Fig. 6. m/e = 83 TOF spectrum at 35°. The signal is due to $CCl_2$ from reaction (6) and is fit with the $P(E_T)$ shown in fig. 7.

Fig. 7. $P(E_T)$ for reaction (6), derived from the data in figs. 6 and 8.

Fig. 8. Top: m/e = 47 TOF spectrum at 35°. The slower peak (— —) is from fragmentation of $CCl_2$ from reaction (6) in the ionizer, and the faster peak (—— –) is from CCl produced in the secondary reaction (8). Bottom: m/e = 35 TOF spectrum at 35°, with contributions from $CCl_2$ (— —) and Cl (- - -) from reaction (6), CCl (—— –) and Cl (—— ——) from the secondary reaction (8), and Cl atoms (—— – – –) from reaction (9), the photodissociation of $Cl_2$ produced in the source.

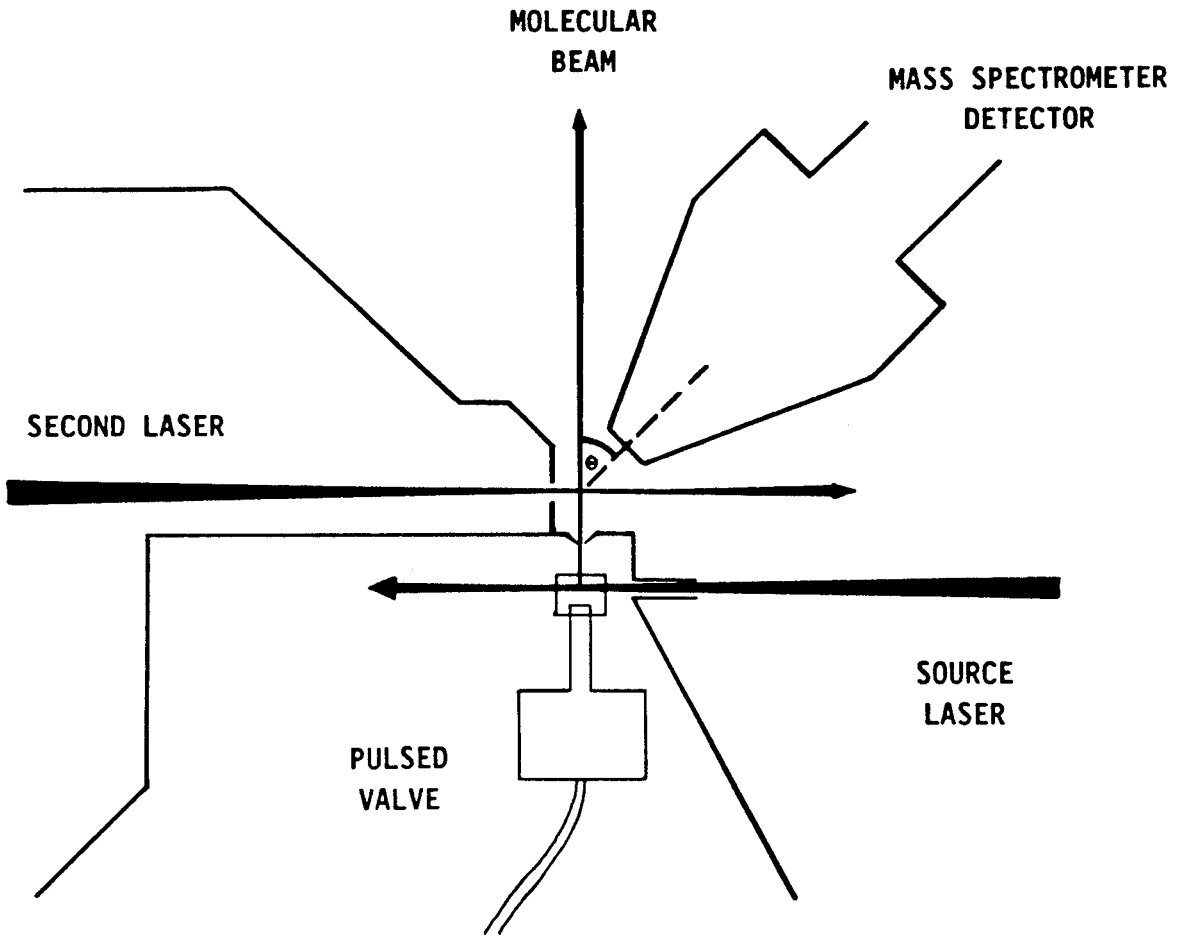


XBL 893-808

Figure 1

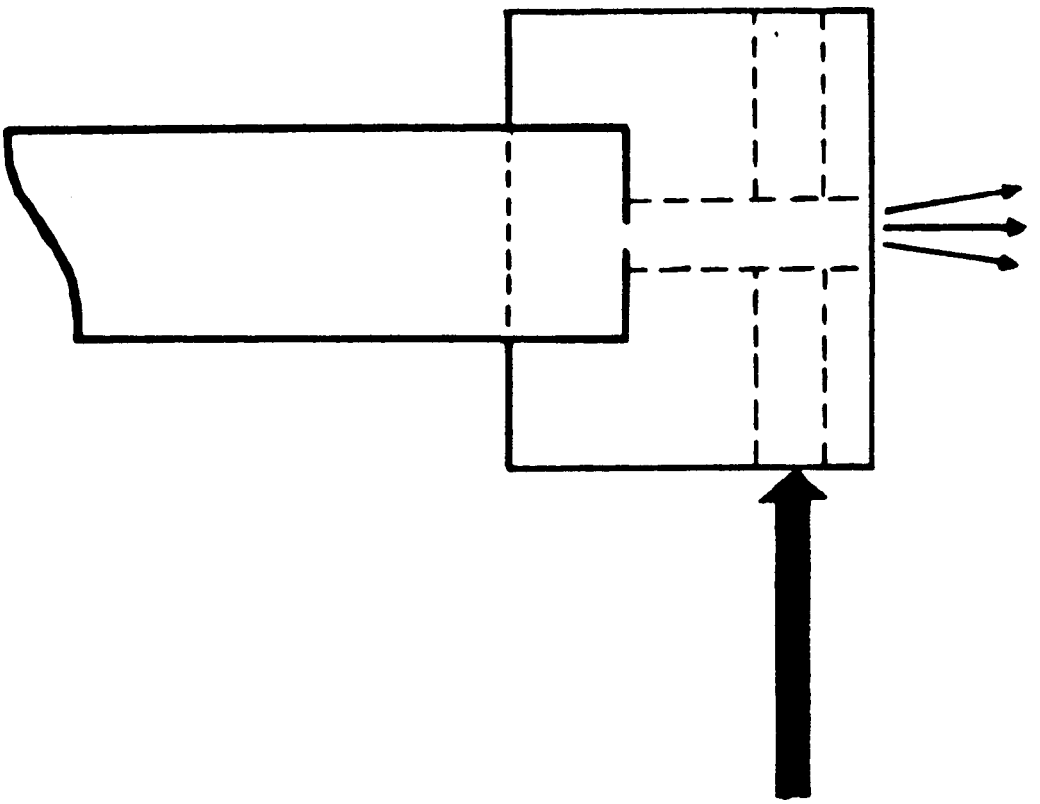

XBL 893-809

Figure 2

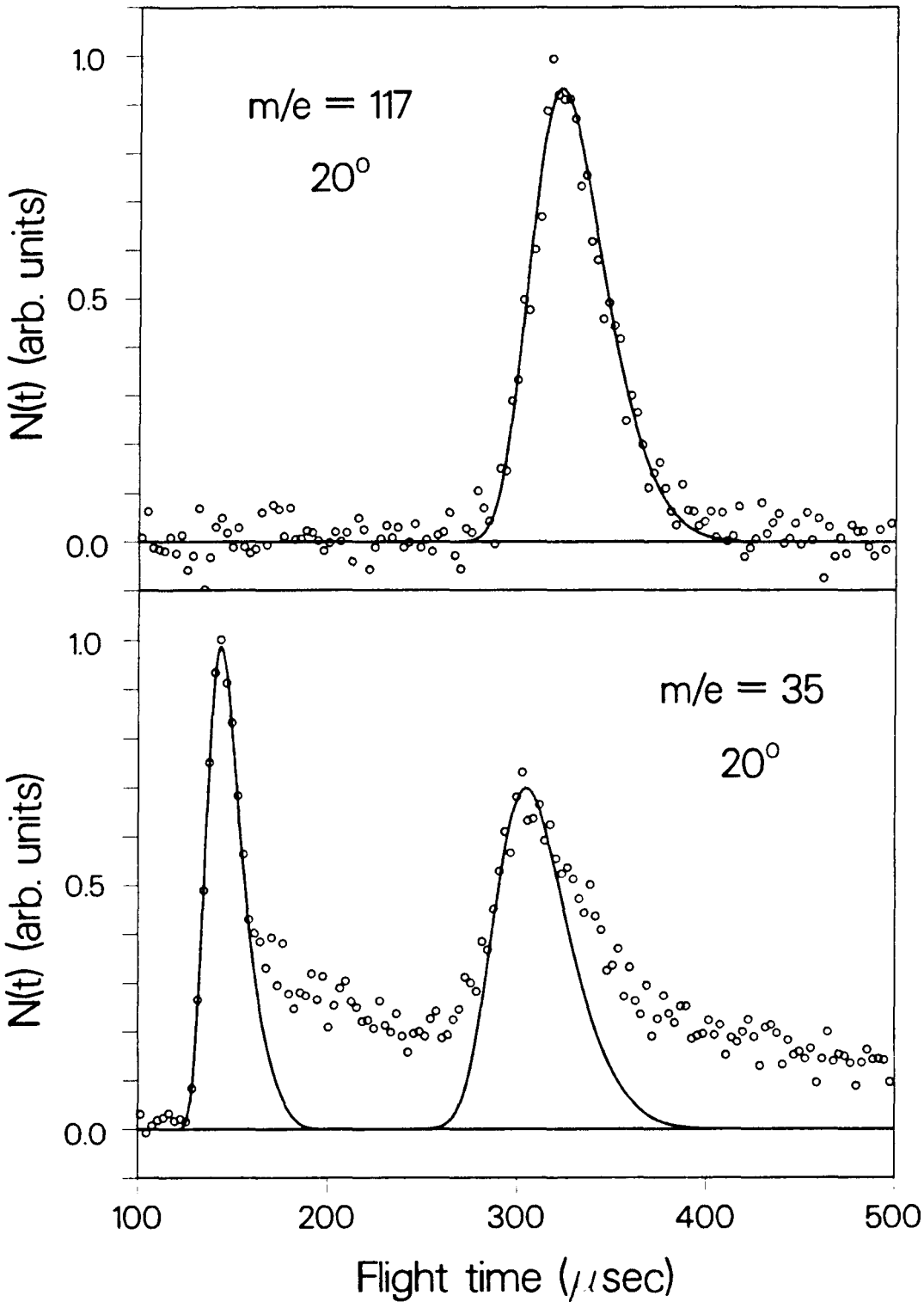


Figure 3

XBL 893-810

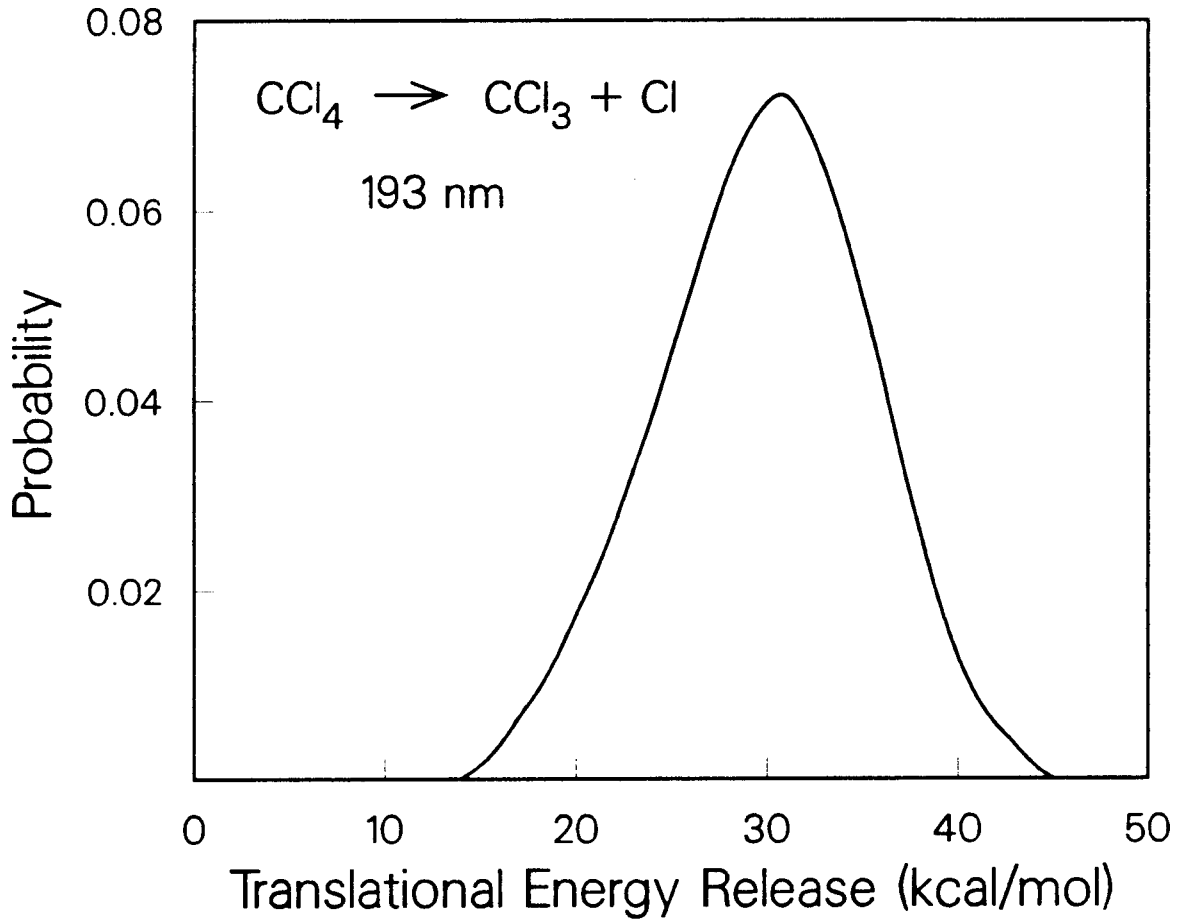


XBL 893-811

Figure 4

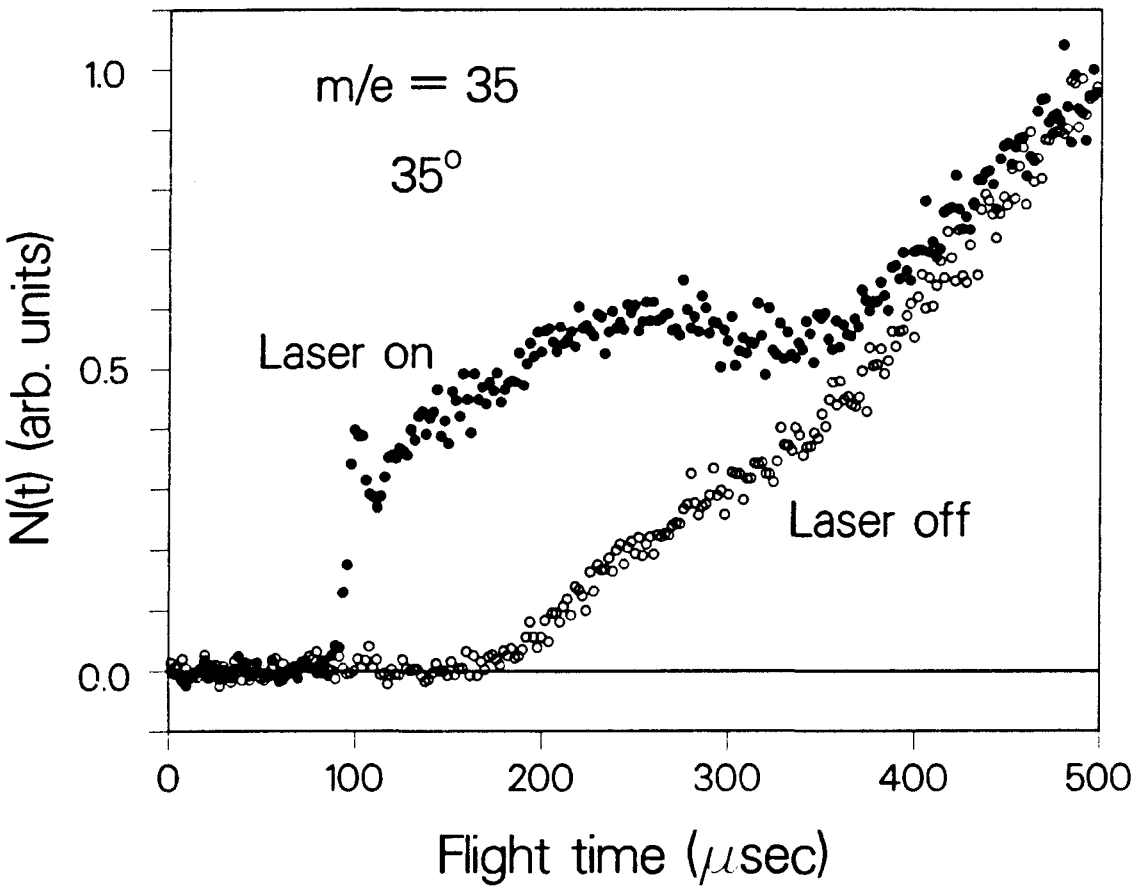


XBL 893-812

Figure 5

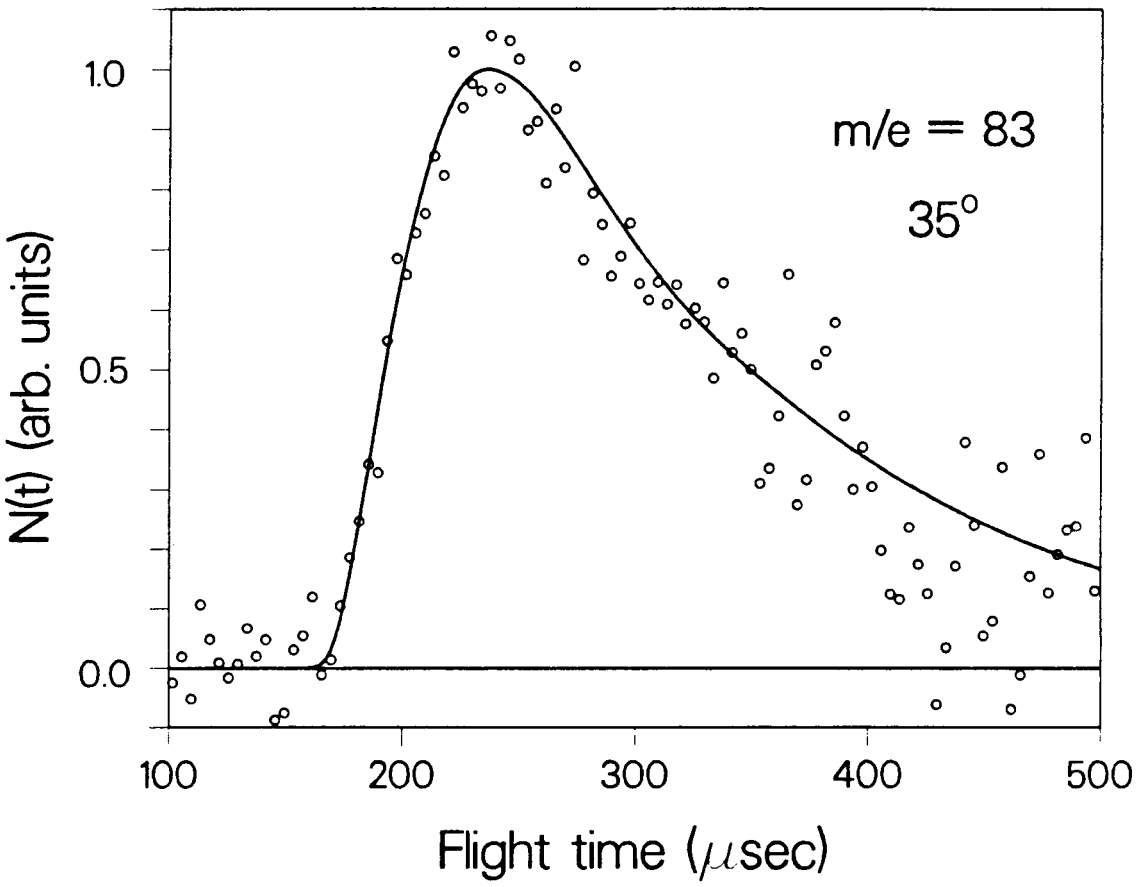


XBL 893-813

Figure 6

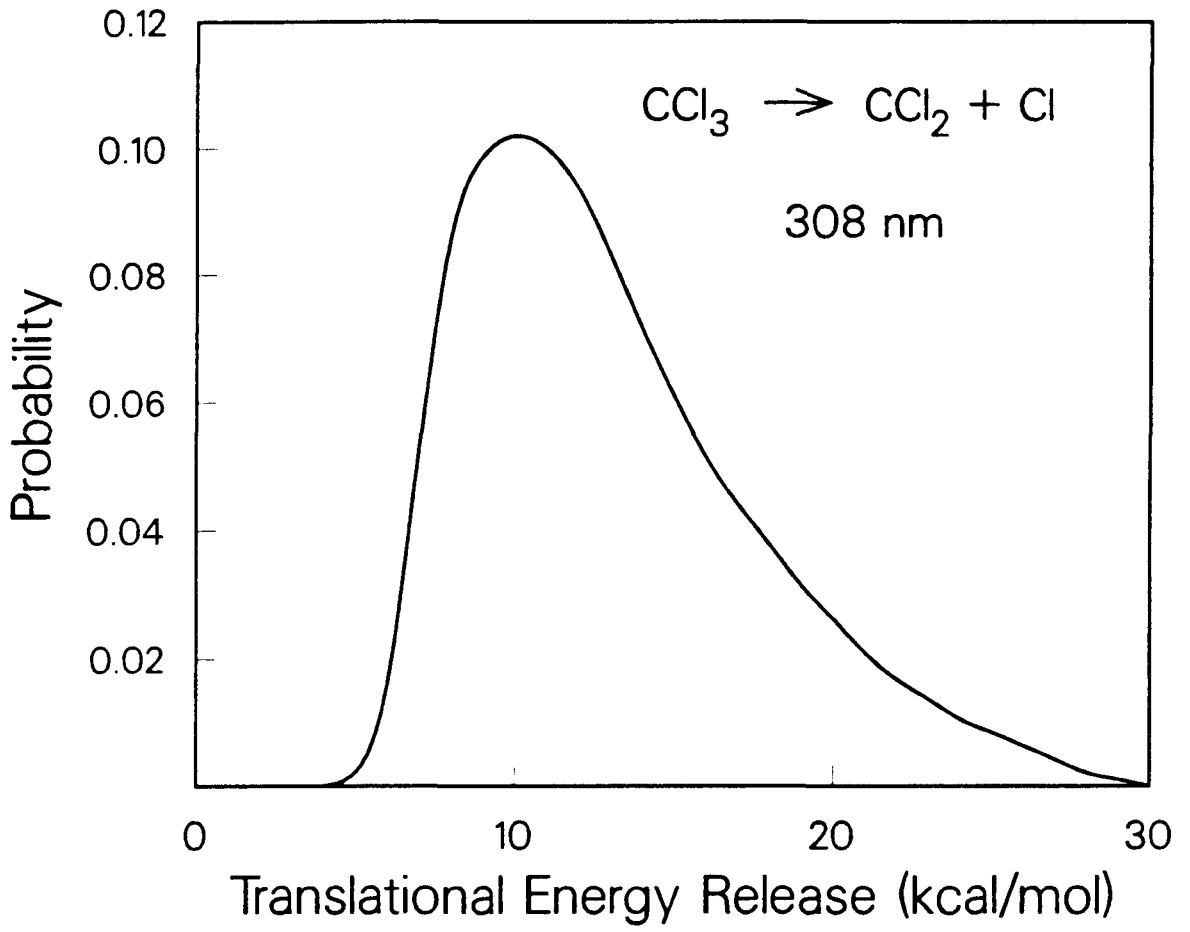


XBL 893-814

Figure 7

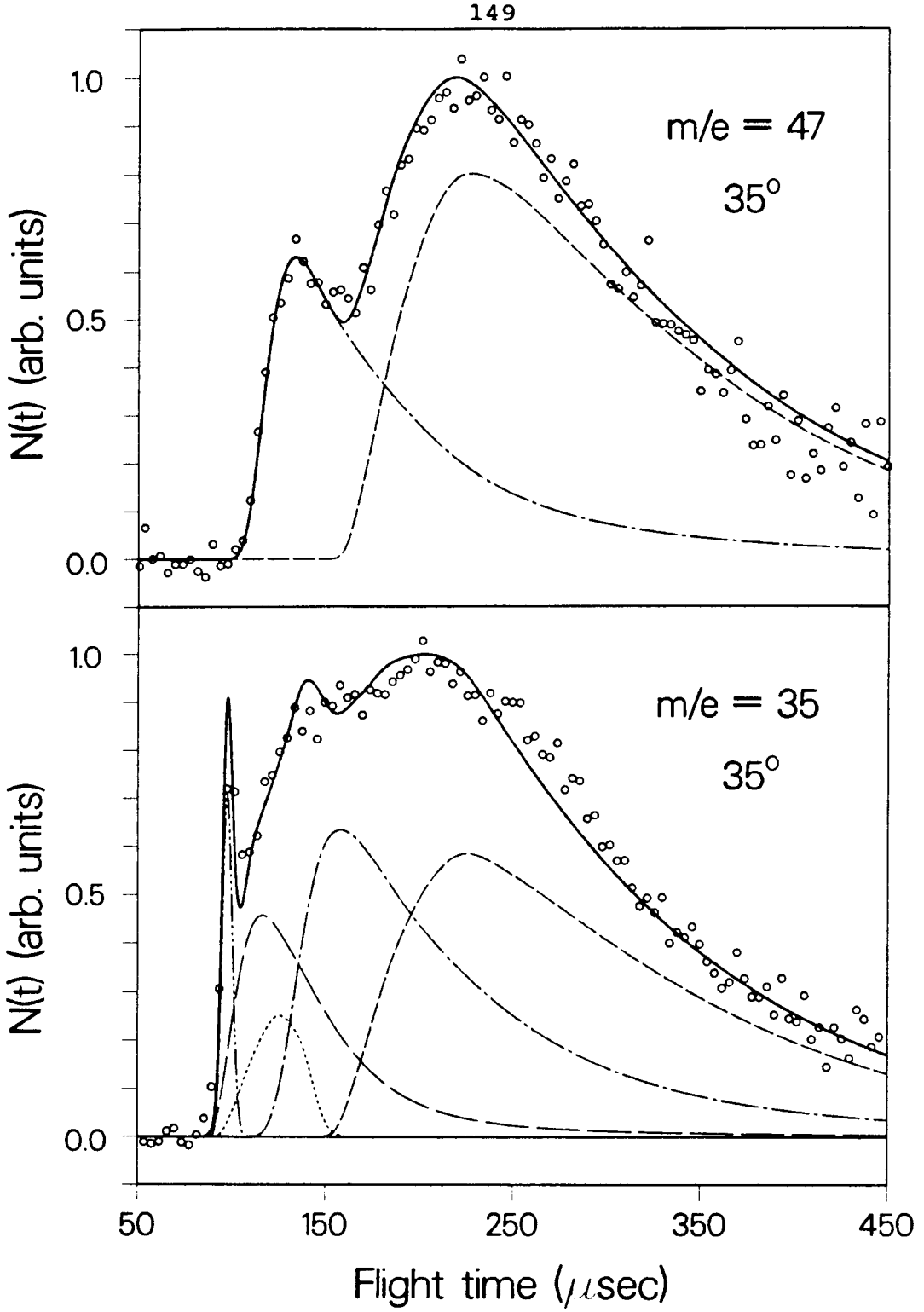


XBL 893-815

Figure 8